DAYLIGHT TRANSMISSION THROUGH A DOUBLE-SECTION SLAT WINDOW

MS. SOMWADEE WONGSIT
ID: 55300700522

A THESIS SUBMITTED AS A PART OF THE REQUIREMENTS
FOR THE DEGREE OF MASTER OF ENGINEERING
IN ENERGY TECHNOLOGY AND MANAGEMENT

THE JOINT GRADUATE SCHOOL OF ENERGY AND ENVIRONMENT
AT KING MONGKUT'S UNIVERSITY OF TECHNOLOGY THONBURI

2ND SEMESTER 2014

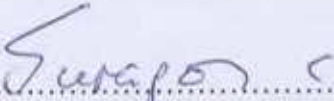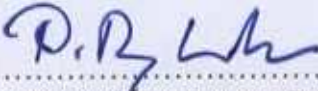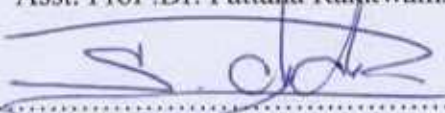Daylight Transmission through a Double-Section Slat Window
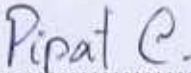
Mr. Somwadee Wongsit
ID: 55300700522

A Thesis Submitted as a Part of the Requirements
for the Degree of Master of Engineering
in Energy Technology and Management

The Joint Graduate School of Energy and Environment
at King Mongkut's University of Technology Thonburi

2nd Semester 2014

Thesis Committee

............*Pipat C.*............
(Asst. Prof. Dr. Pipat Chaiwiwatworakul   )   Advisor

....
(Prof. Dr. Surapong Chirarattananon   )   Member

....
(Asst. Prof .Dr. Pattana Rakkwamsuk   )   Member

....
(Dr. Surawut Chuangchote   )   Member

....
(Asst. Prof. Dr. Atch Sreshthaputra   )   External Examiner

Thesis Title: Daylight Transmission through a Double-Section Slat Window

Student's name, organization and telephone/fax numbers/email

      Ms. Somwadee Wongsit

      The Joint Graduate School of Energy and Environment (JGSEE)

      King Mongkut's University of Technology Thonburi (KMUTT)

      126 Pracha Uthit Rd., Bangmod, Tungkru, Bangkok 10140 Thailand

      Telephone: 0-8809-80995

      Email: bbb_noina@hotmail.com

Supervisor's name, organization and telephone/fax numbers/email

      Asst. Prof. Dr. Pipat Chaiwiwatworakul

      The Joint Graduate School of Energy and Environment (JGSEE)

      126 Pracha Uthit Rd., Bangmod, Tungkru, Bangkok 10140 Thailand

      Telephone: 0-2470-8309 ext. 4107

      Email: pipatc@gmail.com

Topic: Daylight Transmission through a Double-Section Slat Window

Name of student: Ms. Somwadee Wongsit   Student ID: 55300700522

Name of advisor: Asst. Prof. Dr. Pipat Chaiwiwatworakul

ABSTRACT

Double-glazing units have become popular in commercial buildings because of their saving potential and sun shading product as slat were designed to insert into double-glazing window. Ordinarily, one-section slat or a set of parallel slats (all tilt the same angle) is used in double-glazed window, but in this study, double-section slat window which consists of two sets of slat (upper and lower sets) and each set of the slat can be tilted to different angles blind is investigated. The aims of this research are to determine the daylight transmission and heat transmission for both cases of the outer edge of the blind slats tilted downward to ground and upward to sky by using computer program in an attempt to maximize energy saving from lighting and air-conditioning system. In this work, the developed model was validated with experimental data collected in a full-scale physical laboratory. Temperature of the two glass planes and blind of double section slat window were measured to determine the heat gain. Results of calculation from the program agreed well with those results from experiments. The validated numerical model were used to evaluate an annual interior daylight from the window and a whole year electrical energy consumption of a continuous dimmable lighting system and air-conditioning system. The results show that two-section slat window can enhance the daylight use in the building by increasing more useful daylight illuminance, and providing better uniformity of the interior daylight distribution than the single-section slat window. In term of energy saving potential, found that the use of two section slat window saves electrical energy consumption as well as one section slat window. Overall, window with slat provides better interior daylight performance and electrical energy savings than single window with heat reflective glasses.

Keywords: double - section slat window, daylighting, heat transfer, energy saving potential

ACKNOWLEDGEMENTS

CONTENTS

CONTENTS (Cont')

LIST OF TABLES

LIST OF FIGURES (Cont')

LIST OF FIGURES (Cont')

LIST OF FIGURES (Cont')

LIST OF ABBREVIATIONS AND SYMBOLS

A	absorbed energy (Wm^{-2})
B	ratio of blind width to blind separation (-)
c_p	specific heat capacity (J kg^{-1} K^{-1})
E_{e0}	extraterrestrial solar irradiance (W m^{-2})
E_{ed}	diffuse horizontal irradiance (W m^{-2})
E_{es}	solar irradiance (W m^{-2})
E_v	illuminance (lux)
E_x	final exitance (lm m^{-2})
E_{xd}	direct exitance (lm m^{-2})
F_b	porosity of the system (-)
F_{ij}	view factor from surface i to surface j
g	constraint
I	irradiance (W m^{-2})
J_i	final radiosity of segment i (W m^{-2})
J_{oi}	initial radiosity of segment i (W m^{-2})
L	luminance (cd m^{-2})
L_i	length of segment i of a blind system (m)
L_g	ground luminance (cd m^{-2})
L_v	disability glare
L_z	zenith luminance (cd m^{-2})
M	final exitance of blind (lm m^{-2})
M_0	initial exitance of blind (lm m^{-2})
q_{bld}	energy absorbed in blinds (W m^{-2})
q_{wi}	energy, from inter-reflected radiation between blinds, absorbed in window glass pane (W m^{-2})
q_{wo}	energy, from inter-reflected radiation between blinds, released out from blinds to ambient (W m^{-2})
R_{ca}	resistance of convection heat transfer between outside glazing and ambient air (m^2 K W^{-1})
R_{co}	resistance of convection heat transfer between outside glazing and the gap (m^2 K W^{-1})

LIST OF ABBREVIATIONS AND SYMBOLS (Cont')

R_{ci} resistance of convection heat transfer between inside glazing and the gap (m^2 K W^{-1})

R_{cr} resistance of convection heat transfer between inside glazing with the inside temperature of the room (m^2 K W^{-1})

R_{rg} resistance of conduction heat transfer between blind and glazing (m^2 K W^{-1})

R_{rg} resistance of radiation heat transfer between ground and outer surface of outside window pane (m^2 K W^{-1})

R_{ri} resistance of radiation heat transfer between slats and inside glazing (m^2 K W^{-1})

R_{ro} resistance of radiation heat transfer between outside glazing and ground (m^2 K W^{-1})

R_{rr} resistance of radiation heat transfer between inner surface of inside window pane and other surfaces of a room   (m^2 K W^{-1})

R_{rs} resistance of radiation heat transfer between sky and outer surface of outside window pane (m^2 K W^{-1})

S_b length of separation between two slats (m)

T_{go} temperature of outside glazing (K)

T_{BL} temperature of slats (K)

T_{gi} temperature of inside glazing (K)

$T_{ambient}$ ambient air temperature (K)

t time (s)

V_L proportion of exterior visible from interior point through blind slats in lower region (-)

V_u proportion of exterior visible from interior point through blind slats in upper region (-)

W_b width of a slat (m)

Greek letters

β blind tilt angle

Δ increment (-), Perez's brightness index (-)

ε emittance (-), Perez's clearness index (-)

φ profile angle and tilt angle measured with respect to the horizontal direction (deg.)

ϕ zenith angle is (deg.)

α altitude angle or elevation angle (deg.)

LIST OF ABBREVIATIONS AND SYMBOLS (Cont')

γ azimuth angle

η incident angle of the sun ray on surface

τ transmittance of glazing

ρ reflectance of surface

σ Stefan–Boltzmann constant $= 5.670373 \times 10^{-8}$ (W m^{-2} K^{-4})

τ transmittance

Ω solid angle

ω solid angle subtended by the window

ψ gradation function

ζ angle between sun and a point in the sky

Subscripts

b beam normal

bl blind

d diffuse horizontal

g ground, global horizontal

c convention

r radiation

l associated with slat

wo associated with outer window

wi associated with inner window

CHAPTER 1

INTRODUCTION

1.1 Rationale

In tropical Thailand where skylight is voluminous and the daytime is long through the year. The large glazed windows and curtain facades with no external shading are currently popular envelope features of commercial buildings and even residential houses. The excessive solar gain and glare condition are concerned, therefore low optical transmittance glasses are recommended for the usage. However, using the low optical transmittance leads to loss of beneficial gain from the daylight use including connectedness between the occupants and exterior scene and also increase the energy demand of electric lamps on the building even the natural daylight is efficient for building interior iiluminance.

Double glazing substantially reduces thermal loss from the inside and solar heat gain from outside which excellent for energy savings. Daylighting from glazed windows with external or internal shading slats has been studied under different climates and locations. The double-pane glazed window with venetian slats located in between is a specific configuration that has been proven to be applicable in various locations.

However, all slat windows in the literature survey are those equipped with single-section slats that all the slats are to be altered with the same tilt angle. This thesis, focuses on double-section slat window. Double-pane glazed window will be equipped with two sets of slat (upper and lower sets) each set of the slat can be tilted to different angles. It is expected that this configuration can improve the daylight utilization in buildings.

1.2 Literature Review

Entirely, many studies were interested in daylight system to estimate the performance of illumination, indoor environmental control, glare, and its energy savings potential. Most of studies were conducted to evaluate the performance of double glazed window with internal slat for the maximum use of daylight to reduce electrical energy consumption in the building. Almost published studies were in sub-tropical region. Athienitis [3] performed an experiment of a double-glazed window with automated blind in Canada. Mathematical

formulas of transmittance were developed empirically for a double-glazed window with automated blind. The results of simulation had shown that energy savings could exceed 75% for overcast sky and 90% for clear sky when compared to the case of no daylighting/dimming control. The studies were conducted by combining both dimmable and non-dimmable lighting system with the automated blind system. Roche [21] carried out the experiment of a double-glazed with non-dimmable lighting system of automatic blind. The result had shown that the automated blind consumed electricity 60 % which is less than non-dimmable lighting system. More results had shown that the movement of blind was depended on the weather, which is varied from less than 1 min to over 6 minutes and the average was about 3 minutes. For the dimmable lighting system of internal blind slats between double-pane windows, the research from tropical climate in daylighting application were studies by Chaiwiwatworakul [7] and Andhy [15]. Chaiwiwatworakul [7] showed that in the automated blind system, the use of electricity for lighting can be reduced up to 80%. The results of Andhy [15] express that dimmable lighting can save more energy than none dimmable lighting. Nielsen [19] had published a method for calculating direct beam illuminance on the surface and work plane. Nielsen [19] also conducted an experimental set up to validate the model in Sweden (sub-tropic area). Unfortunately, Nielsen [19] didn't show the result for direct beam illuminance calculation specifically on the paper.

In case of heat gain through windows, the internal blind in double-glazed window is used to prevent heat gain. In Canada, Rheault [20] perform the experiment to get the effect of the using of double glazing windows with internal multiple slats. Rheault [20] selected the seven days of summer season where the weather was vary significantly day by day to show the different results of transmitted solar radiation through the window. The result had shown that cooling load had been reduced up to 61% (in 6 days) by using doubled glazed window with internal blinds. Cho [10] made several simulations to examine the effect of the angle of slat blind in double glazed window on solar radiation absorption in summer and winter season. The simulations had shown that the orientation of the angle of slats play a part in solar radiation absorption into the window. Lee [18] performed the full scale experiment of the two adjacent rooms in the same building over a year to study thermal and daylighting performance of automated blind system. The first room was conducted with the automated blind in the double glazed window, another with the particularly fixed angle blind. The result had shown that the automated blind can reduce cooling load higher than the fixed angle blind. Therefore, energy consumption of the air-conditioning system was reduced.

More energy savings were obtained during clear days. In tropical country, Chaiyapinunt [7] conducted research on double glazed window with automated blind. The study was focused on in short wave and long wave optical properties part of the double glazed window with fixed-angle blind system, which longwave and shortwave part were done separately. Chaiwiwatworakul et al. [7] conducted experiments in a lab-scale building by separating the building into 2 rooms. A window system with automate blinds was installed in one room and a window without blind was in another room. Many illuminance sensors were instrumented to measure illuminance and glare in the room. The results showed that the room with automated blinds and dimmable lighting system consumed electrical energy for lighting less than the room with lights fully on by 82% in average. Electricity consumption for lighting system was in the range of 5 to 10 kWh per month where daylight can be used to illuminate interior space efficiently without causing glare problem. Andhy [15] performed the full scale experiment with fixed blind slats at tilt angles of 0°, 30° and 45° and developed simulation software to evaluate the suitable configuration for tropical climate. In the simulation were performed by changing the types of glass using (clear glass, heat reflective glass and tilted glass), the position of blind slats at the angles of 0°, 30° and 45° and four main cardinal orientations of window: north, east, south and west. The result has shown that using the clear glass at the slats angle of 30 degree performs a suitable configuration in terms of maximized electrical energy savings from lighting system and air conditioning system.

In tropical region, the sky is luminous and solar radiation is highly intense. As a result, the luminance is excessive. Since the office buildings are commonly air-conditioned, the use of daylight to illuminance interior space frequently encounters undesirable effects of excessive glare and thermal discomfort. However, all of the published studies were the automatic single-section slat with the same tilt angle.

1.3 Objectives of the Study

The main objective of this research is to investigate an appropriate daylight use through double-section slat window for buildings in tropical climate. To achieve the main objective, the specific objectives are as follows:

1) To develop a mathematical model of the daylight transmission through a double-section slat window

2) To develop a mathematical model of the solar radiation gained through a double-section slat window

3) To determine the daylight gained and heat gained through a double-section slat window

4) To evaluate the electrical energy saving potential from lighting and air-conditioning systems of a room equipped with the double-section slat window

1.4 Scope of Research Work

The research activities include a development of simple energy balance models for the determination of the daylight transmission, and solar and heat gains through double-section slat windows. The capacity of developed models will enhance from those of [9] and [14]. The developed model can determine the daylight transmission for both cases of the outer edge of the blind slats tilted downward to ground and upward to sky. The developed heat transfer model assumes no thermal resistance of glazing panes and slats but accounts for the thermal storage of the window system. One dimensional heat transfer is applied for both slat sections of the window. The models were implemented into a computer program.

Physical experiments were conducted in an outdoor laboratory room with a double-section window oriented south. The laboratory is located at King Mongkut's University of Technology Thonburi, Bang Khun Tien campus. A set of measurement results from experiments on particular days under different daylight conditions will be used to validate the calculations from the developed models.

A whole year's record of solar radiation and daylight illuminance from a meteorological station at the campus was employed for yearly simulation of the double section slat window to determine the resulting energy savings potentials from lighting and air-conditioning.

CHAPTER 2

THEORIES

2.1 Heat transfer through the slat window

A non-steady heat transfer model was developed for the slat window. Figure 2.1 shows the slat window model consisting of two adjacent slats located at the middle between two glass panes. The slats have a width of W_l and a separation of S_l and are tilted at an angle of φ_l measured with respect to the horizontal direction. The outer glass pane with a thickness of e_o is set apart at a distance of D from the inner glass panes with a thickness of e_i. The distance from the edges of the slats to the surfaces of both outer and inner glass panes is d.
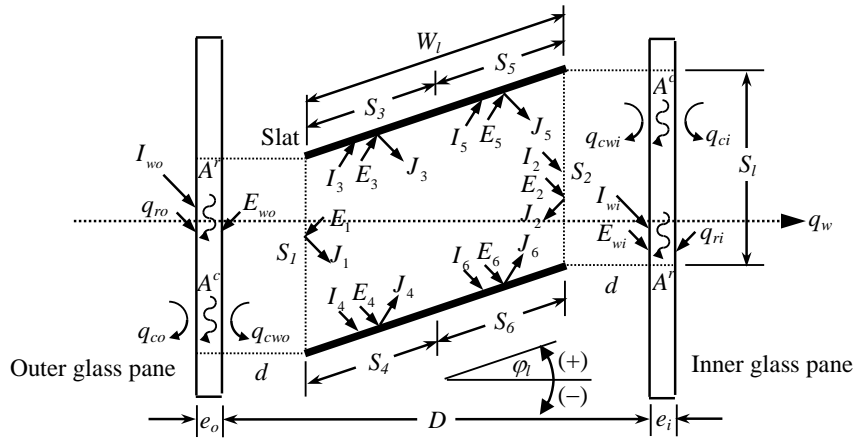
Figure 2.1 The heat transfer model of the slat window

In the figure, the heat transfer through the slat window (q_w) is analyzed based on mechanisms of radiation exchanges and heat convections. The analysis determines the net radiative energy absorbed (A^r) by the slats and the glasses from the exchanges of the solar (shortwave) and thermal (longwave) radiations within the air gap of the slat window. The analysis also determines the net energy absorbed due to the heat convection of the air within the gap between either side of the slat edge and the glass pane (A^c).

The energy balances of the whole window system are simultaneously performed at the slats and the two glass panes by considering the incident solar radiations, the net absorbed energy from the heat exchanges within the air gap, and the heat convection on the glass

surfaces by the surrounding air. In the energy balances, the effects of thermal storage and delay in the temperature and the heat transfer are taken into account as a result of the slat and glass properties.

For the slat window, the slats can be rotated counterclockwise from the horizontal line at which the angle is measured as a positive value $(+\varphi_l)$. Rotating the slats clockwise from the horizontal line, the measured angle is assigned as a negative value $(-\varphi_l)$.

2.1.1 Solar (shortwave) radiative exchanges

As illustrated in Figure 2.1, a fictive cavity is established for the analysis of the solar radiative exchanges within the air gap. The fictive cavity is enclosed by the slat surfaces of S_3 to S_6 and the fictive surfaces of S_1 and S_2. In the analysis, the incident solar radiations on the surfaces are first determined. Figure 2.2 shows the incidences of the beam normal radiation (E_{eb}) on the slat window at the slat angle of $+\varphi_l$.

a) Beam radiation is fully shaded   b) Beam radiation is partially shaded
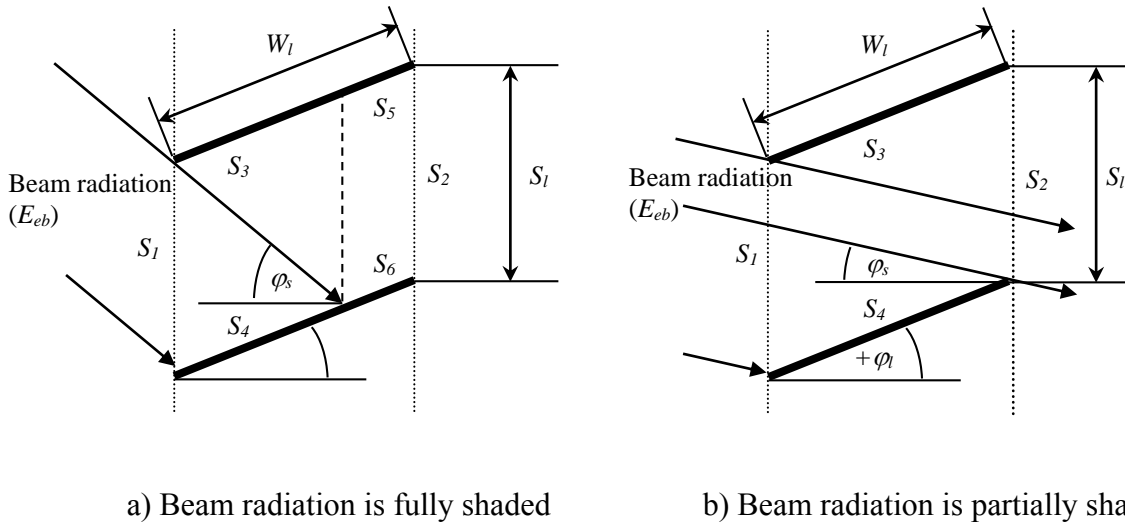
Figure 2.2 Incidences of beam radiation on the slat window

The amount of the incident beam radiation on the slat surface S_4 (W/m^2) can be calculated as

$$I_4^b = \tau_{wo}(\eta_{wo}) \cdot E_{eb} \cdot \cos\eta_l, \tag{1}$$

where τ_{wo} is the solar transmittance of the outer glass pane. η_{wo} and η_l are the incidence angles of the beam radiation on the outer glass and on the slat, respectively. According to [16], the dependence of the glass transmittance on the incidence angle can be expressed as

$$\tau_{wo}(\eta_{wo}) = \tau_{wo}(0°) \cdot \left[1.018 \cdot \cos\eta_{wo} \cdot (1 + \sin^3\eta_{wo})\right], \tag{2}$$

where $\tau_{wo}(0°)$ is the solar transmittance of the outer glass at the normal incidence.

Examining Fig. 2.2(a), the beam radiation is completely shaded by the slats. The length of S_4 can be determined from the geometrical position of the sun relative to the slat:

$$S_4 = \frac{1}{\cos\varphi_l \tan\varphi_s + \sin\varphi_l} \cdot S_1, \qquad (3)$$

where φ_s is the solar profile angle, defined as the angle between the outward normal of the window and the projection of the vector from the window to the sun on the vertical plane containing the outward normal, and can be written as

$$\varphi_s = \tan^{-1}\left(\frac{\tan\alpha_s}{\cos(\gamma_s - \gamma_W)}\right), \qquad (4)$$

where α_s is the solar altitude angle and γ_s is the solar azimuth angle. γ_W is the azimuth angle of the window.

In the figure, the length of the sun shaded surface S_6 can be obtained by subtracting W_l by S_4. The lengths of S_3 and S_5 are assigned equal to S_4 and S_6, respectively. The lengths of S_1 and S_2 are both equal to S_l.

Figure 2.2(b) shows another case where part of the beam radiation is intercepted by the slats and the other part directly reaches on the inner glass pane. In this case, the upper surfaces of the slats are fully sunlit, thus S_4 equals to W_l (S_6=0). The proportion of the sunlit area on the total area of the inner glass pane (F_b) can be determined by using the relationships presented in Table 1.

Table 2.1 Proportion of the sunlit area on the inner glass pane of the slat window (F_b)

Slat angle	Condition	Portion of the sunlit area on the inner glass pane
$\varphi_l \geq 0°$	All values of φ_s	$F_b = 1 - \dfrac{W_l \sin\varphi_l}{S_l} - \dfrac{W_l \cos\varphi_l \tan\varphi_s}{S_l}$
$\varphi_l < 0°$	$\varphi_s < |\varphi_l|$	$F_b = 1 - \dfrac{W_l \sin|\varphi_l|}{S_l} + \dfrac{W_l \cos|\varphi_l| \tan\varphi_s}{S_l}$
	$\varphi_s \geq |\varphi_l|$	$F_b = 1 + \dfrac{W_l \sin|\varphi_l|}{S_l} - \dfrac{W_l \cos|\varphi_l| \tan\varphi_s}{S_l}$

The average amount of the incident beam radiation on the inner glass surface S_2 (W/m^2) is thus calculated as

$$I_2^b = F_b \cdot \tau_{wo}(\eta_{wo}) \cdot E_{eb} \cdot \cos\eta_{wi} , \tag{5}$$

where η_{wi} is the beam incidence angle on the inner glass surface. The F_b value is obtained from the relationships in Table 3.

By assuming all the surfaces are perfectly diffusive, the solar radiative exchange due to the multiple reflections of the incident beam radiation can be resolved by

$$J_i^b = \rho_i I_i^b + \rho_i \sum_j J_j^b \cdot F_{ij} , \tag{6}$$

where J_i^b is the beam solar radiosity of surface i (W/m^2). ρ_i is the solar reflectance of surface i. F_{ij} is the view factor from surface i to surface j. I_i^b is the incident beam radiation on surface i (W/m^2).

In a consequence, the beam solar irradiation on surface i (E_i^b) and the absorbed energy on surface i (A_i^b) can be obtained from

$$E_i^b = \sum_i J_i^b \cdot F_{ij} , \text{ and} \tag{7}$$

$$A_i^b = \alpha_i \cdot E_i^b , \tag{8}$$

where α_i is the solar absorptance of surface i.

By Eq. (6)-(8), the calculated values of surfaces 1 and 2 are to be correspondent with the values of the outer glass and the inner glass, respectively (i.e. $J_{wo}^b = J_1^b$, $J_{wi}^b = J_2^b$, and $E_{wo}^b = E_1^b$, $E_{wi}^b = E_2^b$, and $A_{wo}^b = A_1^b$, $A_{wi}^b = A_2^b$). For the slats, its values can be obtained by averaging the calculated values of surfaces 3 to 6 weighted by the surface length (e.g. $J_l^b = \sum_{i=3}^6 J_i^b \cdot S_i \Big/ \sum_{i=3}^6 S_i$).

The slats and the glasses also receive the diffuse radiations from the sky and the ground. Figure 3.3 shows the incidences of the diffuse radiations. At this step, the lengths of S_3, S_4, S_5 and S_6 are all set equal to half of the slat width. The incident diffuse radiation on surface i (I_i^d) can be calculated as:

$$I_i^d = \int_{\gamma_w - \pi/2}^{\gamma_w + \pi/2} \int_{\alpha_{ll}}^{\alpha_{ul}} \tau_{wo}(\eta_{wo}) R \cos\eta_i \, d\alpha \, d\gamma , \tag{9}$$

where R is radiance values of the sky or the ground. α_{ul} and α_{ll} are the lower and upper limits of the elevation angle of the surface for sky or ground-reflected radiation.

a) Slat angle > 0°   b) Slat angle < 0°
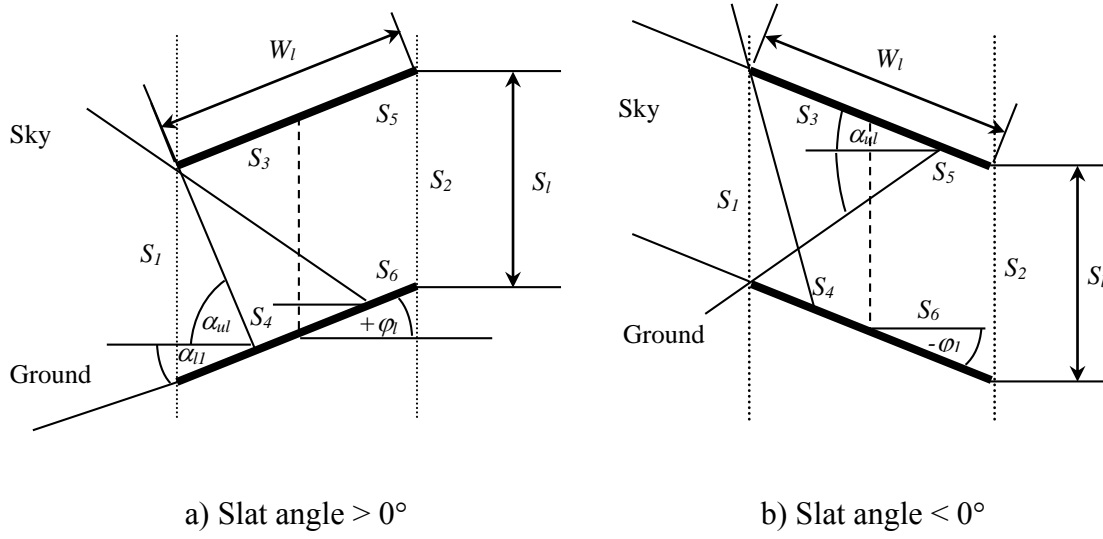
Figure 2.3 Incidences of diffuse radiation on the slat window

In Eq. (9), the radiance values (R) at any points over the sky can be calculated from the ASRC-CIE sky model that is suitable for our tropical sky by Chaiwiwatworakul [5] Radiance value of the ground can be derived by dividing the reflected global radiation from the ground by π.

According to the slat geometry at the positive tilted angle as shown in Figure 2.3(a), values of the lower and upper limits of each surface in Eq. (9) can be exhibited as in Table 2. The variable B in the table represents the ratio of slat width to slat separation, $B=W_l/S_l$.

Table 2.2 Lower and upper limits of the elevation angle used to determine values of diffuse light from sky and ground incident on the six surfaces of the slats.

Blind segment	Visible part	Elevation angle (α)	
		Lower limit (α_l)	Upper limit (α_{ul})
S_1	Sky	n/a	n/a
	Ground	n/a	n/a
S_2	Sky	0	$\tan^{-1}\left(\dfrac{0.5 - B\sin\varphi_l}{B\cos\varphi_l}\right)$
	Ground	$-\tan^{-1}\left(\dfrac{0.5 + B\sin\varphi_l}{B\cos\varphi_l}\right)$	0
S_3	Sky	n/a	n/a
	Ground	$-\tan^{-1}\left(\dfrac{1 + 0.25B\sin\varphi_l}{0.25B\cos\varphi_l}\right)$	$-\varphi_l$
S_4	Sky	0	$\tan^{-1}\left(\dfrac{1 - 0.25B\sin\varphi_l}{0.25B\cos\varphi_l}\right)$
	Ground	$-\varphi_l$	0
S_5	Sky	n/a	n/a
	Ground	$-\tan^{-1}\left(\dfrac{1 + 0.75B\sin\varphi_l}{0.75B\cos\varphi_l}\right)$	$-\varphi_l$
S_6	Sky	0	$\tan^{-1}\left(\dfrac{1 - 0.75B\sin\varphi_l}{0.75B\cos\varphi_l}\right)$
	Ground	$-\varphi_l$	0

By substituting I_i^d for I_i^b in Eq. (6), and J_i^d for J_i^b in Eq. (7), and E_i^d for E_i^b in Eq. (8), the absorbed energy due to the incident diffuse radiation (A_i^d) can be obtained. Values of the form factors of the six surfaces are calculated in accordance with the configuration in Figure 3.3. Finally, the total solar radiosity (J_w^s), total solar irradiation (E_w^s) and the solar energy absorbed (A_w^s) by the slats and the glasses due to the solar radiative exchange can be calculated as

$$J_w^s = J_w^b + J_w^d, \tag{10a}$$

$$E_w^s = E_w^b + E_w^d, \tag{10b}$$

$$A_w^s = A_w^b + A_w^d, \tag{10c}$$

where *w* stands for the window components that are the outer glass (*wo*), the inner glass (*wi*) and the slat (*l*).

It should be noted that the limit values in Table 2 are to be applied in inverse fashion when the slats are tilted at the angle of negative values as shown in Fig. 3.3(b).

2.1.2 Thermal (longwave) radiative exchange

The fictive cavity is also applied for analyzing the thermal radiative exchange between the slats and the glasses. The six surfaces are assumed to be the gray-diffusive. By using the radiosity method, the thermal radiosity of the six surfaces can be written as

$$J_i^t = \varepsilon_i \sigma T_i^4 + (1-\varepsilon_i)\sum_j J_j^t \cdot F_{ij} , \tag{11}$$

where J_i^t is the thermal radiosity of surface *i* (W/m^2). ε_i is the emittance of surface *i*. T_i is the temperature of surface *i* (K).

As the temperatures of the six surfaces are also unknown, an iterative process is used to obtain the solution of these non-linear equations. In the calculation, the temperatures of S_3-S_6 are assigned with the same value and represent the slat temperature.

The net thermal energy absorbed by surface *i* (A_i) can be calculated from

$$A_i^t = E_i^t - J_i^t , \tag{12}$$

where $E_j^t = \sum_j J_j^t \cdot F_{ij}$.

At this moment, total radiative energy absorbed (A_w^r) by the slats and the glass panes can be obtained by summing absorbed solar and thermal radiations:

$$A_w^r = A_w^s + A_w^t , \tag{13}$$

where *w* stands for the outer glass (*wo*), the inner glass (*wi*) and the slat (*l*).

2.1.3 Convective heat exchange

Examining Figure 2.1 again, the outer glass pane is also subjected to the heat convention by the outdoor air. The rate of the heat convection (q_{co}) can be calculated as

$$q_{co} = h_{co}(T_o - T_{wo}) , \tag{14}$$

where T_o is the outdoor air temperature (K). T_{wo} is the surface temperature of the outer glass (K). h_{co} is the convective heat transfer coefficient (W/(m^2.K)) determined by the relationships suggested by Finlayson et al. [11].

$$h_{co} = 8.07 \cdot V_o^{0.605} , \text{ for } V_o < 2 \text{ m/s, and} \tag{15a}$$

$$h_{co} = 12.27 , \text{ for } V_o > 2 \text{ m/s,} \tag{15b}$$

where V_o is the velocity of the outdoor air (m/s).

For the inner glass pane, the glass itself is subjected to the heat convection by the room air (q_{ci}) that can be calculated as

$$q_{cr} = h_{cr}(T_{wi} - T_r),\tag{16}$$

where T_{wi} is the surface temperature of the inner glass (K). T_r is the room air temperature (K). h_{cr} is the convective heat transfer coefficient of the indoor air film (W/(m^2.K)) defined as

$$h_{cr} = 5.6 + 3.8 \cdot V_r,\tag{17}$$

where V_r is the velocity of the room air (m/s).

The natural air circulation within the air gap also causes the heat transfer between the slats and the glass panes. According to Collins et al. [14], the convective heat transfer (q_{cw}) can be calculated for either side of the slats and the glasses as follows:

$$q_{cw} = h_{cw}(T_w - T_l),\tag{18a}$$

$$h_{cw} = \frac{Nu \cdot k}{L},\tag{18b}$$

$$Nu = \left[1 + \left(\frac{0.0665 Ra^{0.33}}{1 + (9000/Ra)^{1.4}}\right)^2\right]^{0.5},\tag{18c}$$

$$Ra = \frac{\rho^2 \cdot g \cdot \beta \cdot \Delta T \cdot (L^3)^2}{\mu} \Pr,\tag{18d}$$

$$L = \frac{D - 0.70 \cdot W_l \cos\varphi_l}{2},\tag{18e}$$

where T_w and T_l are the temperatures of the glass panes and the slats (K), respectively. h_{cw} is the convective heat transfer coefficient (W/(m^2.K)). k is the thermal conductivity of the gas in the gap (W/m.K). Nu is the Nusselt number of the half-gap cavity. Ra is the half-gap Rayleigh number. Pr is the Prandtl number. W is the the gap width (m). g is the gravitational acceleration (m/s^2). β is the coefficient of thermal expansion. ρ is the gas density (kg/m^3). μ is the gas viscosity (N.s/m^2). ΔT is the temperature difference between the gas pane and the slats (K).

By substituting T_{wo} for T_w in Eq. (18a), the calculation determines the convective heat transfer between the outer glass and the slat (q_{cwo}). Similarly, substituting T_{wi} in the equation, the convective heat transfer between the inner glass and the slat (q_{cwi}) is calculated. In this

study, the gas within the window gap is air, thus the values of the parameters relating to the gas in Eq. (18) can be assigned as follows: $k=0.027$, $\rho=1.13$, $\mu=16.97\times10^{-6}$, and $Pr=0.71$.

2.1.4 Energy balances of the slat window

Figure 2.4 shows the thermal resistance network for the energy balance analysis of the slat window system. The analysis is to be simultaneously performed at the outer glass pane, the slats, and the inner glass panes to determine their temperature values. Due to the high thermal conductance of the glasses and the slats, the temperatures of each component can be represented with a single value. As shown in the resistance network, the thermal storage effect of each window component is included in the analysis.
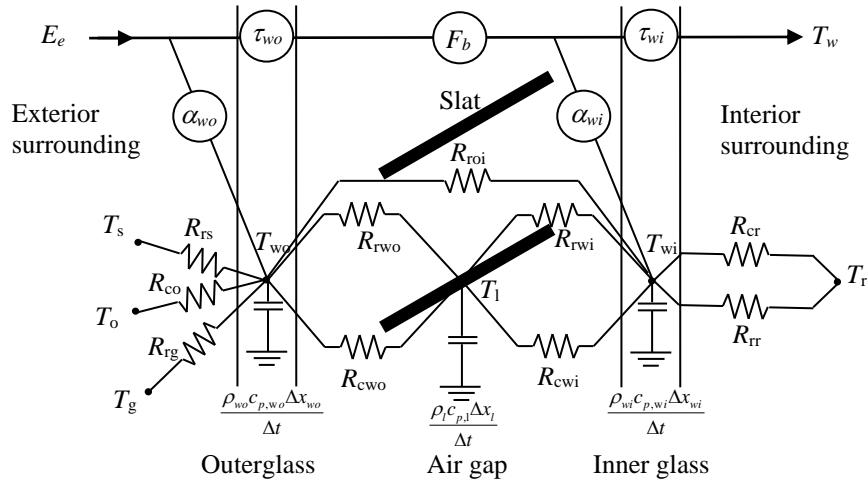
Figure 2.4 The thermal resistance network of the slat window

a) The outer glass (Node T_{wo})

In Figure 2.4, the front surface of the outer glass pane is subjected to the incident solar radiation (I_{wo}), the radiative exchanges with the sky (q_{rs}) and the ground (q_{rg}) and the heat convection by the outdoor air (q_{co}). The back surface of the glass is subjected to the radiative exchanges and natural heat convection within the air gap. Equation 19 expresses the formulation of the energy balance at the outer glass:

$$\alpha_{wo}I_{wo}+\frac{T_o-T_{wo,t}}{R_{co}}+\frac{T_s-T_{wo,t}}{R_{rs}}+\frac{T_g-T_{wo,t}}{R_{rg}}+A_{wo}^r=\frac{T_{wo,t}-T_{l,t}}{R_{cwo}}+\frac{\rho_{wo}C_{p,wo}x_{wo}}{\Delta t}\left(T_{wo,t}-T_{wo,t-1}\right) \quad (19)$$

where I_{wo} is the incident solar radiation on the outer glass. T_o is the outdoor air temperature (K). T_s is the sky temperature (K). T_g is the ground surface temperature (K). $T_{wo,t}$ and $T_{wo,t-1}$ is the outer glass temperature at time t and $t-1$ (K), respectively. $T_{l,t}$ is the slat temperature at time t. ρ_{wo} is the density of the outer glass (kg/m^3). $C_{p,\,wo}$ is the specific heat capacity of

the outer glass (kJ/kg.K). x_{wo} is the glass thickness (m). Δt is the calculation time step (s). R_{co} is the thermal resistance of the convective heat transfer between the outer glass and the outdoor air, and can be expressed mathematically as the reciprocal of h_{co} ($R_{co} = 1/h_{co}$). R_{cwo} is the thermal resistance of the heat transfer between the outer glass and the slat by the natural air convection ($R_{cwo} = 1/h_{cwo}$). R_{rs} and R_{rg} are thermal resistance of the radiative heat transfer between the outer glass and the sky and between the outer glass and the ground, respectively. A_{wo}^r is the net energy absorbed by the outer glass due to the radiation exchange within the air gap.

b) The slats (Node T_l)

In this model, the slats are subjected to the solar and thermal radiative heat exchanges and the convective heat exchanges with the two glass panes. The energy balance at the slats can be formulated as

$$A_l^r + \frac{T_{wo,t} - T_{l,t}}{R_{cwo}} + \frac{T_{l,t} - T_{wi,t}}{R_{cwi}} = \left(\frac{\rho_l c_{p,l} x_l}{\Delta t}\right)\left(T_{l,t} - T_{l,t-1}\right), \tag{20}$$

where ρ_l is the density of the slat (kg/m^3). $C_{p,l}$ is the specific heat capacity of the slat (kJ/kg.K). x_l is the thickness of the slat (m). $T_{l,t}$ and $T_{l,t-1}$ is the slat temperature at time t and $t-1$ (K), respectively. A_l^r is the net energy absorbed by the slats due to the radiation exchange within the air gap. R_{cwi} is the thermal resistance of the heat transfer between the slat and the inner glass by the natural air convection ($R_{cwi} = 1/h_{cwi}$).

c) The inner glass (Node T_{wi})

For the inner glass, its front surface is subjected to the radiative exchange and the convective heat transfer within the air gap and also receive the direct-transmitted solar radiation. The back surface of the glass is subject to the interior thermal environment of the room through the convection and radiation. The energy balances can be formulated as

$$\alpha_{wi} I_{wi} + \frac{T_{l,t} - T_{wi,t}}{R_{cwi}} + A_{wi}^r = \frac{T_{wi,t} - T_r}{R_{cr}} + \frac{T_{wi,t} - T_r}{R_{rr}} + \left(\frac{\rho_{wi} c_{p,wi} x_{wi}}{\Delta t}\right)\left(T_{wi,t} - T_{wi,t-1}\right), \tag{21}$$

where I_{wi} is the incident solar radiation on the inner glass. ρ_{wi} is the density of the inner glass (kg/m^3). $C_{p,wi}$ is the specific heat capacity of the inner glass (kJ/kg.K). x_{wi} is the thickness of the inner glass (m). $T_{wi,t}$ and $T_{wi,t-1}$ is the inner glass temperature at time t and $t-1$ (K), respectively. A_{wi}^r is the net energy absorbed by the inner glass due to the radiation exchange within the air gap.

Now, the temperatures of the slats and the glasses and the resulting heat transfer can be calculated by solving the energy balance equations of the whole window system. At a particular time t, the solar radiation exchanges within the air gap are first analyzed by using Eqs. (1)-(10), and the values of A_w^s are obtained as the result. The unknown values of the slat and the glass temperatures are then assumed for the analysis of the thermal radiative and convective exchanges within the air gap. The analysis is performed by using Eqs. (11)-(18) and the values of A_w^t and q_{cw} are obtained as the result. All calculated values are next substituted into Eqs. (19)-(21) to evaluate their satisfactions. At this step, an iterative process of Newton-Raphson method is applied to produce the new estimated values of the slat and the glass temperatures for their new assumed values in the next iteration round. The process will be repeated until the energy balance equations are satisfied. For this model, the convergence criterion is set at the residual sum from energy balances on both glasses and the slats less than 0.05 W. After obtaining the temperature values, the total heat transfer through the slat window (q_w) can be calculated as

$$q_w = \tau_{wi} \cdot E_{wi}^s + q_{cr} + q_{rr}, \tag{22}$$

where E_{wi}^s is the total solar irradiation on the front surface of the inner glass pane. q_{cr} and q_{rr} are the convective and radiative heat transfer between the back surface of the inner glass pane and the room interior.

2.1.5 A model for a single-pane glazed window

In this study, a model of a single-pane glazed window was also developed to facilitate the determination of the thermal performance of the heat reflective glass. Figure 2.5 shows the thermal resistance network of the model. Compared with Figure 2.4, the model excludes the heat exchanges within the air gap, but the other parts are all identical.
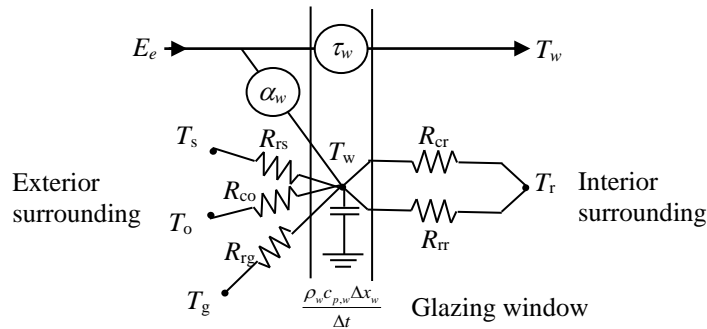

Figure 2.5 The thermal resistance network of a single-pane glazed window

2.2 Daylight from the Slat Window

In this study, the daylight model developed in our previous works was adopted to determine the interior workplane daylight from the slat window according to Chaiwiwatworakul [7, 9]. The model requires the coordinates of the window and of the room as the input. The interior surfaces (wall, floor and ceiling) of the room are first divided into a number of small segments to determine the daylight distribution by using Eq. (23):

$$E_{di} = \int_{\gamma} \int_{\phi} L_W \cos \eta \sin \phi \, d\phi \, d\gamma .$$
$$(23)$$

In Eq. (23), E_{di} is the daylight from the slat window that directly reaches on the surface segment i. L_w represents the window luminance that varies with the line of sight from point i to the patch da on the window as shown in Figure 3.6.
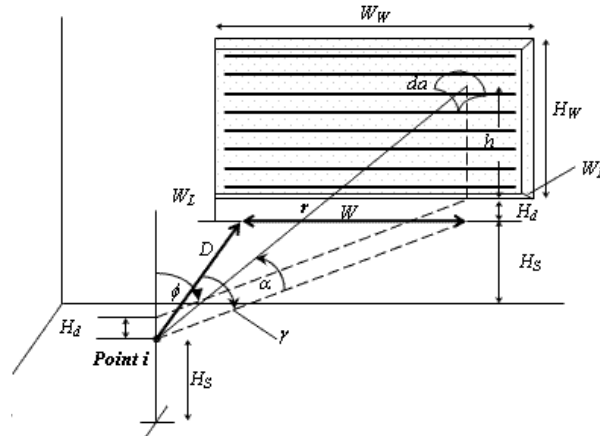
Figure 2.6 Light flux from a patch of window reaching segment i on interior room surface

Value of L_w is obtained as the weighted average between the luminance of the exterior source (sky or ground) and that of slat surface (either lower or upper surface). The luminance value of a patch of sky can be computed using ASRC-CIE sky model by Chaiwiwatworakul [5]. The luminance values of the upper and lower slat surfaces are calculated from reflections of lights from the sun, the sky and ground on the slat surfaces and the two panes of the glazed window. η stands for the angle of incidence between the line of sight and the normal to plan of the wall segment. ϕ and γ are angular variables defined by the window configuration.

For the distribution of the non-slat-reflected sunlight from the slat window onto the interior room surfaces, the daylight model simply determined using Eq. (24)

$$E_{si} = \tau_{wo} \cdot \tau_{wi} \cdot F_b \cdot E_{vb} \cdot A_w \cdot \frac{\cos \eta_i}{\sum\limits_{j=1}^{n} A_j \cdot \cos \eta_j} \cdot \qquad (24)$$

In the equation, E_{vb} stands for the sunlight on the outer glass pane. τ_{wo} and τ_{wi} are the visible transmittances of the outer and inner glazed windows, respectively. A_w is the window area. A_j is the area of the sunlit segment j. η_i is the incident angle of the sunlight on the segment i, and n is the total number of the segments in the room lit by the sunlight. In the equation, F_b represents a fraction of the sunlit area to the total window area that the value can be obtained from Table 1. A surface segment is assumed to receive the sunlight if a line drawn from the center point of the segment to the sun is within the field of view from the point to the window scene. The total direct illuminance from the window on segment i (E_i) can be calculated as the sum of E_{di} and E_{si}.

To deal with the exchange of the light flux by multiple reflections between the small segments of the room interior surfaces, form factors are calculated for the whole segments. The form factors are then used in radiosity method in determining the internally reflected components of the daylight and the total daylight illuminance on the segments. In the final step, the configuration factors between points on the work plane and the segments are determined and used to calculate the workplane daylight illuminance.

2.3 Determination of Total Energy Consumption

The objective of this step is to find the amount of energy consumed by the double-section slat window system that leads the sun of lighting and cooling energy under each condition of a combination of glazing type and slat angle. The set of lamp in the partially daylighted zone were operated so that the level of illuminance at the inner boundary of the zone always attains at a value 300, 500 and 800 lux. To determine the energy consumption of the air conditioner, it was assumed that the air-conditioner operated from 7:00 to 18:00 of each day. Air conditioning load was also assumed just from heat gain of double-section slat window and from electrical lighting system by using the coefficient of performance (COP) of the air-conditioning to be 2.7. Therefore, the total energy is calculated from Equation 25.

$$\text{Total energy} = \text{electrical lighting energy} + \frac{\text{electrical lighting energy} + heat\ gain\ through\ window}{COP}$$

$$(25)$$

CHAPTER 3

METHODOLOGY

Developing a suitable mathematical model for daylight application and heat transferring of the double-section slat window system in the tropical country condition was investigated in this research. The methodology to perform the objectives completely were divided into two schemes: experimental and simulation studies. The measured results from the full-scale physical experiment are compared to the results from the simulated software. The validated model is used to estimate the energy saving potential of the system. The working procedure is illustrated by the chart in Figure 3.1.
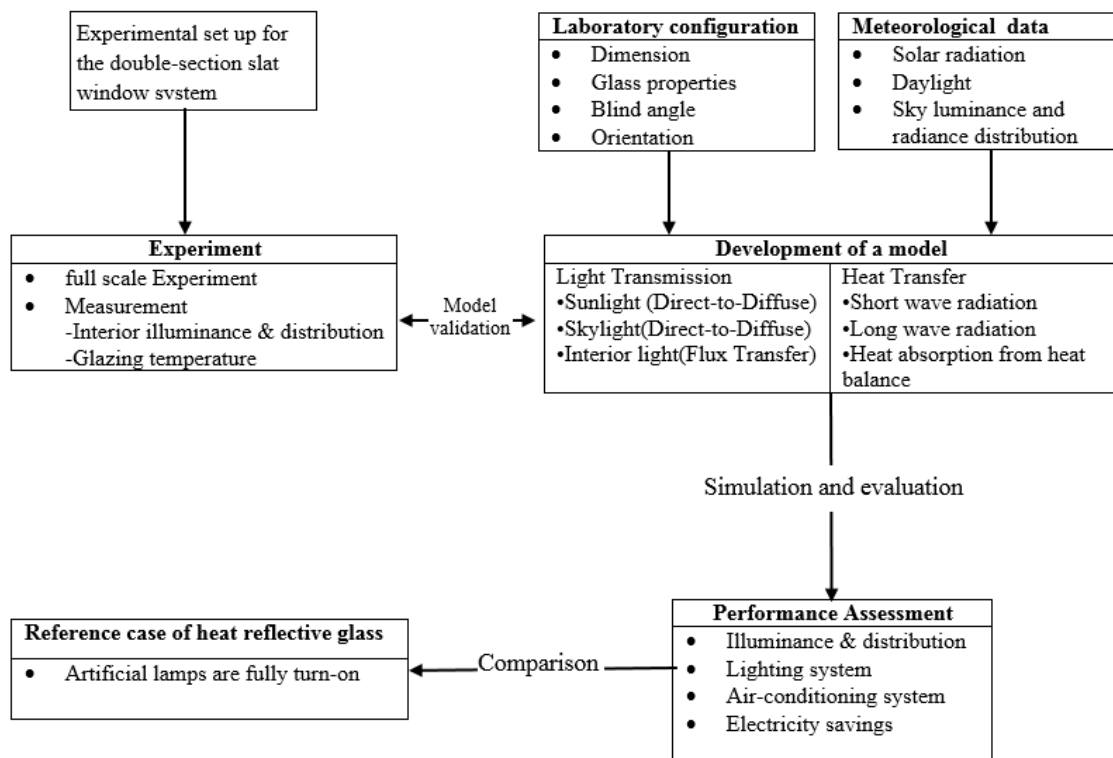

Figure 3.1 Proposed methodology for the research study

3.1 Development of mathematical model

In this research, there are two mathematical models to be developed; daylight transmission solar radiation gain through double-section slat window. The knowledge from the literature review is used in the calculation. The first algorithm is the calculation of the interior illuminance from daylight flux transmitted through the double-section slat window. The principals of the model are:

- to identify the daylight distribution in the daylit space
- to account for the penetration of beam light to the interior of the space

The second is the calculation of the solar radiation gain through the double-section slat window. This algorithm was developed together with the first one and the purposes of the model are:

- to determine the temperature of the exterior and interior glass panes and blind slats
- to calculate heat transfer across the double-section slat window

The model algorithms are coded using Visual Basic language for a program. In the model calculation, the solar irradiance and daylight illuminance at the location, temperatures of ambient air temperature and the air in the daylit space are required.

3.2 Experimental Study

The experiment was conducted at the full scale outdoor laboratory building. The room was located at Bang Khun Tien campus of King Mongkut's University of Technology, Thonburi (latitude 13.57°N and longitude 100.44°E).. The double-section slat window system was set up at the South window of the building. To evaluate light gain and heat gain, a data acquisition system was installed to measure daylight illuminance in the experimental room. The daylight illuminance on the outmost surface of the double-section slat window and temperatures of the window panes and the slat were measured .The exterior daylight illuminances were measured and recorded by a meteorological station. The experimental facilities, equipment and measurements are described below.

3.2.1 The experimental room

The experimental room was a 3.0 m. by 3.0 m. room with a 2.65 m. height. The room had a 6 mm. green glass window on the south wall. The window was 2.8 m. wide by 1.5 m.

high and its sill was 0.85 m. above the floor. The interior wall surfaces were painted white with a reflectance value of 0.73. The surface reflectance of the ceiling and floor was measured at 0.73 and 0.43, respectively. A fan coil unit was installed for the room air-conditioning. To validate the model, the measured values from experiments will be compared with the simulated results from the program. For of the interior illuminance, the comparison will be made at three points located on a line perpendicular to the window wall across the center of the room on the work plane level (0.75 m above floor). the illuminance sensor (EKO: model ML-020S-O) were positioned along the line at 10%D, 50%D, and 90%D depths of the room (D) as shown in Figure 3.2. Platinum RTD (Pt100) sensors were used to measure the surface temperatures of the glass panes and a slat, and the temperature of the room air. A data logging system was used to acquire all measured data from the sensors every 5 min.The measured illuminance on the external surface of the exterior glass pane of the double-section slat window was compared with the calculation. Temperature profiles of each component in the double-section slat window between the measurement and calculation were compared to validate heat transfer calculation.
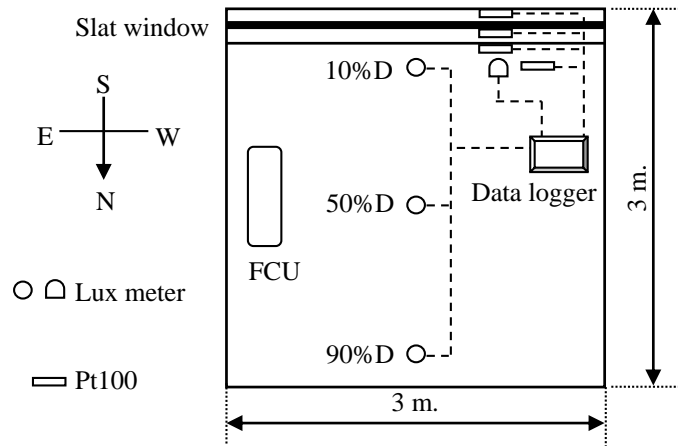

Figure 3.2 The experimental setup

3.2.2 The slat window

The slat window used in the experiments was formed by mounting a set of venetian blinds behind the existed green glass and then affixing with another set of the same glass. Figure 3.3(a) shows the outside environmental of the experimental room where the slat window faced to the South orientation. Figure 3.3 (b) shows the slat blind has two sections where each section can alter the slat blind to different tilted angles. The measured distance

between the two glass panes was 10 cm. The blind slats were 5.0 cm wide and white-painted aluminum. The distance between two adjacent slats was 4.2 cm. The optical properties of the glass and the slats are summarized in Table 1.

(a) South window of the experimental room (b) Installation of a double-section slat in the

testing room

Figure 3.3 Configuration of a laboratory building at

KMUTT, Bang Khun Tien campus

Table 3.1 Optical properties of the glass and the shading slats of the slat window

Description		Green glass	Slat
Solar range	Transmittance	0.44	-
	Reflectance	0.05	0.68
	Absorptance	0.51	0.31
Visible range	Transmittance	0.74	-
	Reflectance	0.06	0.77
Infrared range	Emittance	0.84	0.65

3.2.3 The meteorological station

During the experiments, the exterior solar radiations and daylight illuminances include the global, diffuse horizontal and beam normal components on four cardinal orientations (North, East, South and West) were measured by The meteorological station where is set up on the roof deck of the building at the School of Bioresources and Technology in the university campus.

3.3 Simulation Study

The developed calculation algorithm was used to determine the daylight transmission and heat transfer to the double glazed windows with internal slat. The results from the developed calculation model were validated to the experimental measurements. The validated calculation model was used to simulate the annual interior daylight from the window and to forecast the electrical energy consumption of a dimmable lighting system and air-conditioning system.

CHAPTER 4

RESULTS AND DISCUSSION

4.1 Experimentation, Results and Discussions

The series of experiment were conducted to measure interior daylight illuminance on the work planes and temperature of glass surfaces and slat of two-section blind window in the experiment room. Measurement results from the experiment were compared to those obtain from the computer program by using Visual Basic 6. The experiments were performed for the -30°, 0°, and 30° slat angles.

4.1.1 Upper slat angle at 0° , Lower slat angle at 0°

The experiment of two section slat at upper slat angle 0° and lower slat angle 0° was performed on 13rdJanuary 2015 as shown in Figure 4.1.
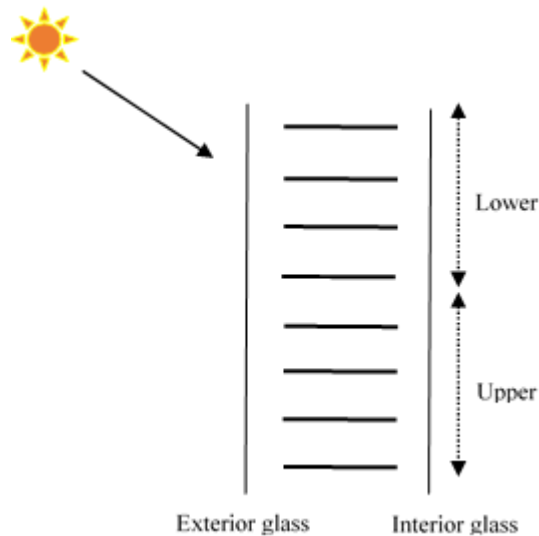

Figure 4.1 Experimental set up of upper slat at 0 degree and lower slat at 0 degree

Figure 4.2 exhibits a plot of exterior global (Evg) and diffuse horizontal illuminance (Evd) on the experiment day. Variation of sky ratio, the ratio of the diffuse to global irradiance, was also presented in the plot. On this day, the sky was partly cloudy and overcast sky in 6am-12pm as the sky ratio was in range 0.9-1, the value of global and diffuse illuminance are nearly the same. But in the noon, the sky was clear, observing from value of

sky ratio varied in the range of 0.2-0.3 and global illuminance was appeared again and its peak reached 83 klux at the noon.
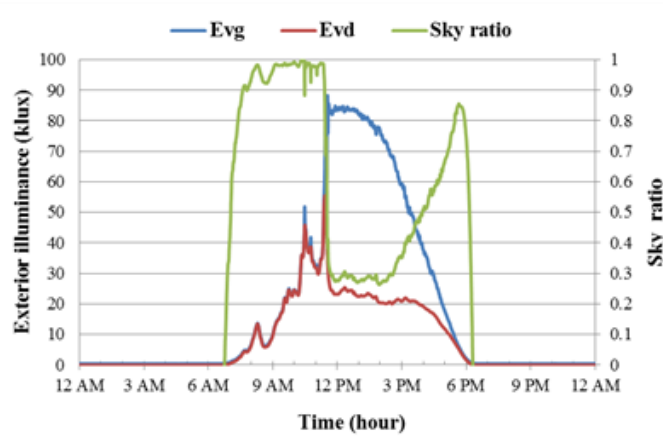

Figure 4.2 Variation of global and diffuse horizontal illuminance and sky ratio on 13/1/2015

Figure 4.3 exhibits the results of the measurements of interior daylight at 10%, 50% and 90% depth of the room (D). The corresponding illuminance obtained from the simulation was also presented in the same plot for comparison. It can be observed that the work plane daylight illuminance had the similar trend to the global illuminance (Evg) in Figure 4.2. The illuminance on work plane at 10%D increased from morning and high up to 2700 lux during noon and drop rapidly to about 1500 lux and 700 lux at 50%D and 90%D, respectively. Overall, the plots show that the calculated values from the model well agree with the measurement.
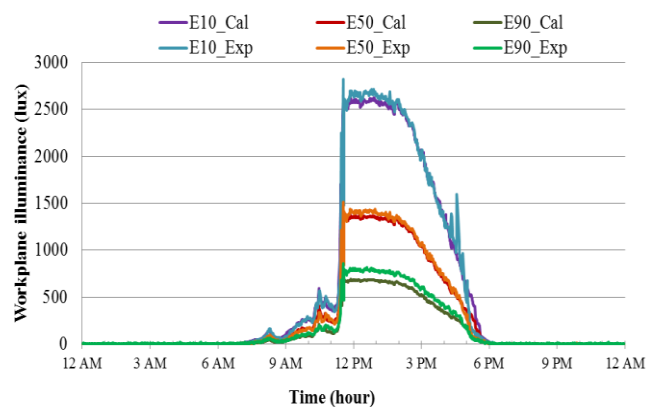

Figure 4.3 Comparison between the measurement of interior daylight illuminance at 10%%, 50% and 90% depth of the room and its corresponding results from simulation on 13/1/2015

Figure 4.4 (a) shows the global (E_{eg}) and the diffuse (E_{ed}) solar radiations on the date of the experiment. Temperature of the ambient air ($T_{\_amb}$) is also shown in the plot. The maximum value of the global radiation was about 800W/m^2 at noon time. Figure 4.4 (b) shows the incident solar radiation on the outer glass pane from the measurement. As the sun stays in front of the window, the incident radiation was high up to 600 W/m^2. In the figure, the corresponding values of the incident radiation from the calculation using the radiation data together with the ASRC-CIE sky model were compared. A good agreement can be observed from the plot.
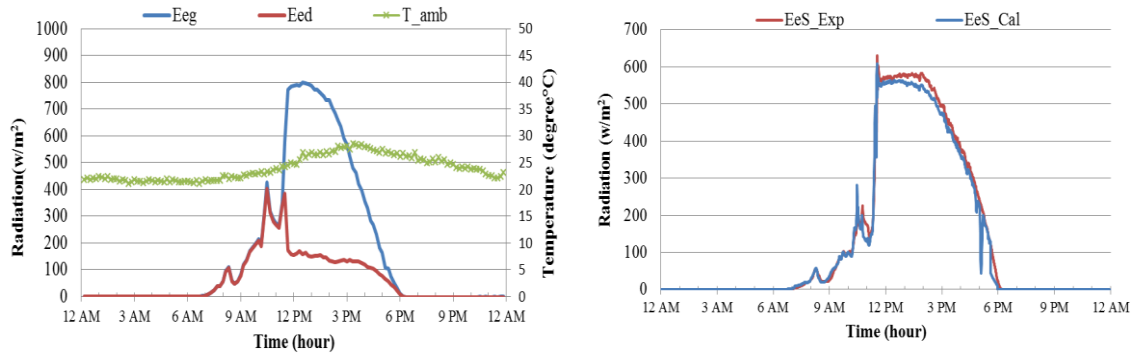
(a) Solar radiation and ambient air temperature (b) Incident and transmitted solar radiation

Figure 4.4 Measurement of solar radiation on 13/1/2015

For the two section slat, the measurement was divided into upper and lower section. The temperature of the outer glass, slat, and inner glass from the measurement and from the calculations are compared in Fig. 4.5 (a), (b), (c), (d), (e) and (f). Again, the plots show that the calculated values from the model well agree with the measurement.

Figure 4.5 (a) and (b), the temperature of the exterior glass (upper and lower) were rising up from 12pm and highest due to incident solar radiation. At the afternoon, the exterior glass temperature slowly decreased and its temperature was closed to the ambient air temperature during the night.

Figure 4.5 (c) and (d) exhibits the good agreement between temperature of upper and lower slat surface from the measurement and calculated values from the model. The temperature of slat have the identical trend with the exterior glass but slightly higher than the exterior glass.
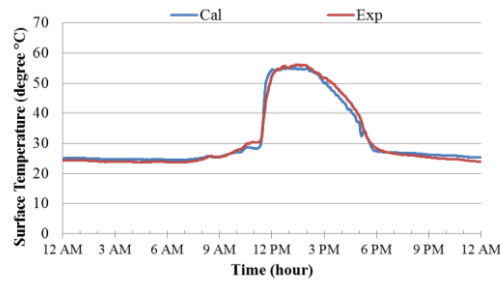
Figure 4.5 (e) and (f) shows the simulation can perform well prediction of the interior glass (upper and lower) temperatures.
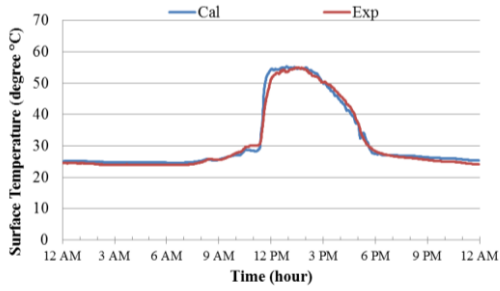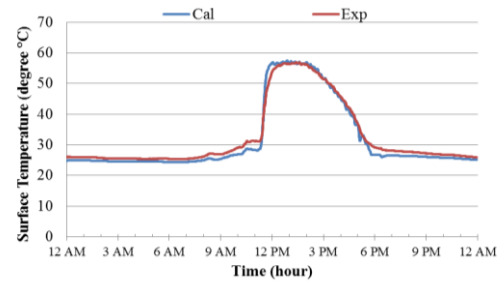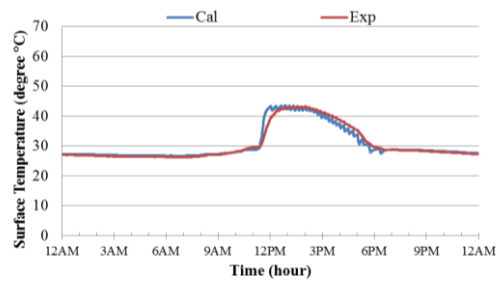
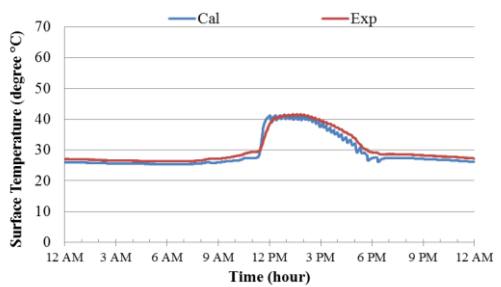a) Temperature of upper exterior glass   b) Temperature of lower exterior glass
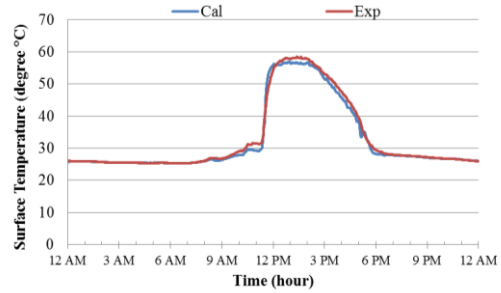
c) Temperature of upper slat   d) Temperature of lower slat

e) Temperature of upper interior glass   f) Temperature of lower interior glass

Figure 4.5 Comparison between temperature measurement and its corresponding results from simulation on 13/1/2015 (continued)

Figure 4.6 shows the resulting heat transfer through the slat window calculated from the model. Both upper and lower slat were set at the same angle therefore heat transfer through window were the same as shown in Figure 4.6(a) and (b). The maximum heat transfer through window was about 180 w/m^2 during the noon. The heat transfer due to the solar radiation is also shown in the plot, the maximum value was high up to about45 w/m^2 at noon.

.
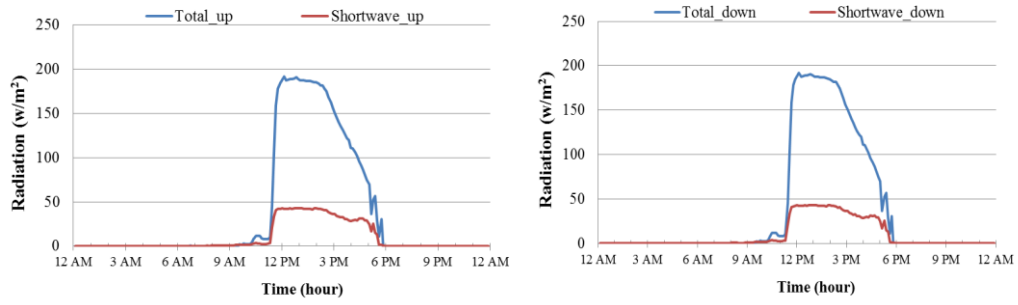
a) upper slat window   b) lower slat window

Figure 4.6 Heat transfer through window on 13/1/2015

4.1.2 Upper slat angle at -30° , Lower slat angle at 30°

On this experiment day, the upper slat was set up at the tilt angle -30° and the lower slat was set at the tilt angle 30° as shown in Figure 4.7
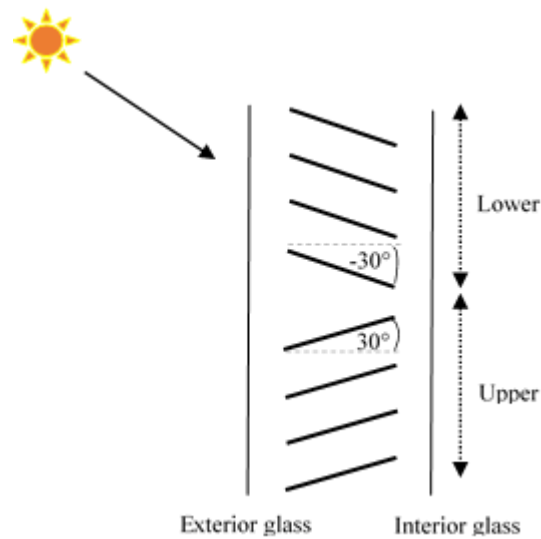
Figure 4.7 Experimental set up of upper slat at -30 degree and lower slat at 30 degree

Figure 4.8 show the variation of global and diffuse horizontal illuminance on 5th February2015. From the plot, value of the sky ratio varied between 0.2-0.4 during 10 am – 3pm. The sky was rather clear on the experiment day except in the early morning and the late noon. The global illuminance was about 87 klux and diffuse illuminance was 23klux at the noon time.
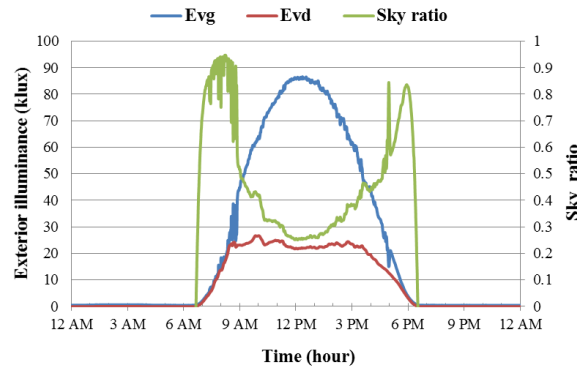
Figure 4.8 Variation of global and diffuse horizontal illuminance and sky ratio on 5/2/2015

Figure 4.9 exhibits the measurements of interior daylight that well agree with the simulation. From the plot, the illuminance on the work plane at 10% D was peak up to 1800lux at noon, and drop rapidly to about 1300 lux and 750 lux at 50% D and 90% D, respectively. Considering at the noon time, the values of interior illuminance on work plane at 10% D and 50% D, were lower than the previous case even though The amount of exterior illuminance (Figure 4.7) at the noon time was quite the higher than the previous case. This is because the lower slat was blocked the daylight to penetrate into the work plane more than the previous case (lower slat tilts at 0°) even though the upper slat opened to see the sky more than the previous case, but at 90% D, the value of the interior illuminance, instead of decreasing as 10%and 50% but its value was quite similar to the previous case. This is because the upper slat had effected to the interior daylight illuminance in the deeper position, it allowed daylight to penetrate more than the previous case (upper slat tilts at 0°).
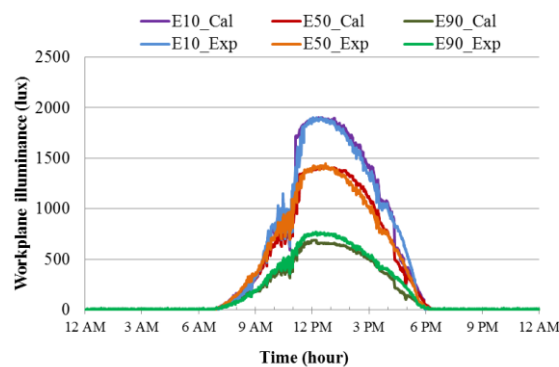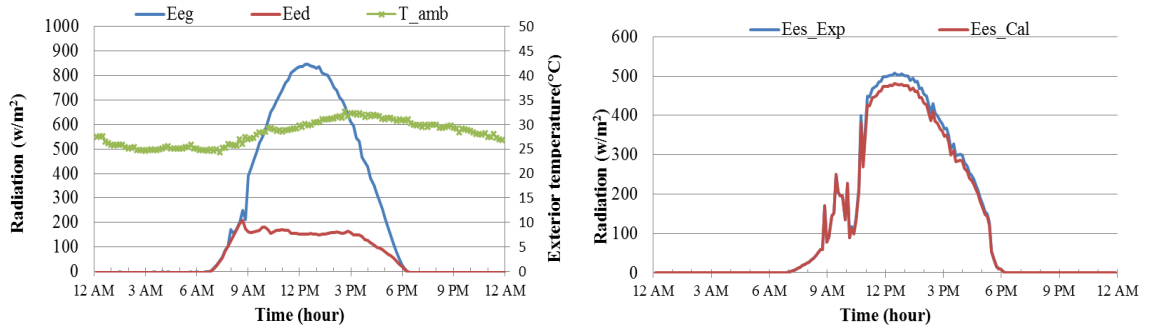

Figure 4.9 Comparison between the measurement of interior daylight illuminance at 10%, 50% and 90% depth of the room and its corresponding results from simulation on 5/2/2015

Figure 4.10 (a) shows the global (E_{eg}) and the diffuse (E_{ed}) solar radiations on the date of experiment. Temperature of the ambient ($T_{\_amb}$) air is also shown in the plot. The maximum value of the global radiation was about 840 W/m^2 at noon time which is higher than the previous case. Figure 4.10 (b) shows the incident solar radiation on the outer glass pane from the measurement. As the sun stays in front of the window, the incident radiation was high up to 500 W/m^2.

(a) Solar radiation and ambient air temperature   (b) Incident and transmitted solar radiation

Figure 4.10 Measurement of solar radiation on 5/2/2015

The comparison between temperature measurement and simulation is shown in Figure 4.11 Similar to Figure 4.5.Figure 4.11(a) and (b) temperatures varied closely with the incident radiation of the outer glass. Figure 4.11(c), (d), (e) and (f) noticed that the temperature profile of lower slat (d) was a bit less than upper slat (c) and the temperature profile of lower interior glass (f) was a bit less than upper interior glass (e). This is because the lower slat angle (30°) tilts more closed, while upper slat angle (-30°) tilts are more opened to receive daylight and radiation. As the upper slat angle allowed the incident radiation falling rather than the lower slat, therefore the temperature of the upper slat and the upper interior glass were higher than the lower parts.
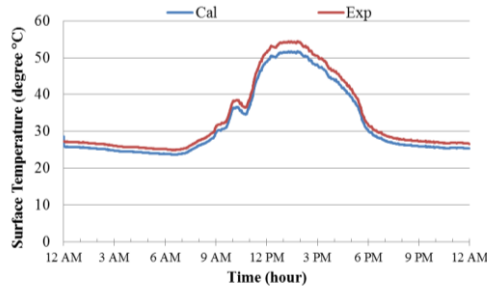
a) Temperature of upper exterior glass
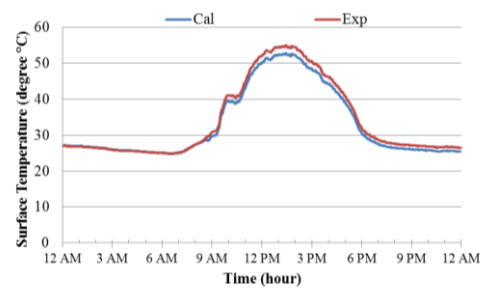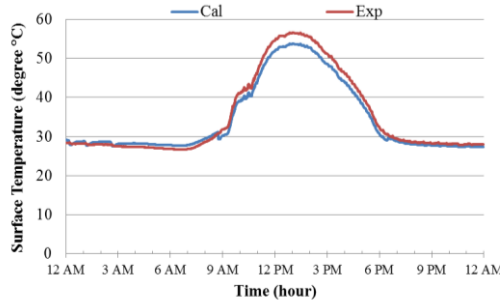
b) Temperature of lower exterior glass

c) Temperature of upper slat
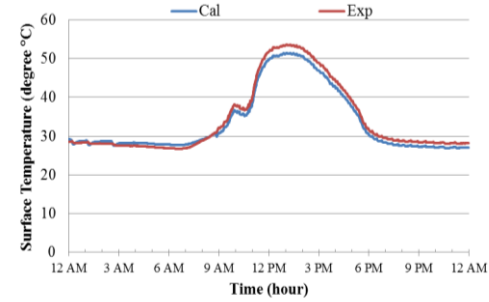
d) Temperature of lower slat
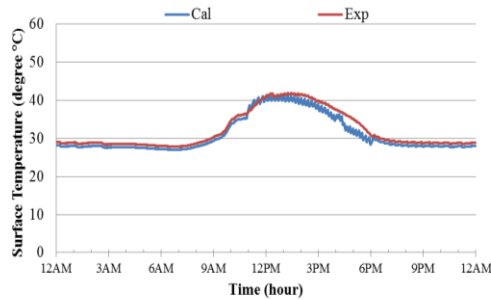
e) Temperature of upper interior glass
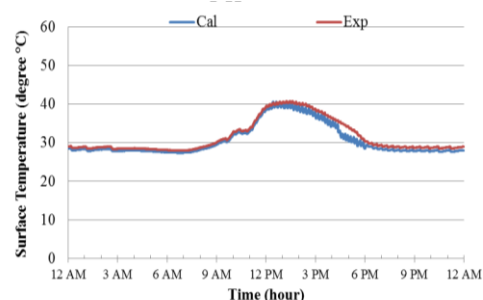
f) Temperature of lower interior glass

Figure 4.11 Comparison between temperature measurements and its corresponding results from simulation on 5/2/2015

The total heat transfer through window from calculation of the upper slat window was high up to $165w/m^2$ and heat transfer from solar radiation was 36 w/m^2 during the noon while total heat transfer through window of the lower slat window was about $145w/m^2$ and heat The heat transfer due to solar radiation was 22 w/m^2 approximately as shown in Figure 4.12 (a) and (b). Values of heat transfer from upper slat window was higher than lower slat window because the angle of upper slat was tilted in negative position as daylight and heat can enter through window more than the positive degree angle of lower slat which prevent

daylight and heat gain through window. Due to incident solar radiation was less than the previous case (Figure 4.6), therefore the amount of heat gain through window on this day was lower.
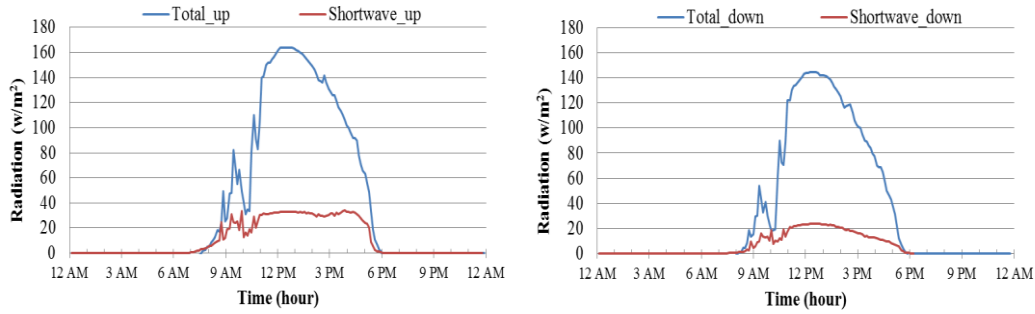
a) Upper slat window   b) Lower slat window

Figure 4.12 Heat transfer through window on 13/1/2015

4.1.3 Upper slat angle at 0°, Lower slat at 30°

The experiment of two section slats at upper slat angle 0° and lower slat angle 30° was performed on 8th February 2015 as shown in Figure 4.13.

Figure 4.13 Experimental set up of upper slat at 0 degree and lower slat at 30 degree

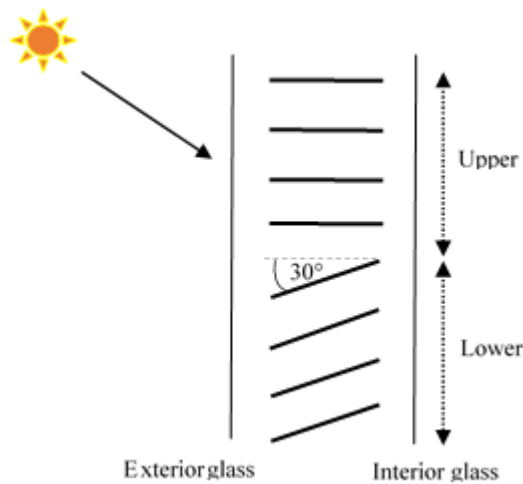Figure 4.14 shows a plot of variations of exterior global (E_{vg}) and diffuse horizontal illuminance (E_{vd}) on the experiment day. From the plot, global illuminance was varied smoothly and its peak reached 78 klux at the noon as same as the maximum diffuse

horizontal reached 40 klux at the noon. The climate on this experiment day was partly cloudy sky condition.
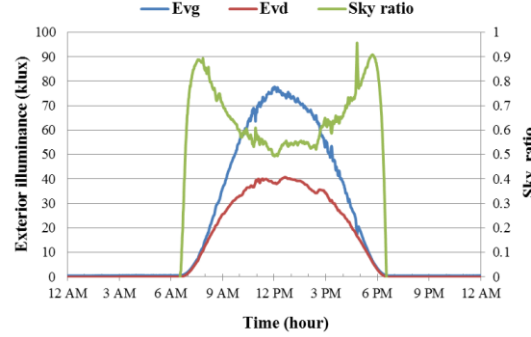
Figure4.14 Variation of global and diffuse horizontal illuminance and sky ratio on 8/2/2015

Figure 4.15 exhibits a plot of the measurements of interior daylight and from simulation. At 10%D, the interior illuminance on work plane was high up 1300 lux, 50%Dwas 900 lux and 90%D was 500lux at the peak, respectively. The interior illuminance on work plane were less than the experiment performed on two previous cases due to on this day had more cloudy and the slat angle prevented daylight transmission into the room more than two experiment cases above. Overall, the experiment and simulation results perform a good agreement.
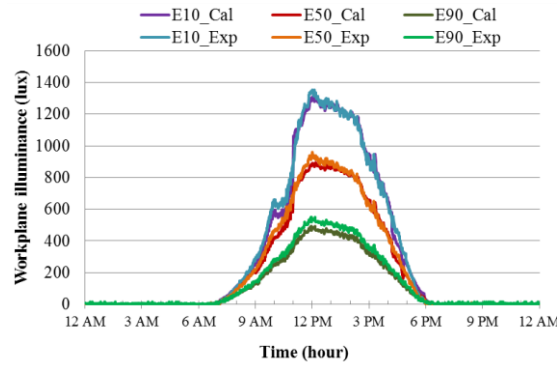
Figure 4.15 Comparison between the measurements of interior daylight illuminance at 10%, 50% and 90% depth of the room and its corresponding results from simulation on 8/2/2015

The global (E_{eg}) and the diffuse (E_{ed}) solar radiations on the experiment day is shown in Figure 4.16 (a). Temperature of the ambient air ($T_{\_amb}$) is also shown in the plot. The maximum value of the global radiation was about 750W/m^2 at noon time which is lower than

the two previous case. Figure 4.16 (b) shows the incident solar radiation on the outer glass pane from the measurement and simulation. The incident radiation was high up to 360 W/m^2 at noon and again, the plot show a good agreement between the simulation and the experiment.
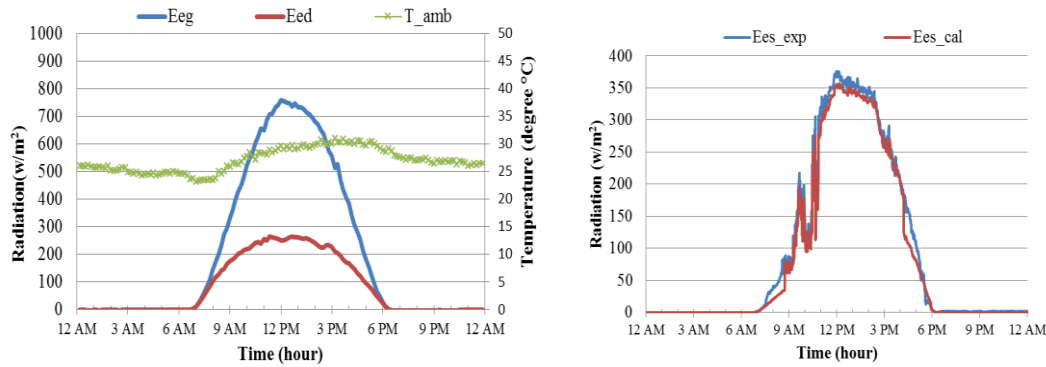
(a) Solar radiation and ambient air temperature   (b) Incident and transmitted solar radiation

Figure 4.16 Measurement of solar radiation on 8/2/2015

The comparison between temperature measurement and simulation is shown in Figure 4.17 Similarly to Figure 4.11, the temperature profile varied correspondingly to radiation falling on the glass surface.
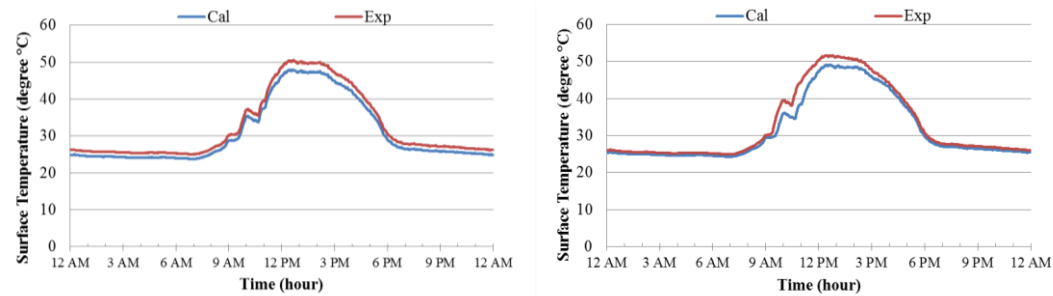
a) Temperature of upper exterior glass   b) Temperature of lower exterior glass

Figure 4.17 Comparison between temperature measurements and its corresponding results from simulation on 8/2/2015
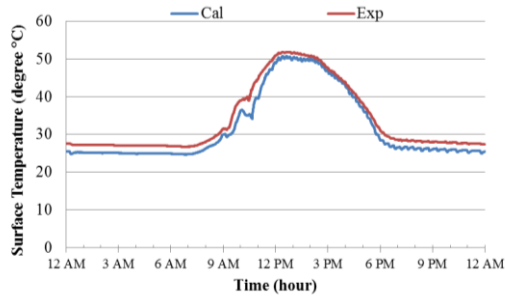
c) Temperature of upper slat
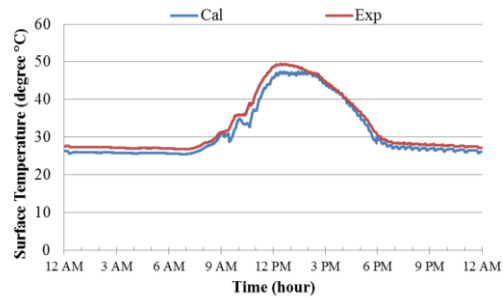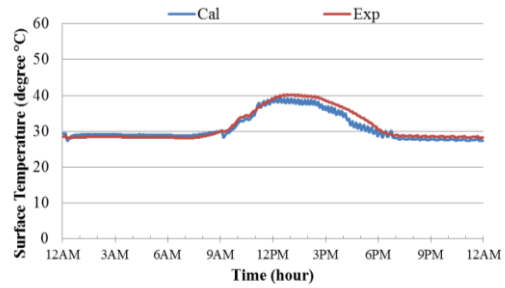
d) Temperature of lower slat

e) Temperature of upper interior glass
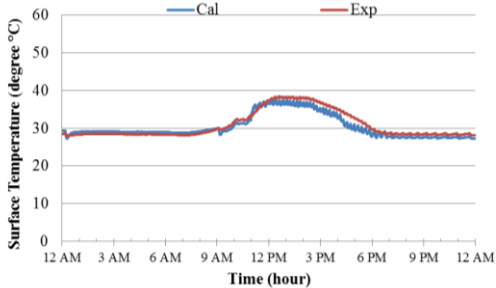
f) Temperature of lower interior glass

Figure 4.17 Comparison between temperature measurements and its corresponding results from simulation on 8/2/2015 (continued)

Figure 4.18 shows the amount of heat transfer through the slat window calculated from the model. In Figure 4.18(a), at the upper slat window, the maximum total heat transfer through window was high up to 120 w/m^2 during the noon. The heat transfer due to the solar radiation was high up 22 w/m^2 at noon. Figure 4.18(b) exhibits the calculated heat transfer of the lower slat window. At noon, the maximum total heat transfer through window was about100 w/m^{2}and heat transfer due to the solar radiation was high up 18 w/m^2. The lower slat provided amount of heat transfer through less than upper slat due to the tilt angle was set in the positive degree, radiation was prevent. Comparing heat transfer through the windows with the two previous case, this case had a lower amount of heat gained than others because the incident solar radiation was lower than others.

a) Upper slat window   b) lower slat window
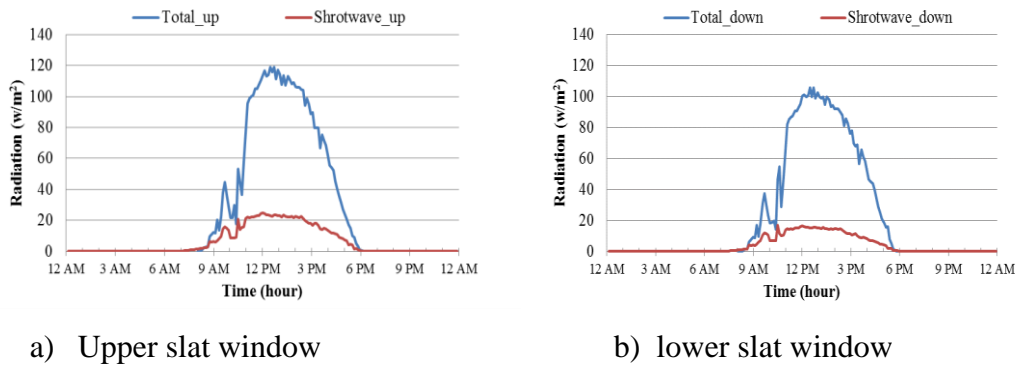
Figure 4.18 Heat transfer through window on 13/1/2015

4.2 Simulation-based analysis

After the calculation model was validated with the experiments, the calculation algorithm was used to simulate the interior daylight and heat transfer through the window from the two-section slat window facing south for a whole year. A completed one-year hourly record of the daylight measured in Thailand was used for the simulation. In the simulation, a model room was set similar to the test room (window to wall ratio =0.6) but its length was extended to 15 m allowing daylight to penetrate deep into the interior without the limit of room depth. A series of simulations was performed by varying the slat angle in upper and lower sections from -60° to 60° at 10° step size. The ratio of the upper and the lower slat sections is kept at 50:50. Calculation of electrical energy consumption are made on during typical office hours 8:00-17:00 for five days a week (Monday-Friday). The COP of system was assumed equal to 2.7. The design room of required illuminance levels at 300 lux, 500 lux and 800 lux are studied. A series of simulation results are shown in appendix

In the simulation results, the two selected months will be shown in here. As January is used to be a representative for the Sun stayed northern hemisphere and June for the Sun stayed southern hemisphere. The values of a window using heat reflective glass without slat was used as a reference case.

4.3 Daylight performance

Figure 4.19 exhibits characteristics of the interior daylight at different points inside the room. D/H values indicate the ratio of depth of the room measured from the window to height of the window. The labels in the plot refer to angles of the upper slats. The values in the horizontal axis are the ratio of depth of the room measured from the window to height of the window D/H of any fixed lower slat angle. At D/H=1(room depth is one time of the window height), the distance of work plane is nearest to window, D/H=9 (room depth is nine times of the window height) is the farthest distance of work plane from window. The slat angles of 60°,-40°,-20°, 0°, 20°, 40° and 60°were selected to show in the plot. In Figure.4.19 (a), the lower slat was fixed at -60° in January.

The plot shows that at any upper slat angle, daylight is entering exponentially as interior daylight illuminance at D/H=1 has the highest value and drops rapidly at D/H=3 to D/H=9, respectively. From the plot, when the upper slat tilts negative angle -10° to -60 °, the interior daylight illuminance on work plane at D/H=1 has higher value than interior daylight illuminance on work plane when the upper slat tilts positive angle 0° to 60 . The angle of upper slat at -40° gives the maximum interior daylight illuminance on work plane at 3500 lux approximately. This is because at this angle, daylight is allowed entering from sky the most. Interior illuminance at -60° degree angle has lower interior daylight illuminance value than -20° because it is almost set in the closed position while at -20° degree angle fully open to receive daylight. For the positive degree angle slat, when turns the angle from 0°, 20°, 40° to 60°, blind slat is performed to closed and closed, respectively. Therefore daylight is more prevented when the slat angle is set more positive degree, for this reason, the upper slat angle at 60° (almost closed) allows daylight penetrate the least, the minimum interior illuminance on work plane is at 1100 lux approximately. Comparing all the lower slat angles in January (on the left hand side) in Figure 4.19 (a), (c), (e), (g), (i), (k) and (m), the lower slat was varied at -60°,-40°,-20°, 0°, 20°, 40° and 60°, respectively. The plots show that at any upper slat angles, the lower slat at -20° gives the maximum interior daylight illuminance on the work plane. In June (on the right hand side), Figure 4.19 (b), (d), (f), (h), (j), (l) and (n) the interior daylight iluuminance on work plane has a similar characteristic as January, but the value of daylight entering is lower than January. This is because in June the sun stay behind the window (Northern hemisphere), the effect of interior daylight is due to diffuse

illuminance only, while in January, the sun stay low in front of the south window during the operate time therefore the daylight penetration is due to beam and diffuse illuminance.

Therefore, high daylight distribution occurs when both upper and lower slat angles are set in the range of negative degree. At upper slat -40° and lower slat -20° of any months, daylight can penetrate into a room the most. In January, the maximum average interior daylight illuminance value is about 5200 lux and in June is about 2500lux at D/H=1. The daylight has less potential in the area deeper than the position of D/H=7. At most of the slat positions, windows with slats provide better daylight performance than windows using heat reflective glass (HR).
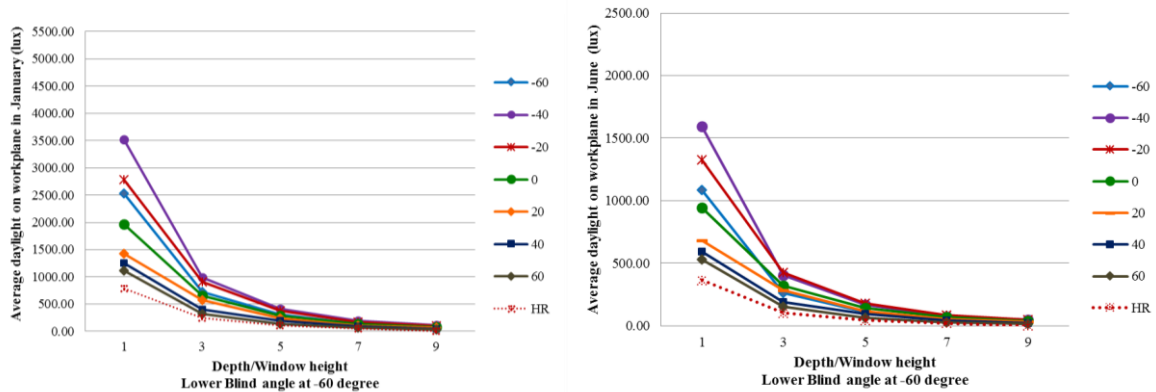
a) Lower slat angle at -60° in January   b) Lower slat angle at -60° in June
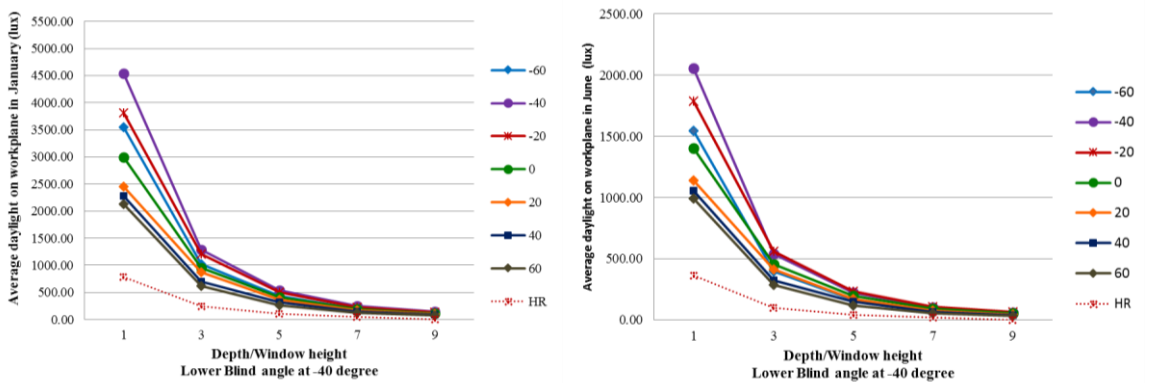
c) Lower slat angle at -40° in January   b) Lower slat angle at -40° in June

Figure 4.19 Interior daylight
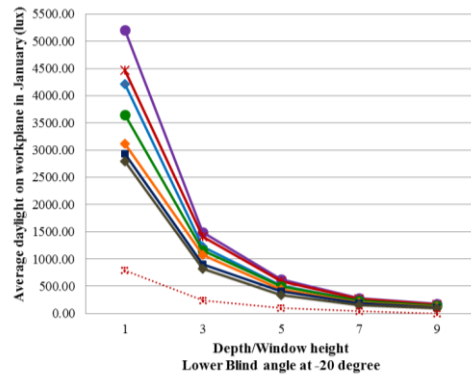
e) Lower slat angle at -20° in January
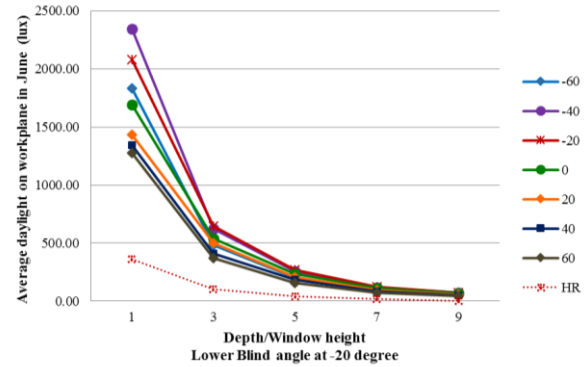
b) Lower slat angle at -20° in June
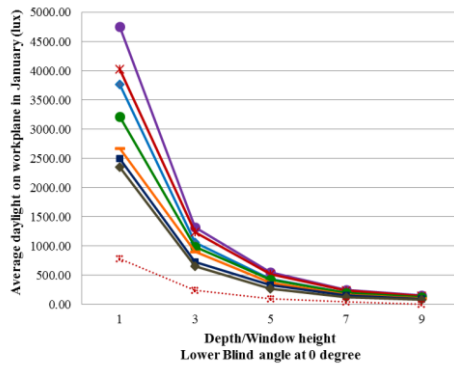
g) Lower slat angle at 0° in January
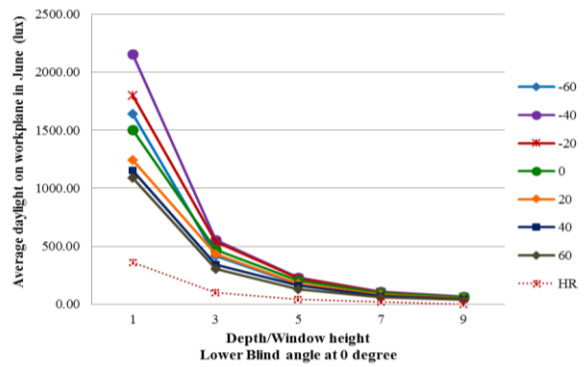
h) Lower slat angle at 0° in June
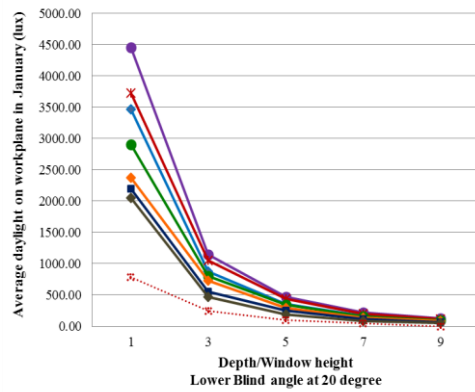
i) Lower slat angle at 20° in January
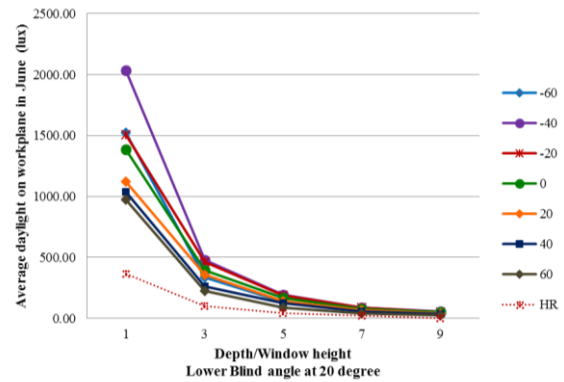
j) Lower slat angle at 20° in June

Figure 4.19 Interior daylight (continued)
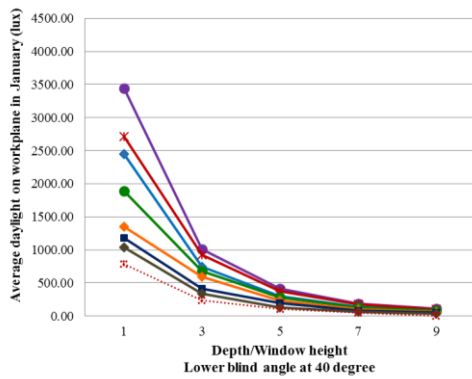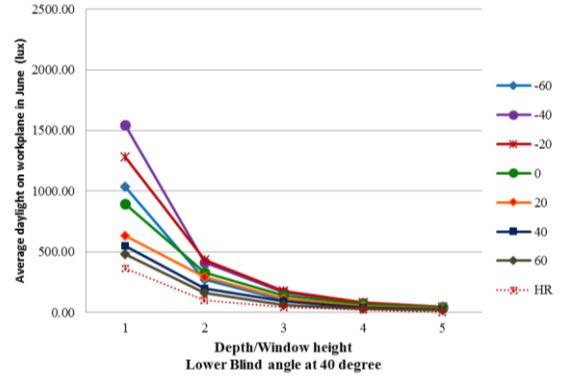
k) Lower slat angle at 40° in January　　　　l) Lower slat angle at 40° in June
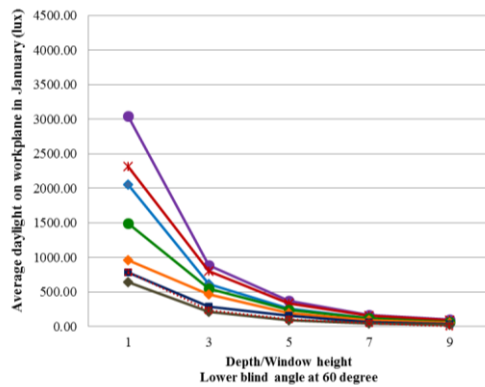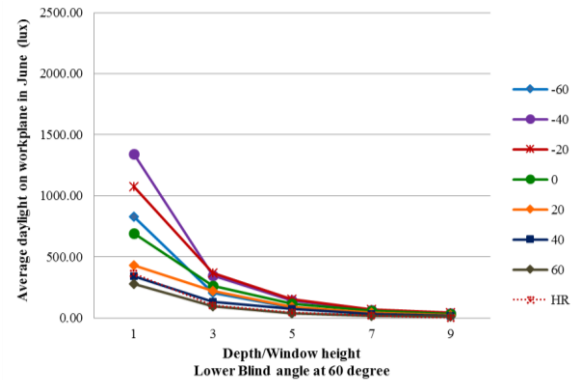
m) Lower slat angle at 60° in January　　　　n) Lower slat angle at 60° in June

Figure 4.19 Interior daylight (continued)

4.3.1 Average daylight illuminance of each room depth

Figure 4.20 (a) shows the average daylight of room depth of 3 m in January. The labels in the plot are referred to angles of the upper slats. The values in the horizontal axis are angles of the lower slats. One section slat blind (1SB) in the plot is the angle of the upper and lower slat tilts same angle. The values of 1SB are included in the plot for comparison. When lower slat angles are positive, most of the average daylight illuminance values of window with two-section slat blinds are higher than that with one-section slat while one section slat blind provide higher daylight illuminance values than two section slat blind when it was set in negative degree angles. The maximum average daylight illuminance value occurs when upper and lower blind of two-section slat window are set at -40 and -20 degree, respectively is about 5200lux. The maximum average daylight illuminance value of one section slat is at -30 degree about 3100 lux. Figure 4.20 (c), (e), (g), and (i) show the average daylight of room depth of 6 m, 9 m, 12 m and 15 m, respectively. The trends of average

daylight illuminance are the similarly to Figure 4.20 (a) but the value of average daylight is decreasing gradually by the depth of the room. As well as average interior daylight in June, the trend of average interior daylight in each room depth is the same with January but the value of average interior daylight comparing with its corresponding angle is less than January because of the sun position. At any room depth, window using heat reflective glass provides the minimum daylight illuminance to the room.
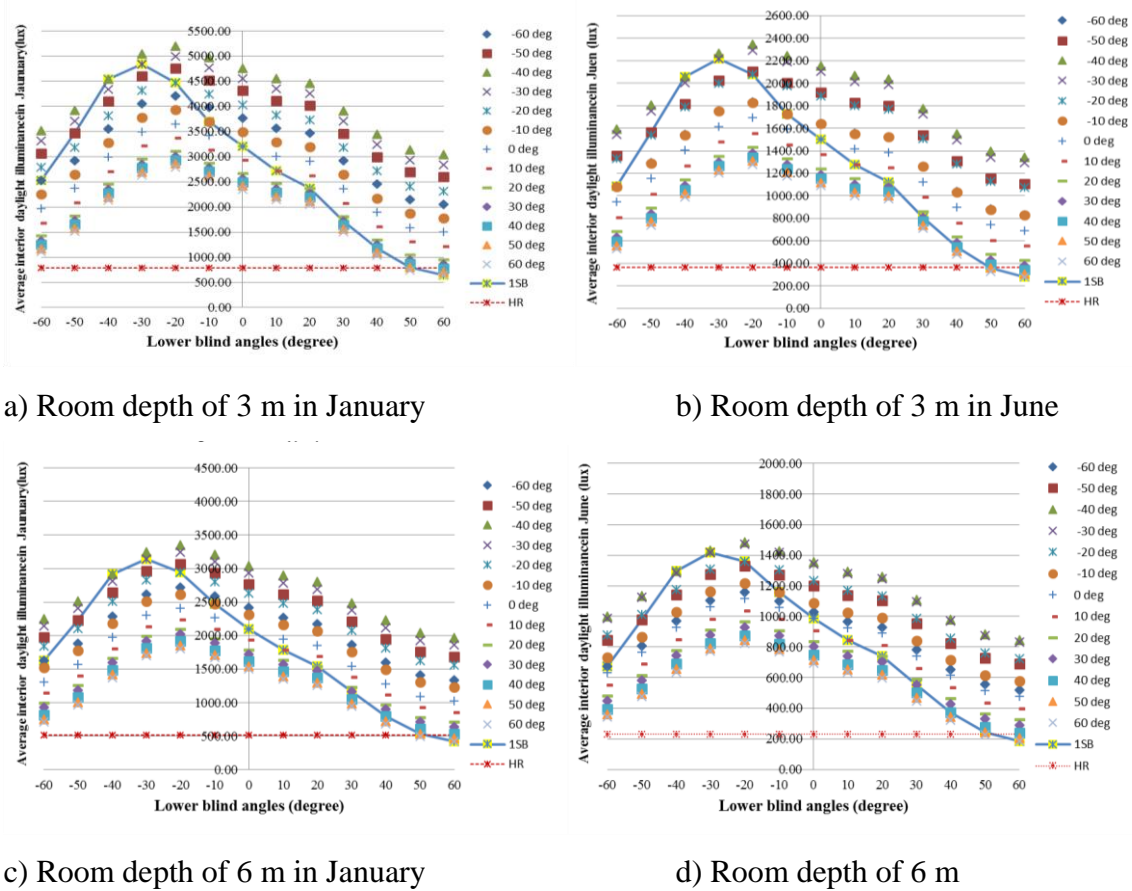
a) Room depth of 3 m in January

b) Room depth of 3 m in June

c) Room depth of 6 m in January

d) Room depth of 6 m

Figure 4.20 Average daylight illuminance at each room depth in January and June
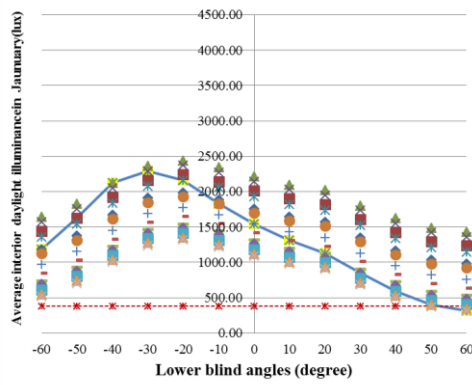
e) Room depth of 9 m in January　　　　　　f) Room depth of 9 m in June
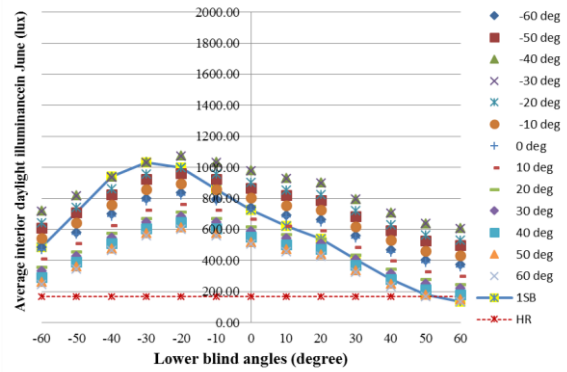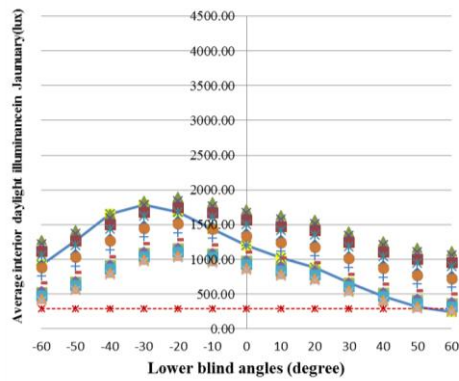
g) Room depth of 12 m in January　　　　　h) Room depth of 12 m in June
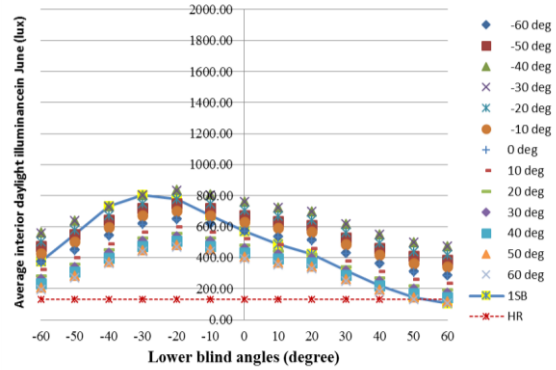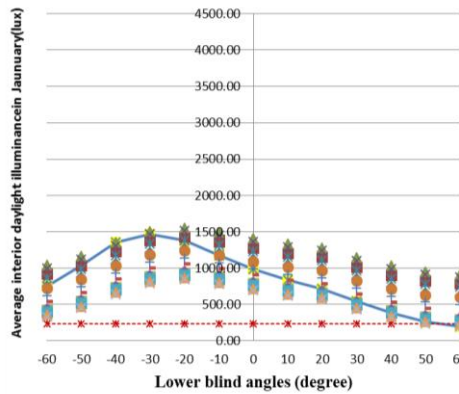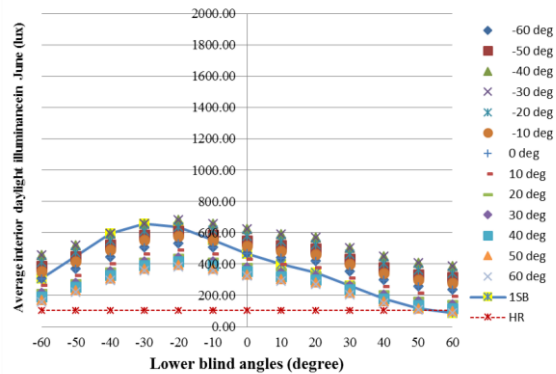
i) Room depth of 15 m in January　　　　　j) Room depth of 15 m in June

Figure 4.20 Average daylight illuminance at each room depth in January and June

(continued)

4.4 Light power density

The study assumes that ceiling-mounted luminaires are used to provide the uniform work plane illuminance at 0.75 m. above floor. Each luminaire is housed with two T8 fluorescent

lamps (36W each) and one electronic ballast (2W). Table 4.1 summarizes the specific information of the luminaires and its rated power calculated using the IESNA Lumen method. From the table, to meet the target illuminance at 800, 500 and 300 lux, the lighting power densities (*LPD*) are at 28.0, 17.5 and 10.5 W/m^2, respectively. For the base case, all the lamps were fully turned on during typical office hours 8:00-17:00 for five days a week (Monday-Friday)

Table 4.1 The luminaire and lighting power density for interior lighting in the modeled room

| Light Luminaire				$E_w = (LLF)\ (CU)\ (L_f/P)\ (P/A)$
Number of lamp			2	
Number of ballast			1	where
Total light flux (lm)			5,360.0	E_w = Target workplane illuminance
Total power (W)			74.0	LLF = Light loss factor (assumed 0.8)
Efficacy (lm/W)			72.4	CU = Coefficient of Utilization
Workplane illuminance (lux)	800	500	300	(assumed 0.5)
				L_f/P = Efficacy
Light power density (W/m^2)	28.0	17.5	10.5	P/A = Light power density

With the daylighting, the dimming controller is used to regulate the light from electric lamps to supplement the daylight. The electric power is lowered linearly with the lighting reduction. However, the system still consumed electricity at 10% of its rated power even when the daylight alone could meet the target illumination level.

Figure 4.21 shows lighting power density required illuminance levels at 300 lux. The labels in the plot are referred to angles of the upper slats. The values in the horizontal axis are the ratio of depth of the room measured from the window to height of the window D/H of fixed lower slat angle. Figure 4.21 (a) exhibits fixed lower slat angle at -50° in January. The trend of *LPD* of each slat angle is increasing when the D/H increase (more depth of the room). *LPD* values are inversely to daylight performance and target illuminance. To reach required illuminance target, if daylight potential is less, the demand of lighting is more, *LPD* value increase. As daylight penetrate to the room exponentially, the daylight has less potential in the area deeper, therefore at D/H=9, *LPD* values of every slat angle are higher. From the plot shows the upper slat angle at 50° has the highest *LPD* value at 8.2 w/m^2, while

the upper slat angle at -30° has the lowest the LPD value at 6 w/m². Figure 4.21 (b) shows the LPD of fixed lower slat angle at -50° in June. The trend of LPD in this month is similar to January but the value of LPD is higher than in January because of the exterior condition. Observing that in January the angle of slat still has impact to LPD in the deeper area while in June every slat angle has similar value.

The results show that at higher required illuminance level in 500 lux as shown in Figure A.1 and 800 lux in shown in Figure A.2, the LPD requirement increases, respectively. However, the patterns of the LPD requirement at these three illuminance levels are similar because daylight potential is identical at the same outside conditions. As the consequence, the interior illuminance distributions of natural light are the same.

The results of annual average *LPD* at 300, 500 and 800 lux required illuminance levels are in the range of 1.8 to10, of 1.8 to 16 and 1.8 to 27 W/m², respectively. The average *LPD* values of window with heat reflective glass are 10.35, 16.79 and 27.66 W/m² for the cases of 300, 500 and 800 lux required illuminance levels, respectively

a) Lower slat angle at -50° in January

b) Lower slat angle at -60° in June

c) Lower slat angle at -30° in January

b) Lower slat angle at -30° in June
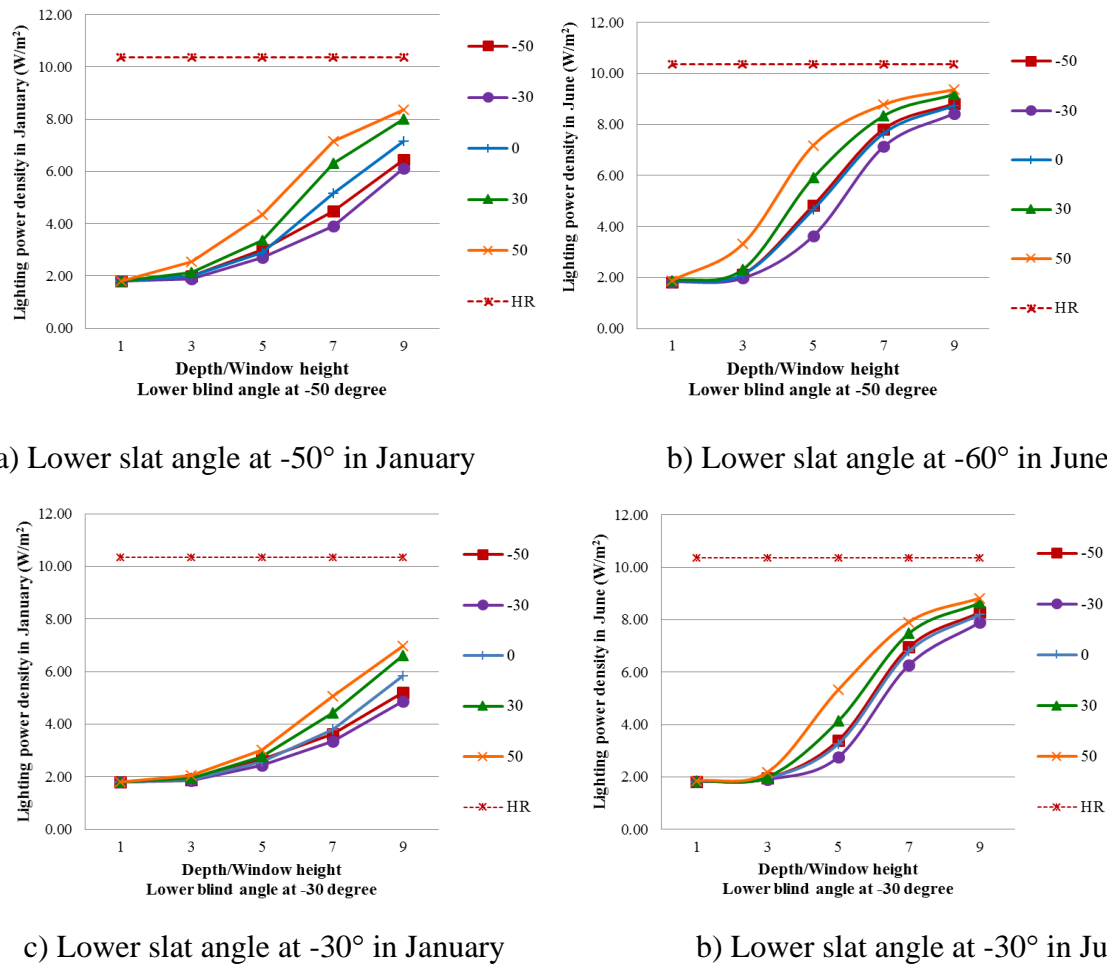
Figure 4.21 Characteristic of lighting power at 300 lux
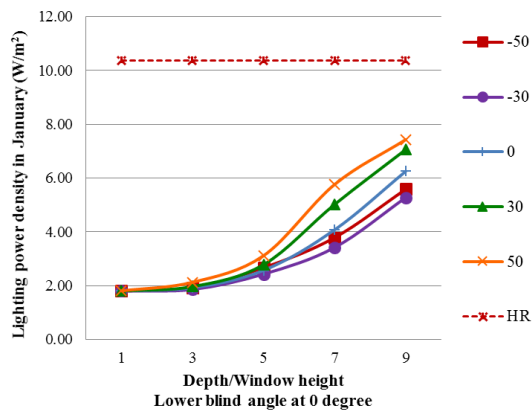
e) Lower slat angle at 0° in January
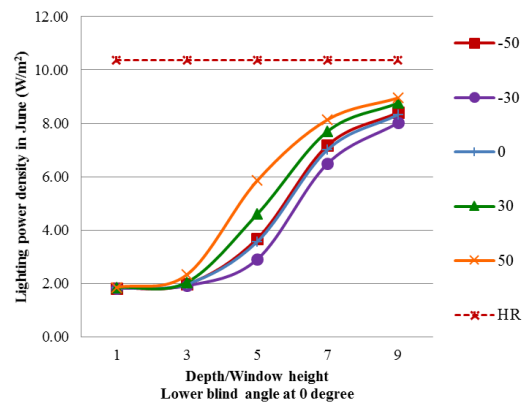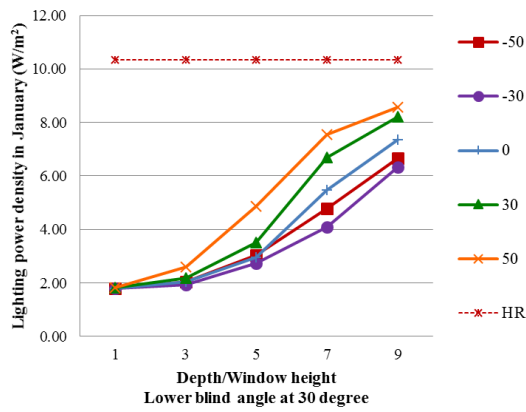
b) Lower slat angle at 0° in June

g) Lower slat angle at 30° in January
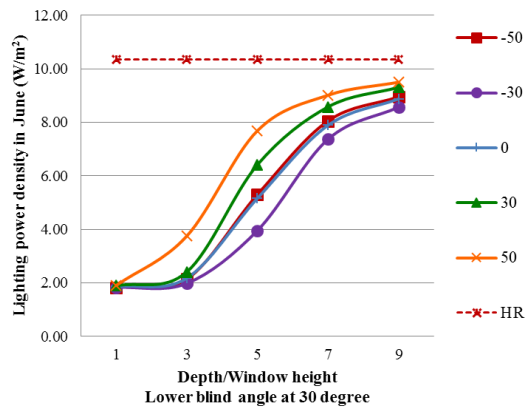
h) Lower slat angle at 0° in June
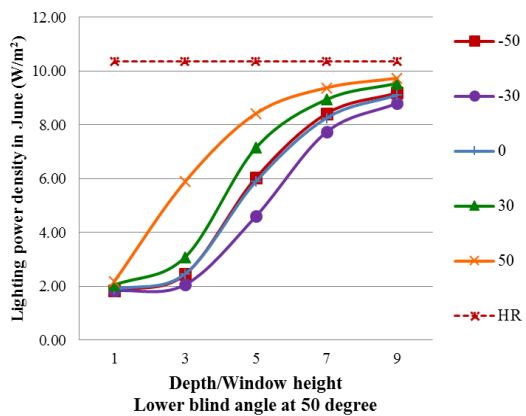
i) Lower slat angle at 50° in January
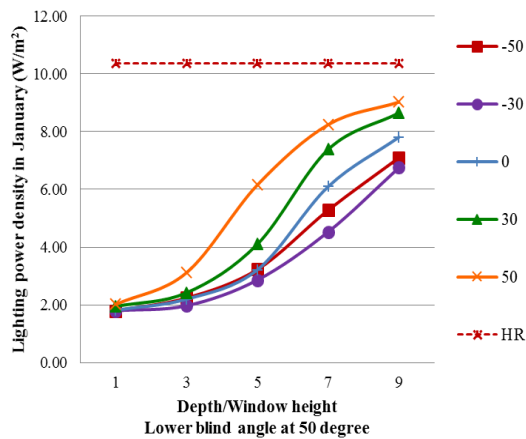
j) Lower slat angle at 50° in June

Figure 4.21 Characteristic of lighting power on work plane 300 lux (continued)

4.4.1 Average Lighting Power density

Figure 4.22 exhibits average light power density at 300 lux of each room depth in January and June. The average *LPD* values are low when the high daylight potential of upper slats and lower slats are set at negative angles in the range of -30 to -10. At room depth of 3m, almost upper and lower slat angles provide the similar average LPD values except for when set the slat angle at the closed position. This is because daylight cannot penetrate through window. From the plots, any target illuminace at room depth of 6m, 9m, 12m and15m in both January and June, upper and lower slat angle at -30° and -20°, respectively provides the minimum average LPD value. According to the same reason, one-section slat window at -20 degree provides the lowest *LPD* value at all illuminance level requirements. Heat reflective glass window always gives the maximum average LPD value of any illuminace requirement and room depths.

Average light power density of 500 and 800 lux are shown in Figures A.3 and A.4.
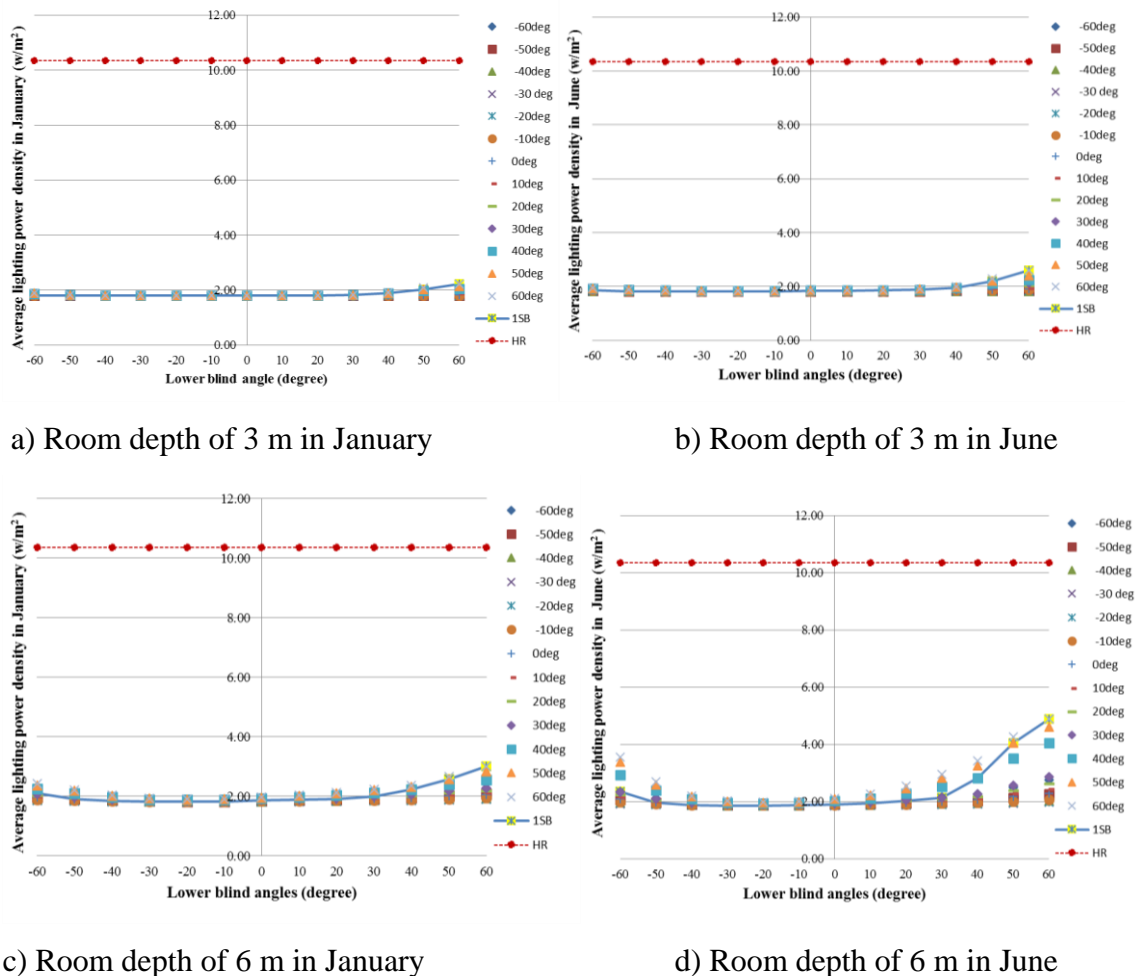
a) Room depth of 3 m in January   b) Room depth of 3 m in June

c) Room depth of 6 m in January   d) Room depth of 6 m in June

Figure 4.22 Average light power density of each room depth at 300 lux in January and June
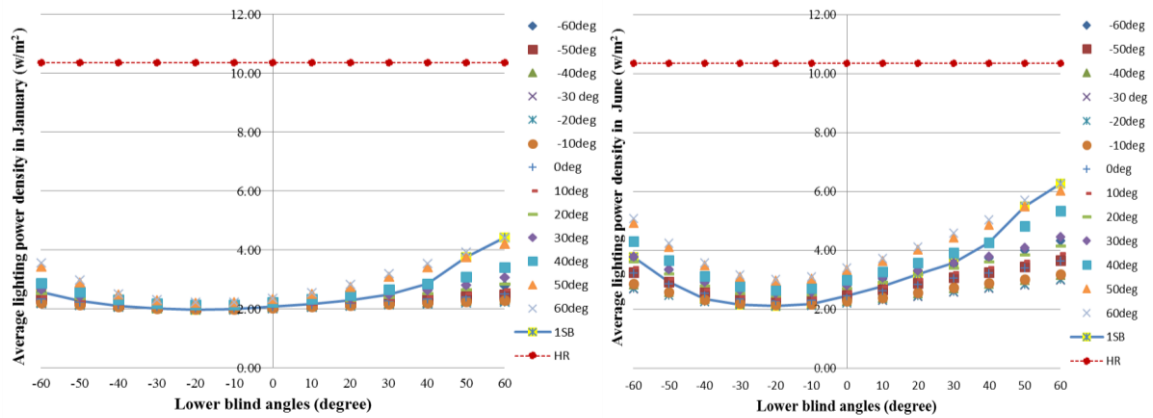
e) Room depth of 9 m in January   f) Room depth of 9 m in June
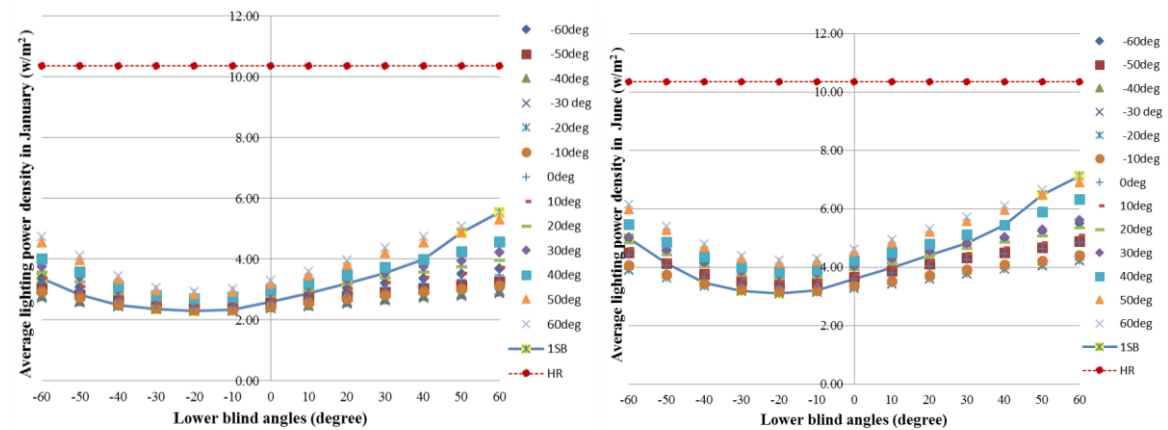
g) Room depth of 12 m in January   h) Room depth of 12 m in June

i) Room depth of 15m in January   j) Room depth of 15 m in June

Figure 4.22 Average light power density of each room depth at 300 lux in January and June (continued)

4.5 Heat Gain through window

Heat transfer through window depends on solar radiation transmission as shortwave radiation and air temperature difference as longwave radiation. When slat angles are negative, there are high chances that slats tilt parallel to beam solar radiation which enters the room. For this reason, the results of negative slat angles show higher heat gain through window as shown in Figure 4.23. At very high degrees of slat angles both in positive and negative directions such as -50, -60, 40,50, and 60 degree, heat gain through window reduces because the blind slats are almost closed and beam radiation cannot penetrate through gaps between blind slats.

When the sun passes through the northern hemisphere in June, at the south window, heat transfer through the window results from diffuse radiation and temperature difference only. Therefore heat gain through window is lesser than the months of sun toward southern hemisphere in January.

The combination of shortwave radiation and longwave radiation gives the maximum of the average heat gain through window in January is high up to 523.44 Watt when upper and lower slat tilts at -30°, while the average heat gain through window in January is high up to 245.74 Watt when upper and lower slat tilts at -20° as shown in Figure 4.23 (a) and (b), respectively. When both upper and lower slat angles are set in the close position slat at 60°, the minimum average heat gain through window occurs at 278.26 Watt in January and 131.82 Watt in June because solar radiation cannot penetrate through gaps between blind slats. The plot show two section the when lower slat angles are in the range of negative degree give the average heat gain through window lower than one section slat angle while in the positive degree angle, two section slat angles provide the average heat gain through window higher than one section slat angle.
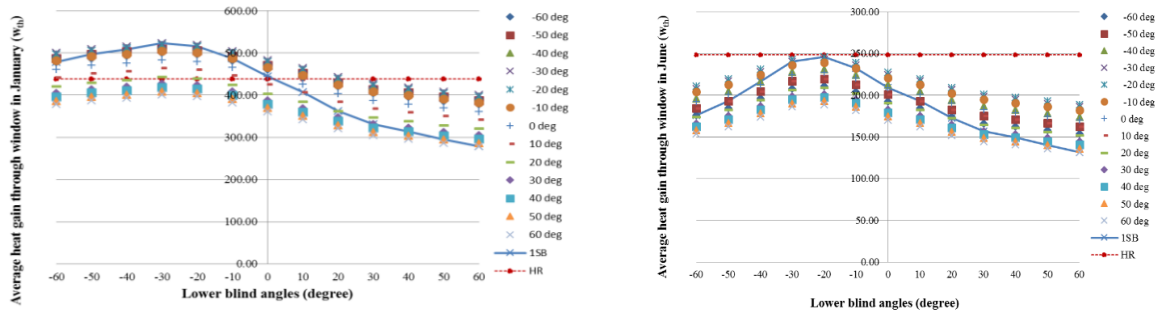
a) January   b) June

Figure4.23 Average heat gain through window in January and June

4.6 Lighting energy consumption

The electricity from lighting system depends on the *LPD* values as a consequence of daylight performance. Figure 4.24 exhibits average lighting energy consumption of each room depth at 300 lux. The trends of lighting energy consumption are identical with average *LPD* as mention previously in Figure 21.The upper slat and lower slat at -30 and -20 provide the minimum electricity from lighting of any room depth and illuminance requirements because this upper and lower slat angle allow maximum daylight to penetrate through window. The average lighting consumption increase as more room depth and more required illuminance level. However, average lighting consumption in June is higher than average lighting consumption in January because of the sun position. Using window with heat reflective glass always gives the highest lighting energy consumption in every room depth and every required illuminance level. For target illuminance at 500, and 800 lux, the average lighting energy consumption are shown in Figures A.5 and A.6, respectively.
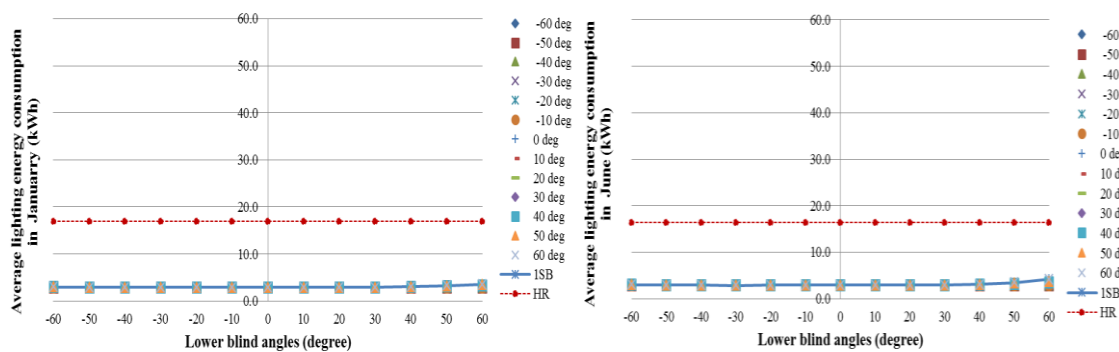
a) Room depth of 3m in January   b) Room depth of 3m in June

Figure 4.24 Average lighting energy consumption at 300 lux in January and June
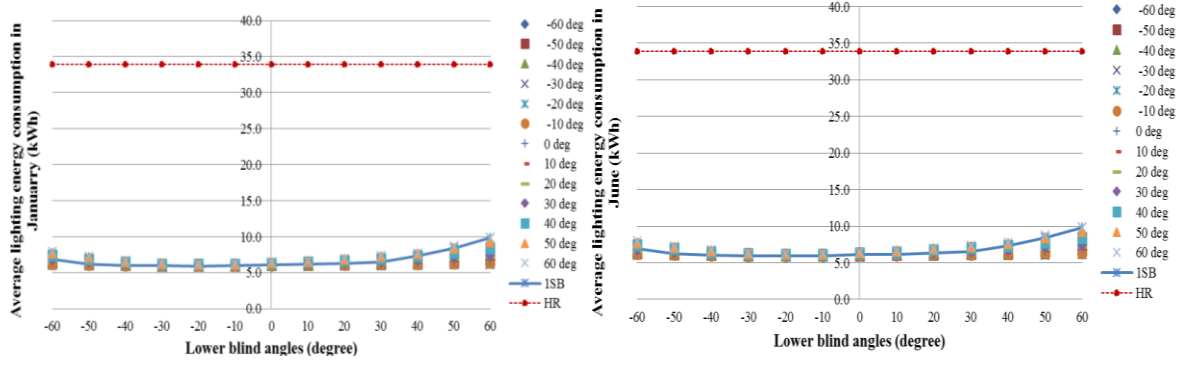
c) Room depth of 6m in January

d) Room depth of 6m in June

e) Room depth of 9 m in January

f) Room depth of 9 m in June

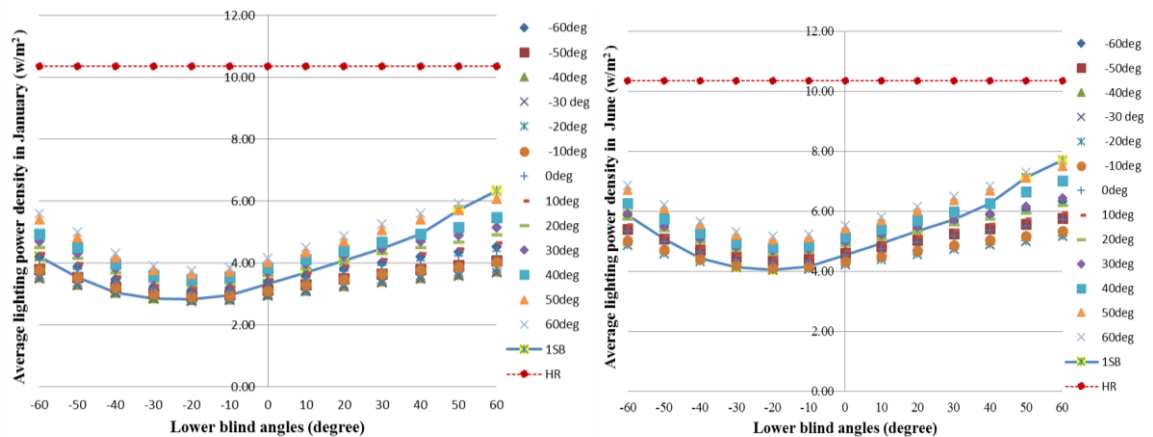g) Room depth of 12 m in January

h) Room depth of 12 m in June

Figure 4.24 Average lighting energy consumption at 300 lux in January and June

h) Room depth of 15 m in January   i) Room depth of 15 m in June

Figure 4.24 Average lighting energy consumption at 300 lux in January and June

(continued)

4.7 Air-conditioning energy consumption

The energy consumption of the air-conditioning system is an effect of cooling load due to lighting system and heat gained through the window. More room depth and illuminance level is required, more air-conditioning energy is used. The proportion of the heat gain from window and heat gain from lighting is varied according to the depth of the room and required illuminance level.

The study has found that the target illuminance of 300 lux in January of any room depth as shown in Figure 4.25 (a),(c),(e),(g) and (h) (on the right hand side), in this month, heat transfer through window is the primary effect to cooling load of air-conditioning system of room. The pattern of air-conditioning energy consumption in each angle is following the trend of heat transfer through window as shown in Figure 4.25 (a). Except for lower slat angles in the range of positive degree at 40°, 50°, 60° of room depth 9 m,12 m and 15 m and lower slat angles in the range of negative degree at -50°,and -60° of room depth 12m and 15m. Observing when the slat angle is set in the closed position, air-conditioning energy consumption is increasing although heat transfer through window is decreasing. This is the effect from the required higher lighting to reach target illuminance, more heat from lighting becomes cooling load of the air-conditioning system. At upper and lower slat angle at -30° and -20°, respectively provides the maximum air-conditioning energy consumption in every room depth.

In June, heat transfer through window is less than January significantly (half of January) but still affected cooling load of air-conditioning system of room depth of 3m and

6m as shown in Figure 4.25 (b) and (d).From the plot, the pattern of air-conditioning energy consumption still following the trend of heat transfer through window in Figure 4.25(b). At room depth of 6 m,9 m, 12 m and 15 m in June as shown in Figure 4.25 (d), (f), (h), and (j), the pattern of air-conditioning energy consumption is the combination between heat transfer through window and lighting. According to the same reason of January, when the slat angle is set in the closed position at -60°,-50°, -40°, 40°, 50° and 60° of lower slat angle, the pattern of air- conditioning energy consumption is increasing due to lighting.

Heat gained through the window is the main effect of air-conditioning energy consumption more than heat gain from lighting when the room depth is short, while heat gain from lighting has primary influence to air-conditioning energy consumption when more illuminance and more depth of the room are required. However, the proportion of air-conditioning energy consumption from heat gain through window and heat gain from lighting is depended on the depth of the room and required illuminance level. As required higher illuminance level 500 and 800 lux are shown in Figures A7 and A8, respectively.

As the reference case, window with heat reflective glass consume the maximum air-conditioning energy consumption compare to any case of window with slat angle except for the negative degree angle of room depth of 3m at required illuminance at 300lux in January as shown in Figure 4.25(a).
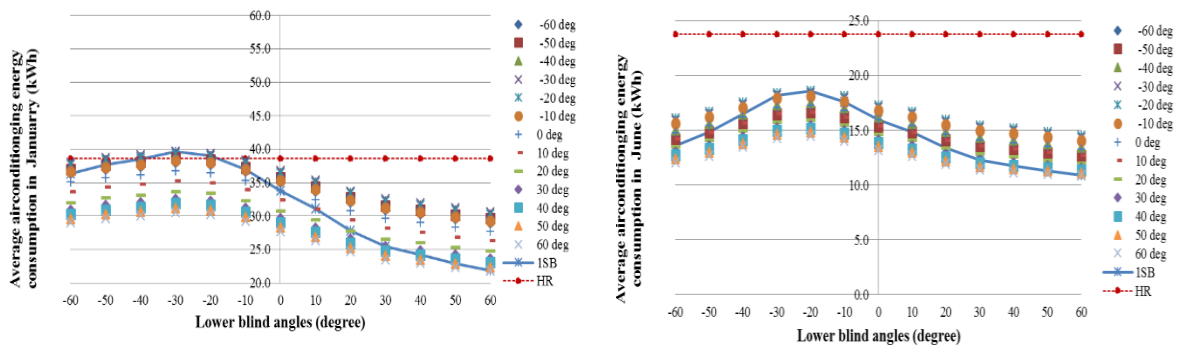
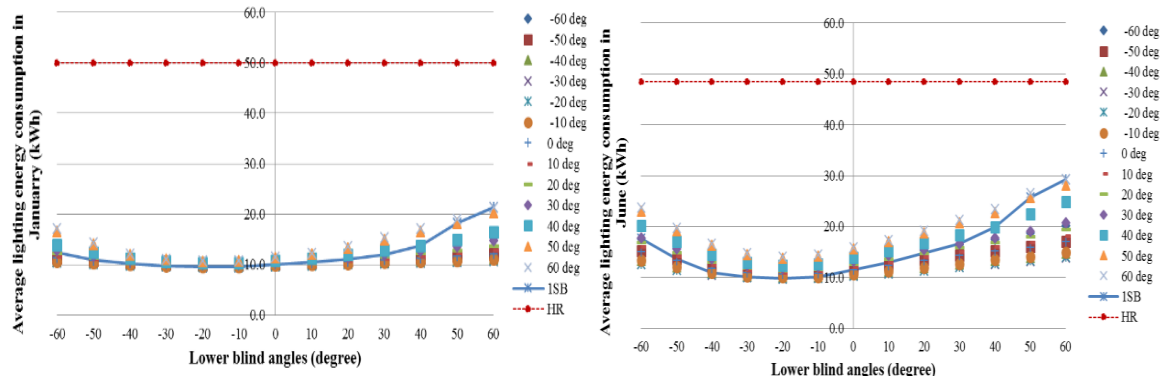a) Room depth of 3 m in January   b) Room depth of 3 m in June

Figure 4.25 Average air-conditioning energy consumption at 300 lux in January and June
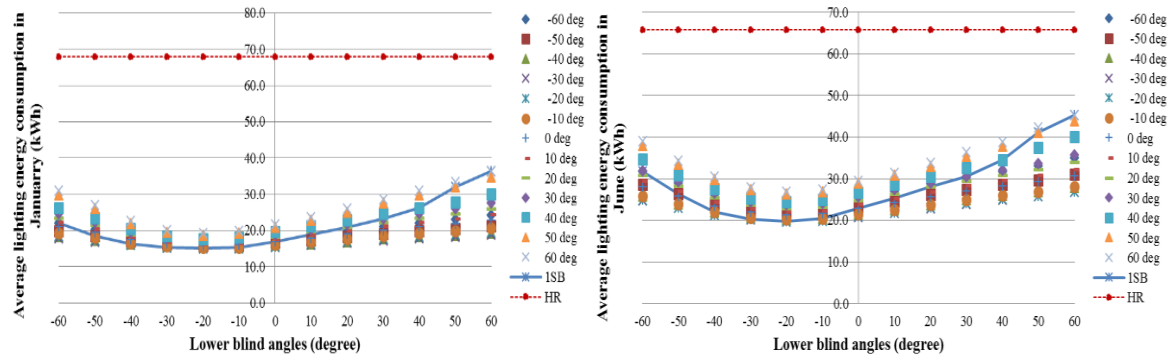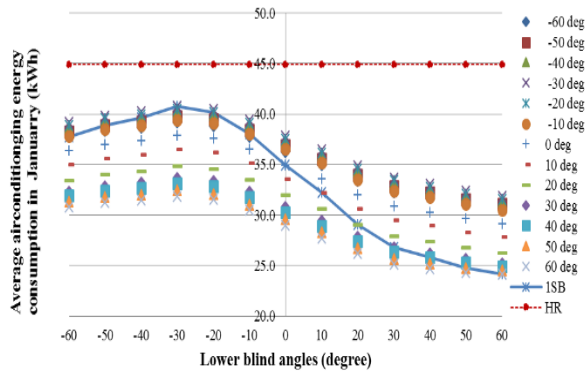
c) Room depth of 6 m in January

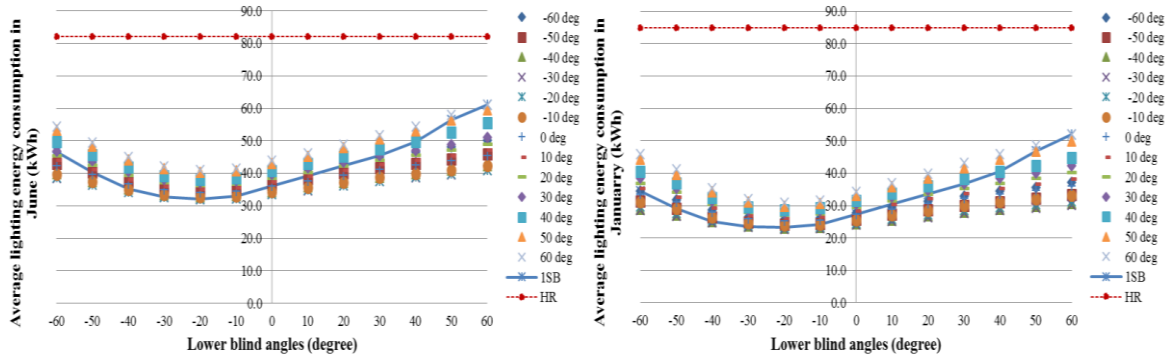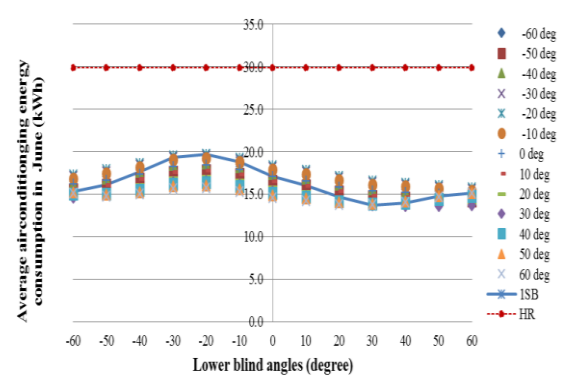d) Room depth of 6 m in June
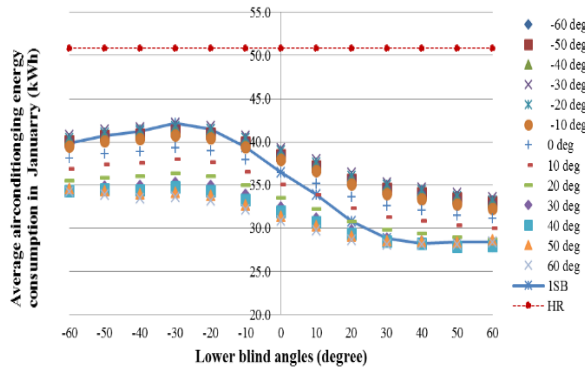
e) Room depth of 9 m in January
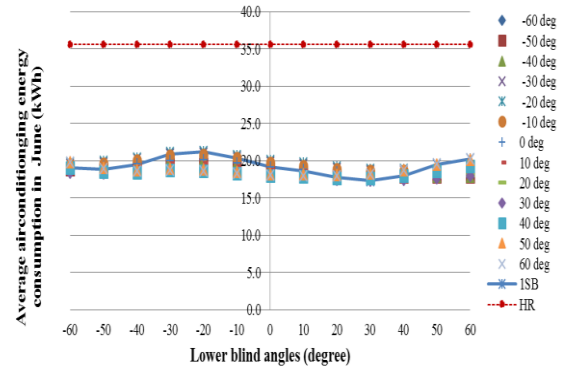
f) Room depth of 9 m in June
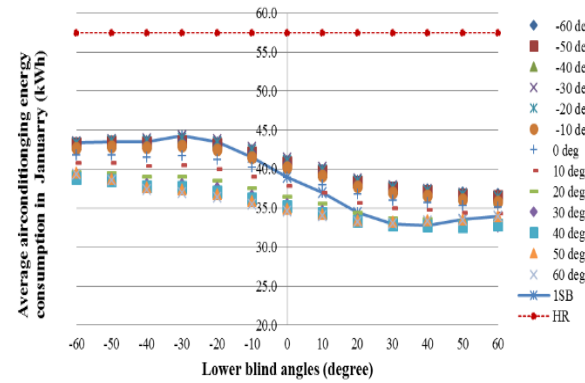
g) Room depth of 12 m in January
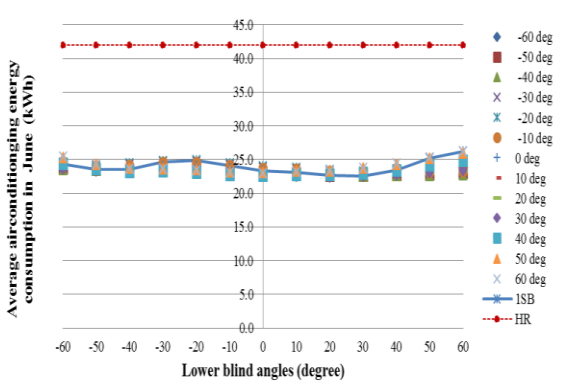
h) Room depth of 12 m in June

Figure 4.25 Average air-conditioning energy consumption at 300 lux in January and June

(continued)

h) Room depth of 15 m in January   i) Room depth of 15 m in June

Figure 4.25 Average air-conditioning energy consumption at 300 lux in January and June

(continued)

4.8 Total energy consumption

Total energy consumption is composed of electric energy from the dimmable lighting system and the room's air-conditioning system as mentioned previously. Therefore, daylight performance has the major effect on the total energy consumption because it influences both in lighting system and air-condition system.

Figure 4.26 exhibits average total energy consumption at 300 lux in January and June. In January, when the room is designed for low illuminance level as shown in Figure 4.26 (a), (c), (e), (g) and (h) (on the right hand side). High daylight level becomes excessive. From the plots, as room depth of 3 m and 6 m as shown in Figure 4.26 (a) and (c) show that heat gain through window play more important role to the total energy consumption. As a result, two-section slat windows with positive angles of the lower slat section provide lower energy consumption because less heat is gained through the window in these cases while their daylight performances are comparable. While room depth of 9m to15 m as shown in Figure 4.26 (e), (g) and (h), daylight began to influence energy consumption, the slat angles are opened to receive more daylight distribution although heat gain to window increase.

In June, heat gain through window still plays more important role to the total energy consumption of room depth of 3 m and 6 m as shown in Figure 4.26 (b) and (d). However, after room depth of 9 m to 15 m, more daylight is required. The lower slat angle is in the negative range of -30° to -10° consume less energy consumption than other angles as shown in Figure 4.26 (f) (h), and (i).

Figure A.9 exhibits average total energy consumption at 500 lux in January and June. Heat gain through window has an effect of room depth 3 m and 6 m in January and only room depth of 3 m in June as shown in Figure A.9 (a), (b), and (c). Besides others room depth, daylight performance plays more important role to the total energy consumption.

Figure A.10 exhibits average total energy consumption at 800 lux in January and June. The results of total energy consumption are similar to total energy consumption at 500 lux.

However, comparing any case of the window with slat to the window with heat reflective glass, the results show that using heat reflective glass window never consumes energy less than window with slat for all case.
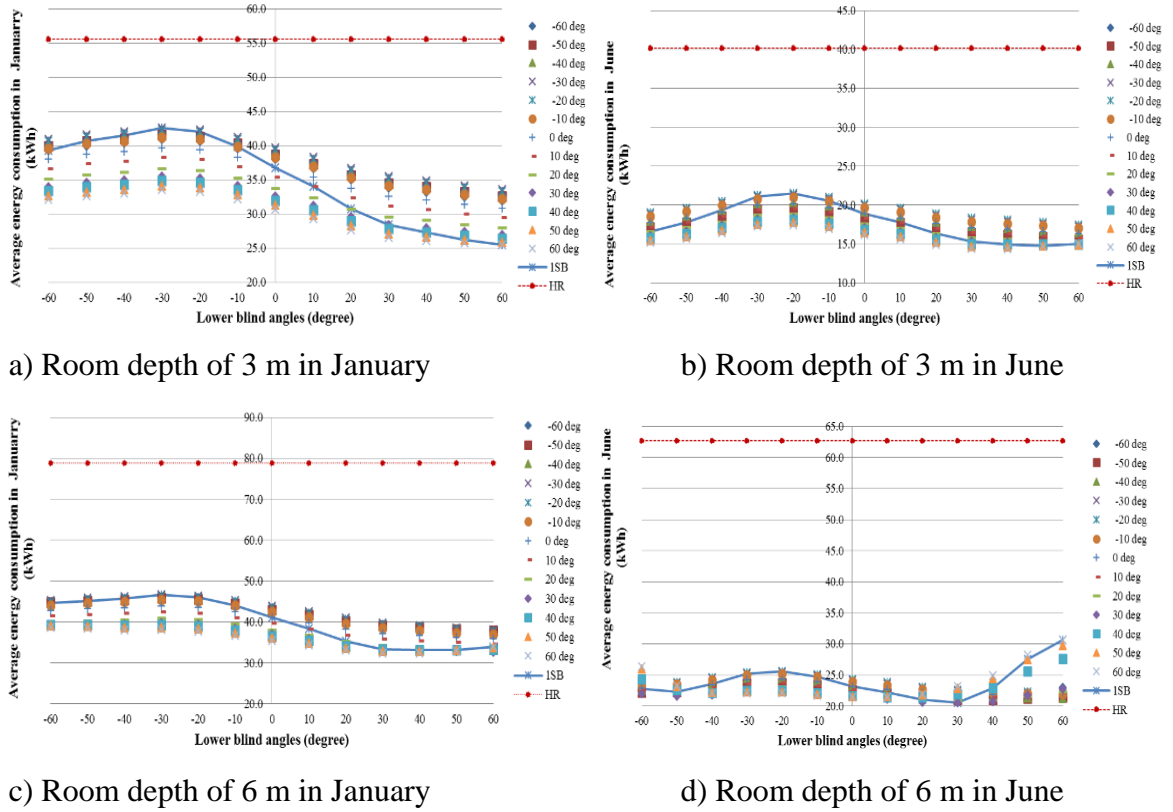
a) Room depth of 3 m in January   b) Room depth of 3 m in June

c) Room depth of 6 m in January   d) Room depth of 6 m in June

Figure 4.26 Average total energy consumption at 300 lux in January and June
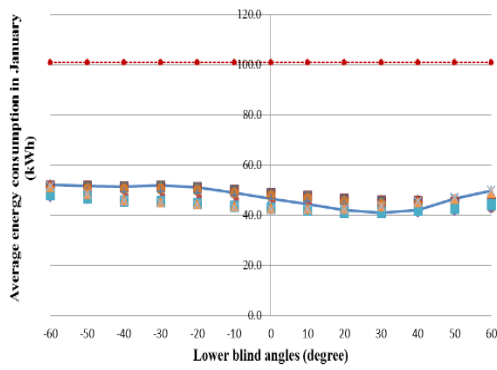
e) Room depth of 9 m in January   f) Room depth of 9 m in June
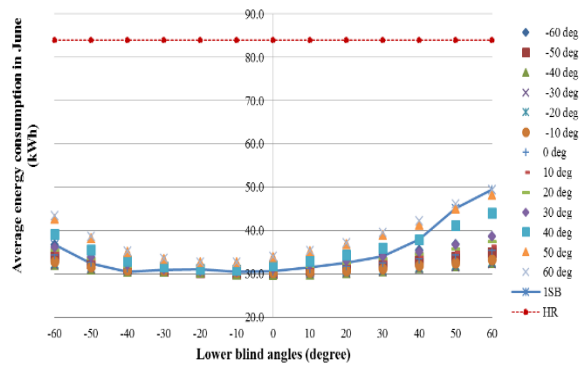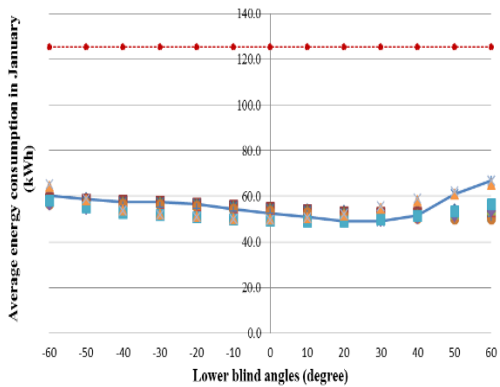
g) Room depth of 12 m in January h) Room depth of 12 m in June
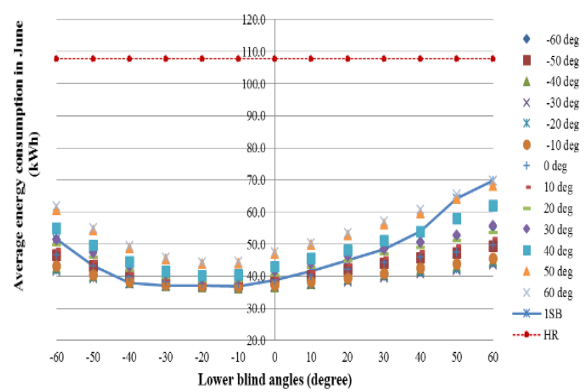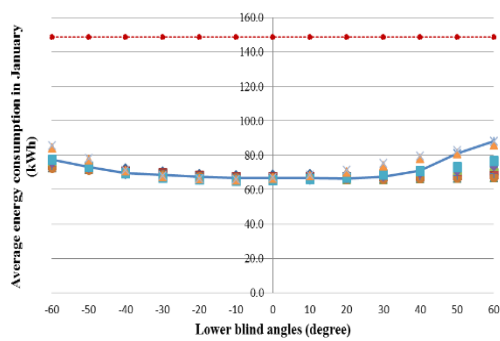
h) Room depth of 15 m in January i) Room depth of 15 m in June
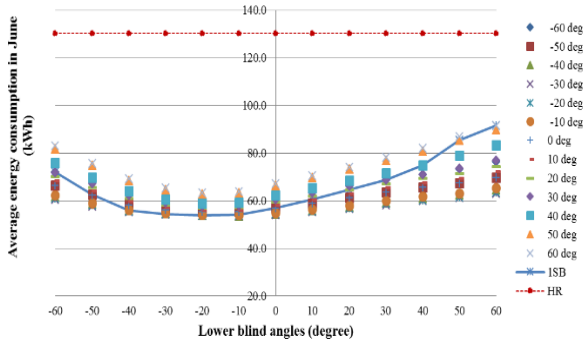
Figure 4.26 Average total energy consumption at 300 lux in January and June (continued)

4.9 Energy Saving

The purpose of the slat window is to shade beam illuminance. Table 4.1 to 4.15 show the angle slats that provide the minimum total energy consumption without beam illuminance in each month of each room depth and required illuminance level. Energy consumption from lighting, heat transfer through window, air-conditioning system of double section slat (2SB),

one section slat (1SB) and heat reflective glass (HR) are also shown in the tables. Energy saving of double section slat is used one section slat and heat reflective glass as references. From the results show that the performance of two section slat is provide higher efficiency than heat reflective glass window significantly but when compare to one section slat window, the performance of two section slat is not much different in term of energy saving.

Table 4.2 Room depth of 3m at 300 lux required illuminance level

300lux	Room depth of 3m																			
	Angle (degree)			Energy consumption without beam illuminance (kWh/month)									Saving(%)						
Month	2SB		1SB	2SB			1SB			HR			compared to HR			compared to 1SB			
	upper	lower		Light	Air-cond	Total	Light	Air-cond	Total	Light	Air-cond	Total	Light	Air-cond	Total	Light	Air-cond	Total	
Jan	60	60	60	3.62	21.86	25.48	3.62	21.86	25.48	16.98	38.61	55.59	78.66	43.39	54.16	0	0	0	
Feb	60	60	60	3.31	17.08	20.40	3.31	17.08	20.40	15.33	31.88	47.21	78.39	46.41	56.79	0	0	0	
Mar	60	40	60	3.55	15.38	18.94	4.34	14.88	19.22	16.98	30.44	47.41	79.06	49.46	60.06	18.16	-3.39	1.48	
Apr	60	40	50	3.08	13.18	16.26	3.32	13.22	16.54	16.43	24.37	40.80	81.26	45.92	60.15	7.14	0.31	1.68	
May	60	40	50	3.53	11.45	14.98	3.41	12.27	15.68	16.98	26.56	43.53	79.22	56.89	65.60	-3.42	6.68	4.49	
Jun	60	40	50	3.17	11.19	14.35	3.48	11.28	14.75	16.43	23.77	40.20	80.72	52.94	64.29	8.85	0.81	2.71	
Jul	60	40	50	3.20	11.62	14.83	3.43	11.69	15.12	16.98	24.68	41.65	81.13	52.90	64.40	6.54	0.55	1.91	
Aug	60	30	50	3.19	12.41	15.60	3.74	12.28	16.02	16.98	25.36	42.34	81.19	51.06	63.14	14.65	-1.03	2.63	
Sep	60	30	60	3.19	13.99	17.19	4.19	13.27	17.47	16.43	27.14	43.57	80.56	48.43	60.55	23.80	-5.44	1.58	
Oct	60	60	60	4.28	17.10	21.38	4.28	17.10	21.38	16.98	32.95	49.93	74.78	48.11	57.18	0	0	0	
Nov	60	60	60	3.26	22.33	25.59	3.26	22.33	25.59	16.43	39.30	55.73	80.16	43.18	54.09	0	0	0	
Dec	60	60	60	3.38	25.78	29.16	3.38	25.78	29.16	16.98	44.10	61.07	80.10	41.54	52.26	0	0	0	
All	30	30	30	36.84	13.65	50.49	36.84	13.65	50.49	199.90	74.04	273.94	81.57	81.57	81.57	0	0	0	

Table 4.3 Room depth of 6 m at 300 lux required illuminance level

300lux	Room depth of 6m																			
	Angle (degree)			Energy consumption without beam illuminance (kWh/month)									Saving(%)						
Month	2SB		1SB	2SB			1SB			HR			compared to HR			compared to 1SB			
	upper	lower		Light	Air-cond	Total	Light	Air-cond	Total	Light	Air-cond	Total	Light	Air-cond	Total	Light	Air-cond	Total	
Jan	60	40	40	7.78	24.69	32.47	7.32	25.82	33.13	33.96	44.90	78.86	77.10	45.01	58.82	-6.31578	4.351959	1.996706	
Feb	60	30	30	6.86	19.87	26.73	5.99	21.03	27.02	30.67	37.56	68.23	77.64	47.08	60.82	-14.4312	5.500195	1.07941	
Mar	30	30	30	7.44	18.35	25.79	7.44	18.35	25.79	33.96	36.72	70.68	78.09	50.04	63.51	0	0	0	
Apr	30	30	30	6.55	15.75	22.30	6.55	15.75	22.30	32.86	30.46	63.32	80.07	48.28	64.78	0	0	0	
May	30	30	30	8.26	14.07	22.33	8.26	14.07	22.33	33.96	32.84	66.80	77.17	56.12	66.82	0	0	0	
Jun	30	30	30	6.82	13.70	20.52	6.82	13.70	20.52	32.86	29.85	62.71	79.26	54.10	67.28	0	0	0	
Jul	30	30	30	6.75	14.17	20.92	6.75	14.17	20.92	33.96	30.96	64.92	80.12	54.24	67.78	0	0	0	
Aug	30	30	30	7.15	14.85	22.00	7.15	14.85	22.00	33.96	31.65	65.60	78.95	53.08	66.47	0	0	0	
Sep	30	30	30	7.13	16.54	23.67	7.13	16.54	23.67	32.86	33.22	66.09	78.30	50.21	64.18	0	0	0	
Oct	30	30	30	7.32	21.00	28.33	7.32	21.00	28.33	33.96	39.24	73.20	78.43	46.48	61.30	0	0	0	
Nov	60	40	50	7.04	25.06	32.09	7.47	25.07	32.54	32.86	45.38	78.24	78.58	44.79	58.98	5.848997	0.048915	1.381153	
Dec	60	50	60	7.74	28.07	35.80	8.42	27.65	36.07	33.96	50.38	84.34	77.21	44.29	57.55	8.102326	-1.52291	0.724469	
All	30	30	30	6.33	311.44	317.77	6.33	311.44	317.77	30.67	812.44	843.11	79.35	61.67	62.31	0	0	0	

Table 4.4 Room depth of 9 m at 300 lux required illuminance level

300lux	Room depth of 9m																			
	Angle (degree)			Energy consumption without beam illuminance (kWh/month)									Saving(%)						
Month	2SB		1SB	2SB			1SB			HR			compared to HR			compared to 1SB			
	upper	lower		Light	Air-cond	Total	Light	Air-cond	Total	Light	Air-cond	Total	Light	Air-cond	Total	Light	Air-cond	Total	
Jan	30	30	30	12.06	28.82	40.87	12.06	28.82	40.87	50.01	50.85	100.86	75.89	43.32	59.47	0	0	0	
Feb	30	30	30	11.68	23.14	34.81	11.68	23.14	34.81	45.17	42.93	88.10	74.14	46.10	60.48	0	0	0	
Mar	30	10	10	13.65	22.41	36.06	12.67	23.81	36.48	50.01	42.67	92.68	72.71	47.49	61.10	-7.69764	5.876716	1.160749	
Apr	-40	0	0	10.60	21.36	31.96	11.16	21.53	32.69	48.39	36.21	84.61	78.10	41.01	62.22	5.03	0.79	2.24	
May	-40	0	-40	11.88	20.19	32.07	12.80	20.02	32.81	50.01	38.79	88.80	76.24	47.96	63.89	7.15	-0.85	2.27	
Jun	-40	0	-40	10.66	19.10	29.75	10.99	19.49	30.48	48.39	35.61	84.00	77.98	46.37	64.58	3.03	2.03	2.39	
Jul	-40	0	0	10.54	19.82	30.36	11.22	19.71	30.93	50.01	36.91	86.92	78.93	46.31	65.07	6.07	-0.53	1.86	
Aug	-40	20	0	11.76	19.52	31.29	11.44	20.53	31.98	50.01	37.59	87.60	76.48	48.07	64.28	-2.80	4.92	2.16	
Sep	-40	30	20	11.33	21.02	32.35	13.02	20.11	33.12	48.39	38.98	87.37	76.59	46.07	62.97	12.95	-4.54	2.33	
Oct	30	20	20	12.98	23.98	36.95	12.57	24.71	37.28	50.01	45.19	95.19	74.05	46.94	61.18	-3.20762	2.966466	0.884251	
Nov	30	30	30	11.09	29.21	40.30	11.09	29.21	40.30	48.39	51.14	99.53	77.09	42.87	59.51	0	0	0	
Dec	40	30	30	11.63	32.66	44.29	11.10	33.22	44.32	50.01	56.33	106.34	76.73	42.03	58.35	-4.83137	1.712041	0.073591	
All	30	30	30	13.47	431.79	445.25	13.47	431.79	445.25	45.17	1056.94	1102.10	70.18	59.15	59.60	0	0	0	

Table 4.5 Room depth of 12 m at 300 lux required illuminance level

300lux	Room depth of 12m																				
	Angle (degree)			Energy consumption without beam illuminance (kWh/month)									Saving(%)							
	2SB		1SB	2SB			1SB			HR			compared to HR			compared to 1SB					
Month	upper	lower		Light	Air-cond	Total	Light	Air-cond	Total	Light	Air-cond	Total	Light	Air-cond	Total	Light	Air-cond	Total			
Jan	30	30	30	23.27	32.97	56.24	23.27	32.97	56.24	67.91	57.48	125.39	65.74	42.64	55.15	0	0	0			
Feb	30	30	30	22.79	27.25	50.04	22.79	27.25	50.04	61.34	48.92	110.26	62.85	44.29	54.62	0	0	0			
Mar	10	10	10	24.30	28.11	52.41	24.30	28.11	52.41	67.91	49.30	117.21	64.22	42.98	55.29	0	0	0			
Apr	-40	-10	-10	20.38	25.82	46.20	19.97	26.47	46.45	65.72	42.63	108.35	68.99	39.43	57.36	-2.02	2.46	0.53			
May	-40	-10	-20	23.36	24.44	47.80	22.65	25.64	48.29	67.91	45.42	113.33	65.60	46.20	57.82	-3.16	4.70	1.01			
Jun	-40	-10	-10	20.50	23.58	44.08	20.41	24.12	44.52	65.72	42.02	107.74	68.81	43.89	59.09	-0.43	2.22	1.01			
Jul	-40	-10	-10	20.16	24.29	44.44	20.06	24.80	44.86	67.91	43.54	111.45	70.32	44.22	60.12	-0.49	2.07	0.93			
Aug	-40	-10	-10	20.11	24.96	45.07	19.98	25.54	45.51	67.91	44.22	112.13	70.39	43.56	59.81	-0.65	2.25	0.98			
Sep	-40	-10	-40	17.77	26.91	44.68	18.83	26.72	45.54	65.72	45.40	111.12	72.96	40.71	59.79	5.62	-0.73	1.89			
Oct	20	10	10	22.35	29.55	51.90	21.47	30.43	51.91	67.91	51.82	119.73	67.09	42.98	56.65	-4	3	0			
Nov	30	30	30	21.86	33.20	55.06	21.86	33.20	55.06	65.72	57.55	123.27	66.74	42.31	55.33	0	0	0			
Dec	30	30	30	15.07	34.70	49.77	15.07	34.70	49.77	67.91	62.96	130.87	77.81	44.89	61.97	0	0	0			
All	30	30	30	238.43	292.97	531.39	238.43	292.97	531.39	799.60	591.38	1390.98	70.18	50.46	61.80	0	0	0			

Table 4.6 Room depth of 15 m at 300 lux required illuminance level

300lux	Room depth of 15m																	
	Angle (degree)			Energy consumption without beam illuminance (kWh/month)									Saving(%)					
	2SB		1SB	2SB			1SB			HR			compared to HR			compared to 1SB		
Month	upper	lower		Light	Air-cond	Total	Light	Air-cond	Total	Light	Air-cond	Total	Light	Air-cond	Total	Light	Air-cond	Total
Jan	30	30	30	36.71	37.95	74.67	36.71	37.95	74.67	84.89	63.77	148.66	56.75	40.48	49.77	0	0	0
Feb	30	30	30	35.51	31.96	67.47	35.51	31.96	67.47	76.67	54.60	131.27	53.69	41.46	48.60	0	0	0
Mar	10	10	10	37.92	33.15	71.07	37.92	33.15	71.07	84.89	55.59	140.48	55.33	40.36	49.41	0	0	0
Apr	-30	-10	-10	32.08	31.12	63.20	32.42	31.08	63.51	82.15	48.72	130.87	60.94	36.12	51.70	1.04	-0.12	0.48
May	-30	-10	-20	36.15	30.00	66.15	35.96	30.57	66.53	84.89	51.71	136.60	57.42	41.98	51.57	-0.53	1.88	0.57
Jun	-30	-10	-20	32.33	28.82	61.15	32.14	29.41	61.54	82.15	48.11	130.26	60.64	40.10	53.05	-0.62	2.00	0.63
Jul	-30	-10	-20	32.01	29.57	61.58	31.80	30.19	61.99	84.89	49.83	134.72	62.29	40.66	54.29	-0.67	2.04	0.65
Aug	-30	-10	-20	31.65	30.17	61.82	31.44	30.82	62.26	84.89	50.51	135.40	62.71	40.27	54.34	-0.68	2.10	0.70
Sep	-40	-10	-20	28.71	30.97	59.67	27.87	32.56	60.42	82.15	51.48	133.63	65.05	39.85	55.34	-3.02	4.88	1.24
Oct	10	10	10	33.97	35.06	69.03	33.97	35.06	69.03	84.89	58.11	142.99	59.98	39.66	51.72	0	0	0
Nov	30	30	30	34.82	38.00	72.82	34.82	38.00	72.82	82.15	63.64	145.79	57.62	40.28	50.05	0	0	0
Dec	30	30	30	26.97	39.10	66.07	26.97	39.10	66.07	84.89	69.25	154.14	68.23	43.53	57.14	0	0	0
All	30	30	30	498.96	389.46	888.42	498.96	389.46	888.42	999.50	665.42	1664.92	50.08	41.47	46.64	0	0	0

Table 4.7 Room depth of 3 m at 500 lux required illuminance level

500lux	Room depth of 3m																	
	Angle (degree)			Energy consumption without beam illuminance (kWh/month)									Saving(%)					
Month	2SB		1SB	2SB			1SB			HR			compared to HR			compared to 1SB		
	upper	lower		Light	Air-cond	Total	Light	Air-cond	Total	Light	Air-cond	Total	Light	Air-cond	Total	Light	Air-cond	Total
Jan	60	30	60	3.47	23.72	27.19	5.85	22.68	28.53	28.30	42.81	71.10	87.73	44.58	61.76	40.62	-4.58	4.68
Feb	60	30	40	3.27	18.54	21.81	3.66	19.21	22.87	25.56	35.66	61.22	87.22	48.01	64.38	10.74	3.47	4.63
Mar	60	30	30	4.29	16.02	20.31	4.07	17.10	21.16	28.30	34.63	62.92	84.85	53.74	67.73	-5.45	6.31	4.05
Apr	60	30	30	3.44	13.62	17.07	3.28	14.54	17.83	27.38	28.43	55.81	87.42	52.09	69.43	-4.91	6.35	4.28
May	60	20	30	4.37	12.30	16.67	4.83	12.80	17.63	28.30	30.75	59.04	84.56	60.01	71.77	9.55	3.91	5.45
Jun	60	20	30	3.24	12.04	15.29	3.45	12.45	15.90	27.38	27.82	55.21	88.15	56.72	72.31	5.87	3.30	3.86
Jul	60	20	30	3.58	12.05	15.63	3.43	12.94	16.37	28.30	28.87	57.17	87.33	58.26	72.65	-4.62	6.87	4.47
Aug	60	20	30	3.59	13.18	16.75	3.88	13.64	17.52	28.30	29.55	57.85	87.33	55.41	71.02	7.63	3.38	4.32
Sep	60	20	30	3.64	14.85	18.50	3.96	15.37	19.33	27.38	31.20	58.58	86.69	52.39	68.42	8.05	3.37	4.33
Oct	60	30	30	4.38	18.52	22.90	4.16	19.83	24.00	28.30	37.15	65.44	84.53	50.14	65.01	-5.09	6.60	4.57
Nov	60	40	60	3.69	23.82	27.51	4.88	22.93	27.81	27.38	43.35	70.74	86.52	45.07	61.11	24.36	-3.88	1.08
Dec	60	60	60	4.85	26.32	31.17	4.85	26.32	31.17	28.30	48.29	76.58	82.87	45.49	59.30	0	0	0
All	30	30	30	44.04	16.31	60.36	44.04	16.31	60.36	333.17	123.40	456.56	86.78	86.78	86.78	0	0	0

Table 4.8 Room depth of 6 m at 500 lux required illuminance level

500lux	Room depth of 6m																	
	Angle (degree)			Energy consumption without beam illuminance (kWh/month)									Saving(%)					
Month	2SB		1SB	2SB			1SB			HR			compared to HR			compared to 1SB		
	upper	lower		Light	Air-cond	Total	Light	Air-cond	Total	Light	Air-cond	Total	Light	Air-cond	Total	Light	Air-cond	Total
Jan	30	30	30	9.31	27.80	37.12	9.31	27.80	37.12	56.59	53.29	109.88	83.54	47.82	66.22	0	0	0
Feb	30	30	30	8.95	22.12	31.07	8.95	22.12	31.07	51.12	45.13	96.25	82.50	50.98	67.72	0	0	0
Mar	30	10	20	10.70	21.32	32.02	11.22	21.25	32.47	56.59	45.11	101.70	81.09	52.74	68.52	4.59	-0.31	1.38
Apr	30	-10	-40	8.24	19.25	27.49	8.02	20.45	28.47	54.77	38.57	93.34	84.96	50.09	70.55	-2.66	5.84	3.44
May	-40	10	-40	9.29	18.39	27.68	9.48	18.79	28.26	56.59	41.23	97.82	83.58	55.40	71.70	1.95	2.12	2.07
Jun	-40	10	-40	7.83	17.49	25.33	7.78	18.30	26.08	54.77	37.97	92.73	85.70	53.92	72.69	-0.68	4.42	2.90
Jul	-40	20	-40	8.13	17.53	25.66	8.09	18.56	26.65	56.59	39.35	95.94	85.64	55.45	73.26	-0.39	5.52	3.73
Aug	-40	20	-40	8.65	18.37	27.01	8.26	19.95	28.21	56.59	40.03	96.62	84.72	54.12	72.04	-4.67	7.93	4.24
Sep	-40	30	20	8.62	20.02	28.63	10.04	19.01	29.05	54.77	41.34	96.11	84.26	51.58	70.21	14.16	-5.32	1.41
Oct	30	20	20	10.36	23.01	33.37	10.08	23.79	33.87	56.59	47.63	104.22	81.69	51.69	67.98	-2.77	3.28	1.48
Nov	30	30	30	8.19	28.14	36.32	8.19	28.14	36.32	54.77	53.50	108.26	85.05	47.40	66.45	0	0	0
Dec	30	30	30	8.28	32.18	40.47	8.28	32.18	40.47	56.59	58.77	115.36	85.36	45.24	64.92	0	0	0
All	30	30	30	11.08	391.56	402.64	11.08	391.56	402.64	51.12	1157.24	1208.36	78.32	66.16	66.68	0	0	0

Table 4.9 Room depth of 9 m at 500 lux required illuminance level

500lux	Room depth of 9m																	
	Angle (degree)			Energy consumption without beam illuminance (kWh/month)									Saving(%)					
	2SB		1SB	2SB			1SB			HR			compared to HR			compared to 1SB		
Month	upper	lower		Light	Air-cond	Total	Light	Air-cond	Total	Light	Air-cond	Total	Light	Air-cond	Total	Light	Air-cond	Total
Jan	30	30	30	23.92	33.21	57.14	23.92	33.21	57.14	83.35	63.20	146.54	71.30	47.44	61.01	0	0	0
Feb	30	30	30	24.19	27.77	51.96	24.19	27.77	51.96	75.28	54.08	129.36	67.87	48.65	59.84	0	0	0
Mar	10	10	10	25.75	28.65	54.40	25.75	28.65	54.40	83.35	55.02	138.36	69.11	47.93	60.69	0	0	0
Apr	-30	-10	-20	19.06	26.29	45.35	18.84	26.93	45.77	80.66	48.16	128.82	76.37	45.40	64.79	-1.16	2.37	0.92
May	-30	-10	-20	23.00	25.61	48.61	23.19	25.85	49.04	83.35	51.14	134.48	72.41	49.92	63.85	0.84	0.91	0.88
Jun	-30	-10	-20	19.42	24.03	43.45	19.22	24.62	43.85	80.66	47.55	128.21	75.93	49.46	66.11	-1.00	2.40	0.91
Jul	-30	-10	-20	18.33	24.50	42.83	18.11	25.12	43.23	83.35	49.26	132.60	78.01	50.26	67.70	-1.17	2.45	0.93
Aug	-30	-10	-20	18.23	25.20	43.42	18.04	25.86	43.89	83.35	49.94	133.28	78.13	49.54	67.42	-1.05	2.54	1.07
Sep	-30	-10	-20	15.97	26.25	42.21	15.55	27.64	43.19	80.66	50.93	131.58	80.21	48.46	67.92	-2.68	5.04	2.26
Oct	10	10	10	21.28	30.36	51.64	21.28	30.36	51.64	83.35	57.53	140.88	74.47	47.23	63.34	0	0	0
Nov	30	30	30	22.24	33.34	55.59	22.24	33.34	55.59	80.66	63.09	143.74	72.42	47.14	61.33	0	0	0
Dec	30	30	30	21.41	37.04	58.45	21.41	37.04	58.45	83.35	68.68	152.02	74.32	46.06	61.55	0	0	0
All	30	30	30	27.59	669.98	697.58	27.59	669.98	697.58	75.28	1564.74	1640.02	63.35	57.18	57.47	0	0	0

Table 4.10 Room depth of 12 m at 500 lux required illuminance level

500lux	Room depth of 12m																	
	Angle (degree)			Energy consumption without beam illuminance (kWh/month)									Saving(%)					
	2SB		1SB	2SB			1SB			HR			compared to HR			compared to 1SB		
Month	upper	lower		Light	Air-cond	Total	Light	Air-cond	Total	Light	Air-cond	Total	Light	Air-cond	Total	Light	Air-cond	Total
Jan	30	30	30	46.64	41.63	88.26	46.64	41.63	88.26	113.19	74.25	187.43	58.80	43.94	52.91	0	0	0
Feb	30	30	30	45.74	35.75	81.49	45.74	35.75	81.49	102.23	64.06	166.29	55.26	44.20	51.00	0	0	0
Mar	10	10	10	48.91	37.23	86.14	48.91	37.23	86.14	113.19	66.07	179.25	56.79	43.65	51.95	0	0	0
Apr	-30	-10	-20	40.03	34.06	74.09	39.70	34.66	74.36	109.53	58.86	168.39	63.45	42.13	56.00	-0.84	1.72	0.36
May	-30	-20	-20	45.57	33.97	79.54	45.80	34.22	80.02	113.19	62.19	175.37	59.74	45.37	54.64	0.49	0.72	0.59
Jun	-30	-20	-20	40.05	32.15	72.20	40.19	32.39	72.58	109.53	58.25	167.78	63.44	44.81	56.97	0.35	0.74	0.52
Jul	-30	-20	-20	38.92	32.65	71.57	39.08	32.88	71.96	113.19	60.31	173.49	65.61	45.87	58.75	0.40	0.71	0.54
Aug	-30	-20	-20	38.43	33.20	71.63	38.50	33.43	71.93	113.19	60.99	174.18	66.05	45.56	58.88	0.19	0.70	0.43
Sep	-30	-20	-20	33.09	34.31	67.41	33.40	34.60	68.00	109.53	61.62	171.16	69.79	44.32	60.62	0.92	0.84	0.88
Oct	10	10	10	42.48	38.21	80.69	42.48	38.21	80.69	113.19	68.59	181.77	62.47	44.29	55.61	0	0	0
Nov	30	30	30	44.15	41.46	85.61	44.15	41.46	85.61	109.53	73.78	183.32	59.69	43.80	53.30	0	0	0
Dec	30	30	30	29.07	39.88	68.95	29.07	39.88	68.95	113.19	79.73	192.91	74.32	49.98	64.26	0	0	0
All	30	30	30	488.48	385.58	874.05	488.48	385.58	874.05	1332.67	788.82	2121.48	63.35	51.12	58.80	0	0	0

Table 4.11 Room depth of 15 m at 500 lux required illuminance level

500lux	Room depth of 15m																	
	Angle (degree)			Energy consumption with shaded-sun (kWh/month)									Saving(%)					
	2SB		1SB	2SB			1SB			HR			compared to HR			compared to 1SB		
Month	upper	lower		Light	Air-cond	Total	Light	Air-cond	Total	Light	Air-cond	Total	Light	Air-cond	Total	Light	Air-cond	Total
Jan	30	30	30	71.39	50.79	122.18	71.39	50.79	122.18	141.48	84.73	226.21	49.54	40.05	45.99	0	0	0
Feb	30	30	30	68.67	44.24	112.91	68.67	44.24	112.91	127.79	73.53	201.32	46.26	39.83	43.91	0	0	0
Mar	10	10	10	73.84	46.46	120.29	73.84	46.46	120.29	141.48	76.55	218.03	47.81	39.31	44.83	0	0	0
Apr	-30	-10	-20	63.32	42.69	106.01	62.94	43.27	106.21	136.92	69.00	205.92	53.75	38.13	48.52	-0.59	1.34	0.19
May	-30	-20	-20	70.16	43.08	113.24	70.41	43.34	113.75	141.48	72.67	214.15	50.41	40.72	47.12	0.36	0.60	0.45
Jun	-30	-20	-20	63.34	40.77	104.11	63.50	41.02	104.52	136.92	68.39	205.31	53.74	40.38	49.29	0.25	0.61	0.39
Jul	-30	-20	-20	62.57	41.41	103.97	62.76	41.65	104.42	141.48	70.79	212.27	55.78	41.51	51.02	0.31	0.60	0.42
Aug	-30	-20	-20	61.78	41.85	103.63	61.88	42.09	103.97	141.48	71.47	212.95	56.33	41.44	51.34	0.16	0.58	0.33
Sep	-30	-20	-20	54.61	42.28	96.89	55.00	42.61	97.61	136.92	71.76	208.68	60.12	41.08	53.57	0.72	0.76	0.74
Oct	10	10	10	66.27	47.03	113.30	66.27	47.03	113.30	141.48	79.07	220.55	53.16	40.52	48.63	0	0	0
Nov	30	30	30	68.05	50.31	118.36	68.05	50.31	118.36	136.92	83.92	220.84	50.30	40.05	46.40	0	0	0
Dec	30	30	30	54.20	49.19	103.39	54.20	49.19	103.39	141.48	90.21	231.69	61.69	45.47	55.37	0	0	0
All	30	30	30	952.71	557.52	1510.23	952.71	557.52	1510.23	1665.83	912.21	2578.04	42.81	38.88	41.42	0	0	0

Table 4.12 Room depth of 3 m at 800 lux required illuminance level

800lux	Room depth of 3m																	
	Angle (degree)			Energy consumption without beam illuminance (kWh/month)									Saving(%)					
	2SB		1SB	2SB			1SB			HR			compared to HR			compared to 1SB		
Month	upper	lower		Light	Air-cond	Total	Light	Air-cond	Total	Light	Air-cond	Total	Light	Air-cond	Total	Light	Air-cond	Total
Jan	60	30	30	5.72	24.55	30.27	5.13	26.25	31.39	45.27	49.09	94.37	87.37	49.99	67.92	-11.37	6.48	3.56
Feb	60	30	30	5.31	19.30	24.60	4.67	20.54	25.20	40.89	41.34	82.24	87.03	53.32	70.08	-13.72	6.04	2.38
Mar	60	20	20	5.76	17.32	23.08	5.22	19.03	24.25	45.27	40.92	86.19	87.27	57.68	73.22	-10.37	9.00	4.83
Apr	-50	20	20	3.33	15.78	19.11	3.99	16.08	20.07	43.81	34.52	78.33	92.39	54.29	75.60	16.52	1.89	4.80
May	-50	20	20	4.69	14.59	19.27	5.09	15.51	20.61	45.27	37.04	82.31	89.65	60.61	76.58	7.98	5.98	6.47
Jun	-50	20	20	3.60	13.74	17.34	4.33	13.89	18.22	43.81	33.91	77.72	91.79	59.48	77.69	16.89	1.12	4.87
Jul	-50	20	20	4.53	12.98	17.51	4.05	14.33	18.37	45.27	35.16	80.43	89.99	63.08	78.23	-12.01	9.40	4.68
Aug	-50	30	20	4.02	15.13	19.15	4.99	15.29	20.28	45.27	35.84	81.11	91.13	57.78	76.39	19.55	1.03	5.59
Sep	60	20	20	5.57	15.57	21.14	5.09	17.17	22.27	43.81	37.28	81.10	87.28	58.24	73.93	-9.43	9.35	5.05
Oct	60	20	20	5.81	19.94	25.75	5.38	22.05	27.43	45.27	43.43	88.71	87.16	54.10	70.97	-7.97	9.58	6.13
Nov	60	30	30	4.80	24.89	29.69	4.37	26.72	31.09	43.81	49.44	93.25	89.04	49.65	68.16	-9.99	6.85	4.49
Dec	60	30	30	4.80	28.60	33.40	4.40	30.75	35.15	45.27	54.58	99.85	89.40	47.60	66.55	-8.99	6.98	4.98
All	30	30	30	75.03	27.79	102.82	75.03	27.79	102.82	533.07	197.43	730.50	85.93	85.93	85.93	0	0	0

Table 4.13 Room depth of 6 m at 800 lux required illuminance level

800lux	Room depth of 6m																		
	Angle (degree)			Energy consumption without beam illuminance (kWh/month)									Saving(%)						
	2SB		1SB	2SB			1SB			HR			compared to HR			compared to 1SB		
Month	upper	lower		Light	Air-cond	Total	Light	Air-cond	Total	Light	Air-cond	Total	Light	Air-cond	Total	Light	Air-cond	Total
Jan	30	30	30	18.87	31.34	50.21	18.87	31.34	50.21	90.55	65.86	156.41	79.16	52.41	67.90	0	0	0
Feb	30	30	30	20.36	26.35	46.70	20.36	26.35	46.70	81.79	56.49	138.27	75.11	53.36	66.22	0	0	0
Mar	10	10	10	21.68	27.14	48.82	21.68	27.14	48.82	90.55	57.68	148.23	76.06	52.95	67.07	0	0	0
Apr	-30	-10	-20	14.01	24.43	38.44	13.87	25.09	38.96	87.63	50.74	138.37	84.01	51.87	72.22	-1.04	2.65	1.34
May	-30	-10	-20	17.74	23.66	41.40	18.25	24.01	42.26	90.55	53.80	144.35	80.41	56.02	71.32	2.81	1.47	2.05
Jun	-30	-10	-20	13.93	22.00	35.93	13.80	22.62	36.42	90.55	50.14	137.76	84.10	56.12	73.92	-0.93	2.72	1.34
Jul	-30	-10	-20	12.62	22.39	35.00	12.48	23.03	35.51	90.55	51.93	142.47	86.07	56.89	75.43	-1.09	2.80	1.43
Aug	-40	-10	-20	13.82	22.63	36.45	13.14	24.04	37.18	90.55	52.61	143.15	84.74	56.98	74.54	-5.19	5.87	1.96
Sep	-40	-10	-40	11.88	24.73	36.61	13.18	24.63	37.80	87.63	53.51	141.14	86.45	53.78	74.06	9.86	-0.43	3.16
Oct	10	10	10	16.79	28.70	45.49	16.79	28.70	45.49	90.55	60.20	150.75	81.46	52.33	69.82	0	0	0
Nov	30	30	30	17.23	31.49	48.72	17.23	31.49	48.72	87.63	65.67	153.29	80.33	52.05	68.22	0	0	0
Dec	30	30	30	15.61	34.89	50.50	15.61	34.89	50.50	90.55	71.34	161.89	82.76	51.09	68.81	0	0	0
All	30	30	30	25.30	631.34	656.64	25.30	631.34	656.64	81.79	1674.45	1756.23	69.06	62.30	62.61	0	0	0

Table 4.14 Room depth of 9 m at 800 lux required illuminance level

800lux	Room depth of 9m																		
	Angle (degree)			Energy consumption without beam illuminance (kWh/month)									Saving(%)						
	2SB		1SB	2SB			1SB			HR			compared to HR			compared to 1SB		
Month	upper	lower		Light	Air-cond	Total	Light	Air-cond	Total	Light	Air-cond	Total	Light	Air-cond	Total	Light	Air-cond	Total
Jan	30	30	30	23.92	33.21	57.14	23.92	33.21	57.14	83.35	63.20	146.54	71.30	47.44	61.01	0	0	0
Feb	30	30	30	24.19	27.77	51.96	24.19	27.77	51.96	75.28	54.08	129.36	67.87	48.65	59.84	0	0	0
Mar	10	10	10	25.75	28.65	54.40	25.75	28.65	54.40	83.35	55.02	138.36	69.11	47.93	60.69	0	0	0
Apr	-30	-10	-20	19.06	26.29	45.35	18.84	26.93	45.77	80.66	48.16	128.82	76.37	45.40	64.79	-1.16	2.37	0.92
May	-30	-10	-20	23.00	25.61	48.61	23.19	25.85	49.04	83.35	51.14	134.48	72.41	49.92	63.85	0.84	0.91	0.88
Jun	-30	-10	-20	19.42	24.03	43.45	19.22	24.62	43.85	80.66	47.55	128.21	75.93	49.46	66.11	-1.00	2.40	0.91
Jul	-30	-10	-20	18.33	24.50	42.83	18.11	25.12	43.23	83.35	49.26	132.60	78.01	50.26	67.70	-1.17	2.45	0.93
Aug	-30	-10	-20	18.23	25.20	43.42	18.04	25.86	43.89	83.35	49.94	133.28	78.13	49.54	67.42	-1.05	2.54	1.07
Sep	-30	-10	-20	15.97	26.25	42.21	15.55	27.64	43.19	80.66	50.93	131.58	80.21	48.46	67.92	-2.68	5.04	2.26
Oct	10	10	10	21.28	30.36	51.64	21.28	30.36	51.64	83.35	57.53	140.88	74.47	47.23	63.34	0	0	0
Nov	30	30	30	22.24	33.34	55.59	22.24	33.34	55.59	80.66	63.09	143.74	72.42	47.14	61.33	0	0	0
Dec	30	30	30	21.41	37.04	58.45	21.41	37.04	58.45	83.35	68.68	152.02	74.32	46.06	61.55	0	0	0
All	30	30	30	27.59	669.98	697.58	27.59	669.98	697.58	75.28	1564.74	1640.02	63.35	57.18	57.47	0	0	0

Table 4.15 Room depth of 12 m at 800 lux required illuminance level

800lux	Room depth of 12m																		
	Angle (degree)			Energy consumption without beam illuminance (kWh/month)									Saving(%)						
	2SB		1SB	2SB			1SB			HR			compared to HR			compared to 1SB		
Month	upper	lower		Light	Air-cond	Total	Light	Air-cond	Total	Light	Air-cond	Total	Light	Air-cond	Total	Light	Air-cond	Total
Jan	30	30	30	89.98	57.68	147.65	89.98	57.68	147.65	181.10	99.40	280.50	50.32	41.97	47.36	0	0	0
Feb	30	30	30	87.79	51.32	139.11	87.79	51.32	139.11	163.57	86.78	250.35	46.33	40.86	44.43	0	0	0
Mar	10	10	10	94.51	54.11	148.62	94.51	54.11	148.62	181.10	91.22	272.32	47.81	40.68	45.42	0	0	0
Apr	-30	-20	-20	79.80	49.23	129.03	79.71	49.48	129.19	175.25	83.20	258.45	54.47	40.83	50.08	-0.11	0.50	0.13
May	-30	-20	-20	88.69	49.94	139.69	79.34	50.35	139.69	181.10	87.34	268.44	51.03	42.82	48.36	0.73	0.80	0.76
Jun	-30	-20	-20	79.61	46.80	126.42	79.91	47.10	127.01	175.25	82.59	257.85	54.57	43.33	50.97	0.37	0.64	0.47
Jul	-30	-20	-20	78.36	47.25	125.62	78.65	47.54	126.19	181.10	85.46	266.56	56.73	44.71	52.87	0.37	0.60	0.46
Aug	-30	-20	-20	77.49	47.67	125.15	77.75	47.97	125.73	181.10	86.14	267.24	57.21	44.66	53.17	0.34	0.64	0.46
Sep	-30	-20	-20	67.92	47.21	115.14	68.58	47.63	116.21	175.25	85.96	261.22	61.24	45.08	55.92	0.95	0.88	0.92
Oct	10	10	10	83.60	53.44	137.04	83.60	53.44	137.04	181.10	93.74	274.83	53.84	42.99	50.14	0	0	0
Nov	30	30	30	86.02	56.97	142.99	86.02	56.97	142.99	175.25	98.12	273.38	50.92	41.94	47.69	0	0	0
Dec	30	30	30	61.43	51.86	113.29	61.43	51.86	113.29	181.10	104.88	285.98	66.08	50.55	60.38	0	0	0
All	30	30	30	1001.66	575.65	1577.31	1001.66	575.65	1577.31	2132.27	1084.96	3217.23	53.02	46.94	50.97	0	0	0

Table 4.16 Room depth of 15 m at 800 lux required illuminance level

800lux	Room depth of 15m																		
	Angle (degree)			Energy consumption with shaded-sun (kWh/month)									Saving(%)						
	2SB		1SB	2SB			1SB			HR			compared to HR			compared to 1SB		
Month	upper	lower		Light	Air-cond	Total	Light	Air-cond	Total	Light	Air-cond	Total	Light	Air-cond	Total	Light	Air-cond	Total
Jan	30	30	30	131.70	73.13	204.83	131.70	73.13	204.83	226.37	116.17	342.54	41.82	37.05	40.20	0	0	0
Feb	30	30	30	126.05	65.50	191.54	126.05	65.50	191.54	204.46	101.93	306.39	38.35	35.74	37.48	0	0	0
Mar	10	10	10	136.40	69.63	206.04	136.40	69.63	206.04	226.37	107.99	334.36	39.74	35.52	38.38	0	0	0
Apr	-30	-20	-20	119.48	63.93	183.40	119.38	64.17	183.55	219.07	99.43	318.49	45.46	35.70	42.42	-0.08	0.38	0.08
May	-30	-20	-20	130.25	65.33	195.58	130.93	65.75	196.67	226.37	104.11	330.48	42.46	37.25	40.82	0.52	0.63	0.56
Jun	-30	-20	-20	119.32	62.14	181.46	119.64	61.82	181.46	219.07	98.82	317.89	45.53	37.75	43.11	0.27	0.50	0.35
Jul	-30	-20	-20	118.98	62.30	181.28	119.31	62.60	181.90	226.37	102.23	328.60	47.44	39.06	44.83	0.28	0.48	0.34
Aug	-30	-20	-20	117.81	62.60	180.41	118.10	62.92	181.02	226.37	102.91	329.28	47.96	39.17	45.21	0.25	0.50	0.34
Sep	-30	-20	-20	105.86	61.26	167.12	106.60	61.72	168.32	219.07	102.19	321.26	51.68	40.05	47.98	0.70	0.73	0.71
Oct	10	10	10	124.37	68.54	192.91	124.37	68.54	192.91	226.37	110.51	336.88	45.06	37.97	42.74	0	0	0
Nov	30	30	30	126.34	71.90	198.25	126.34	71.90	198.25	219.07	114.35	333.42	42.33	37.12	40.54	0	0	0
Dec	30	30	30	105.74	68.28	174.02	105.74	68.28	174.02	226.37	121.65	348.02	53.29	43.87	50.00	0	0	0
All	30	30	30	1737.24	848.08	2585.33	1737.24	848.08	2585.33	2665.33	1282.40	3947.73	34.82	33.87	34.51	0	0	0

CHAPTER 5

CONCLUSION

5.1 Conclusions

The application of double-pane window with two section slat tilt at different angles for daylight and heat transfer was studied through a series of experiments and simulations under tropical climate.

The experiments have presented the system of two section slat window can provide and maintain sufficient interior daylight through the day. The simulation program was validated to the experiment measurement. The results show a good agreement between the measurements and the calculations.

Daylighting and energy consumption was studied for target illuminance at 300 lux, 500 lux and 800lux of room depth of 3 m, 6 m, 9 m, 12 m and 15 m. The study results show that daylight from a two-section slat window that when the slats in the lower and the upper sections were tilted to proper angles, the two-section slat window can enhance the interior daylight use beyond the one-section slat window. It can also improve the uniformity of the interior daylight distribution. Total energy consumption comes from lighting system, and air-conditioning system. Heat gain through window and heat from electric lamps become cooling load to air-conditioning system. At the low required illuminance level (300 lux), the studied results found that heat transfer through window plays an important role for total energy consumption. High daylight become excessive, therefore slat angle was set to close position to prevent heat transfer through window. While daylight potential has become a greater roles especially the room design for higher illuminance levels and more depths. Therefore, the slat angle was adjusted to the negative degree angle which allow more daylight distributes into the room for reducing lighting energy consumption. Two section slat window with dimming control can save much electric energy consumption than window using heat reflective glass, while the performance of two section slat window is a little bit higher to one section slat window in term of energy savings.

Far as the beam penetrate to the window is concerned, the suggestion of the use of slat angles that provide the minimum energy consumption in each month at different room

depth and required illuminance without beam illuminance was analyzed in the studied in Tables 4.2-4.16.

For a whole year, the fixed angle at 30 degree of lower and upper slat (one section blind at slat tilts at 30 degree) provides the maximum energy saving by slat can shade beam illuminance.

5.2 Recommendations

The sizes of windows and walls should be studied
The performance of two section slat windows in qualitative terms of glare conditions and thermal comfort should be studied.

REFERENCES

1   Arasteh, D., Reilly, S., Rubin, M.A., (1989). A versatile procedure for calculating heat transfer through windows. *ASHRAE Transactions,* Vol.95 Pt. 2, pp.755-765.

2   ASHRAE. (1997), Handbook of fundamental. *ASHRAE Inc*., Atlanta,USA

3   Atheinitis,A.K, and Tzempelikos, A. (2002), A Methodology for Simulation of Daylight Room Illuminance Distribution and Light Dimming for a Room with a Controlled Shading Device, *Solar Energy*,72,4,pp.271-281.

4   Bessoudo, M., Tzempelikos, A., Athienitis, A.K., and Zmeureanu, R. (2010), Indoor thermal environmental conditions near glazed facades with shading devices-Part I: Experiments and building thermal model, *Building and Environment*, **45**, 11, pp. 2506-2516.

5   Chaiwiwatworakul, P. and Chirarattananon, S. (2004), Evaluation of Sky Luminance and Radiance Models Using Data of North Bangkok, *The Journal of the Illuminance Engineering Society*, **1**, 2.

6   Chirarattananon, S., and Chaiwiwatworakul, P. (2007), Distributions of sky luminance and radiance of North Bangkok under standard distributions, *Renewable Energy*, **32**, 8, pp. 1328-1345.

7   Chaiwiwatworakul P., Chirarattananon S., Rakkwamsuk P., Application of automated blind for daylighting in tropical region, Energy Conversion and Management 50 (12) (2009) 2927-2943.

8   Chaiyapinunt, S. and Worasinchai, S. (2009), Development of a model for calculating the longwave optical properties and surface temperature of a curved venetian blind, *Solar Energy*, **83**, pp. 817-831.

9   Chaiwiwatworakul P., S. Chirarattananon, A double-pane window with enclosed horizontal slats for daylighting in buildings in the tropics, Energy and Buildings 62 (2013) 27-36.

10   Cho, S.H., Shin., K.S., Zaheer-Uddin,M. (1995), The Effect of Slat Angle of Windows with Venetian Blinds on Heating and Cooling Loads of Buildings and of Buildings in South Korea, *Energy*, 20, 12, pp. 1255-1236.

11   E.U. Finlayson, D.K. Arastech, C. Huizenga, M.D. Rubin, M.S. Reilly, Window 4.0: Documentation of calculation procedures. Publication LBL-33943/UC-350, Lawrence Berkeley Laboratory, Energy & Environmental Division, Berkeley, CA. (2008).

12 Collins, M.R., Harrison, S.J., (2004a). Estimating the solar heat and thermal gain from a window with an interior venetian blind. *ASHARE Transactions*, Vol. 110, Pt. 1, pp. 486-500.

13 Collins, M.R., Wright, J.L.,(2006) .Calculating Centre-Glass Performance Indices of Windows with a Diathermanous Layer, *ASHRAE Transactions*, Vol. 112, Pt. 2. pp. 22-29.

14 Collins, M.R, S.Tasnim, J. Wright, Determination of convective heat transfer for fenestration with between-the-glass louvered shades, International Journal of Heat and Mass Transfer 51 (2008) 2742-2751

15 Fathoni A.M., (2011) Double-Pane window with internal Fixed-Angle Slats for Day light Applications in the Tropics, *Copyright of the Joint Graduate School of Energy and Environment,Thesis Submitted As a Part of the Requirements for the Degree of Master of Philosophy in Energy Technology* , pp 8-54.

16 Hollands, K.G.T., J.L Wright, and C.G. Granqvist (2001). Glazings and coatings. *Solar Energy- The State of Art-ISES Position Papers*, Chapter2, pp.29-50.

17 K.A.R. Ismail a., J.R. Henrı. (2005), Two-dimensional model for the double glass naturallyventilated window,*International Journal of Heat and Mass Transfer* 48 ,pp. 461–475.

18 Lee, E.S, DiBartolomeo D.L and SelkowitZ, S.E (1988), Thermal and Daylighting Performance of an Automated Venetian Blind and Lighting System in a Full-Scale Private Office, *Energy and Bulindings*, 29,1,pp.47-63

19 Nielsen, M.V ., Nielsen, T.R.,   and Svendsen, S. (2005), Calculation of daylight distribution abd utilization in room with solar shadings and light redirecting devices, paper presented in *The 7ᵗʰ symposium on building Physics in the Nordic Countries*, June 13-15th, Reykjavyk, Iceland.

20 Rheault, S. and Bilgen, E. (1989), Heat transfer analysis in an automated venetian blind window system, *Journal of Solar Energy Engineering*, **111**, pp. 89-95.

21 Roche, L. (2002), Summertime Performance of an Automated Lighting and Blinds Control System, *Lighting Research and Technology*, 34, 1, pp. 11-27

22 Tzempelikos, A. (2008), The impact of venetian blind geometry and tilt angle on view, direct light transmission and interior illuminance, *Solar Energy*, **82**, 12, pp. 1172-1191.

23 Wright, J.L., Kotey, N.A., (2006). Solar Absorption by Each Element in a Glazing/Shading Layer Array, *ASHRAE Transactions,* Vol. 112, Pt. 2. pp. 3-12.

24 Yahoda, D.S., Wright, J.L., (2004a). Heat transfer analysis of a between panes venetian blind using effective longwave radiative properties. *ASHRAE Transactions* Vol.110,Pt.1, pp. 445-462.

25 Yahoda, D.S., Wright, J.L., 2(004b). "Methods for calculating the effective longwave radiative properties of a venetian blind layer". ASHRAE Transactions Vol.110, Pt 1, pp463-473.

Average Lighting Power Density on work plane 500 lux
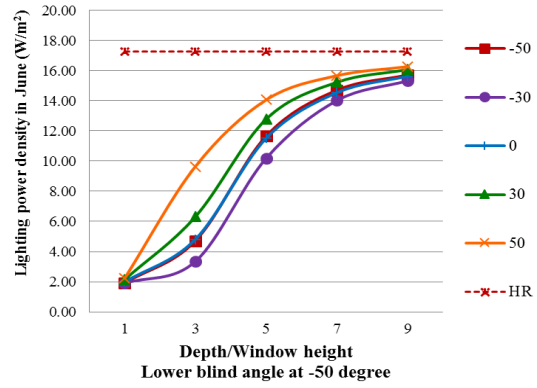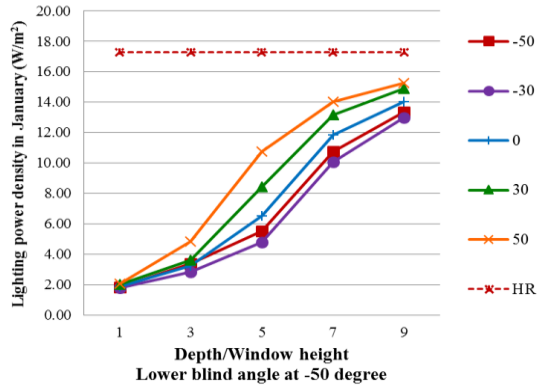
a) Lower slat angle at -50° in January
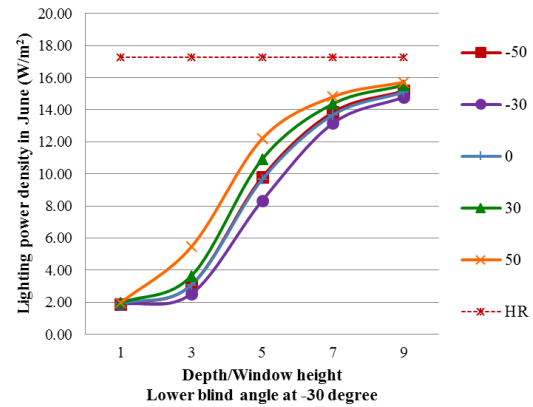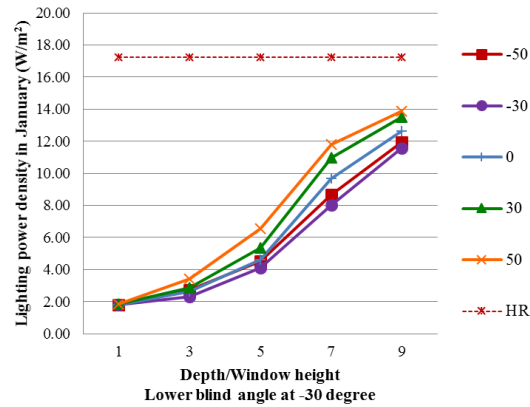
b) Lower slat angle at -60° in June

c) Lower slat angle at -30° in January

b) Lower slat angle at -30° in June
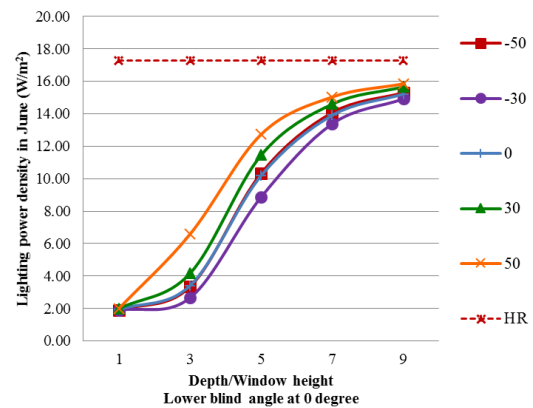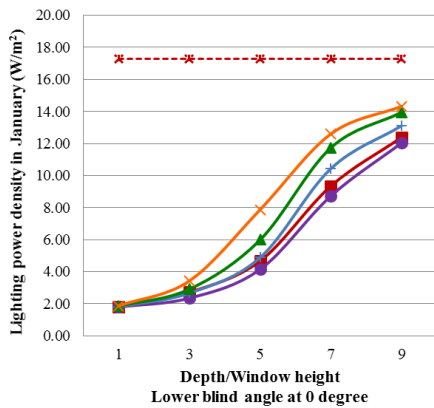
e) Lower slat angle at 0° in January

b) Lower slat angle at 0° in June

Figure A1 Characteristic of lighting power on work plane at 500 lux
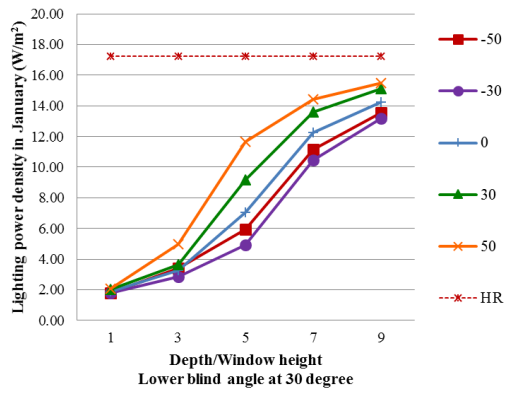
g) Lower slat angle at 30° in January
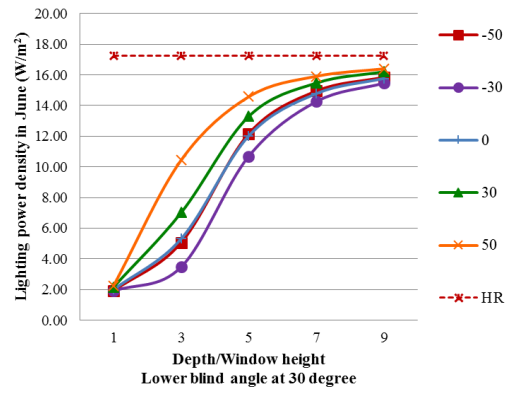
h) Lower slat angle at 0° in June
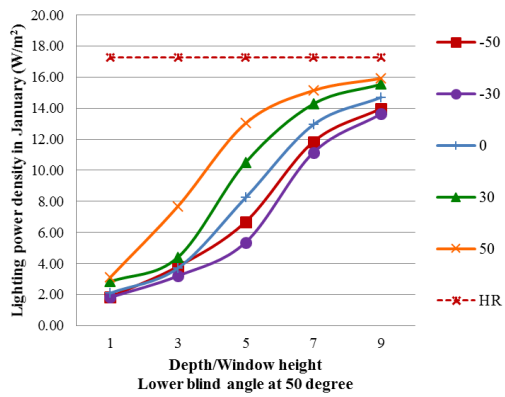
i) Lower slat angle at 50° in January
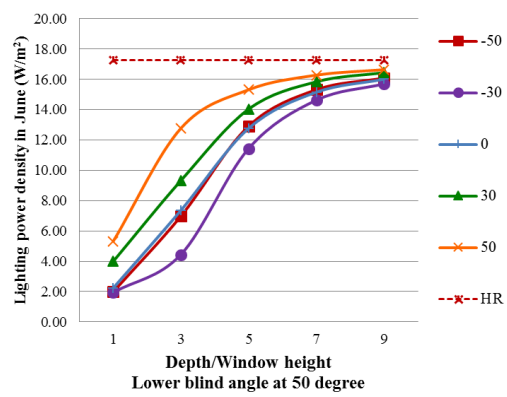
j) Lower slat angle at 50° in June

Figure A1 Characteristic of lighting power on work plane 500 lux (continued)

Average Lighting Power Density at 800 lux
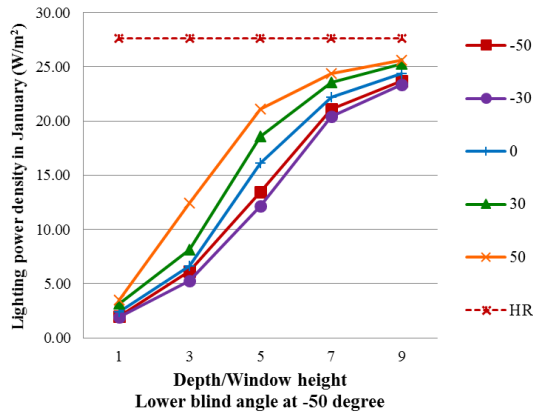
a) Lower slat angle at -50° in January
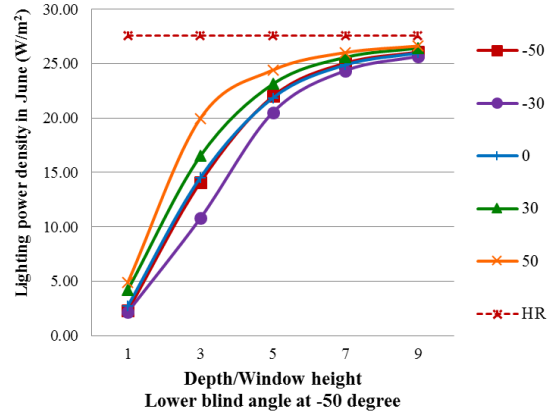
b) Lower slat angle at -50° in June
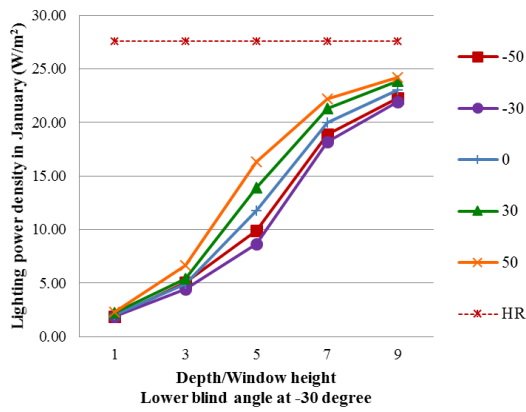
c) Lower angle at -30° in January
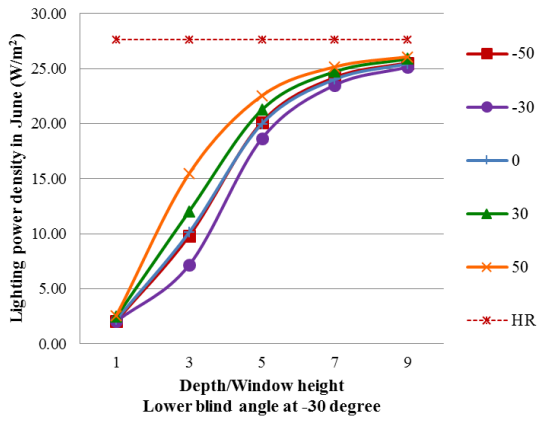
b) Lower slat angle at -30° in June
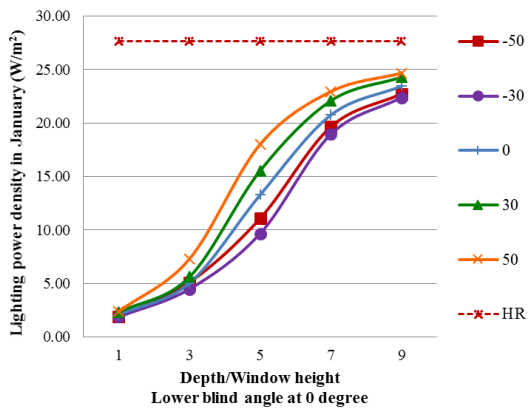
e) Lower slat angle at 0° in January
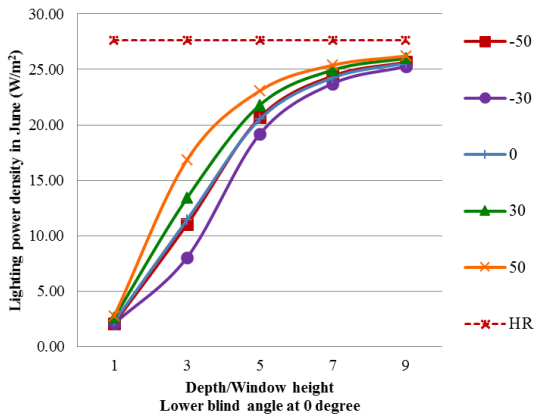
b) Lower slat angle at 0° in June

Figure A2 Characteristic of lighting power on work plane at 800 lux
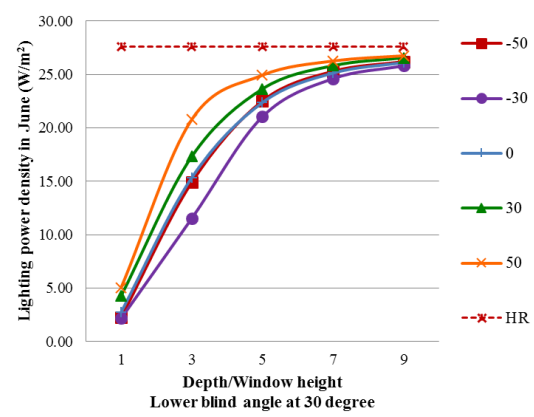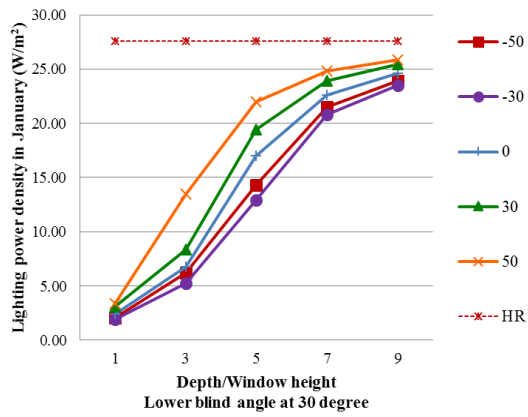
g) Lower slat angle at 30° in January

h) Lower slat angle at 0° in June
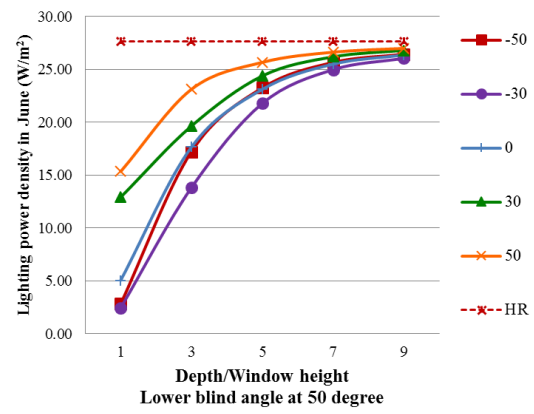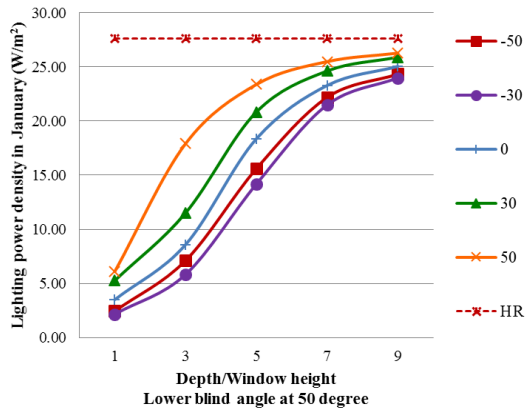
i) Lower slat angle at 50° in January

j) Lower slat angle at 50° in June

Figure A2 Characteristic of lighting power at 800 lux (continued)

Average light power density at 500 lux
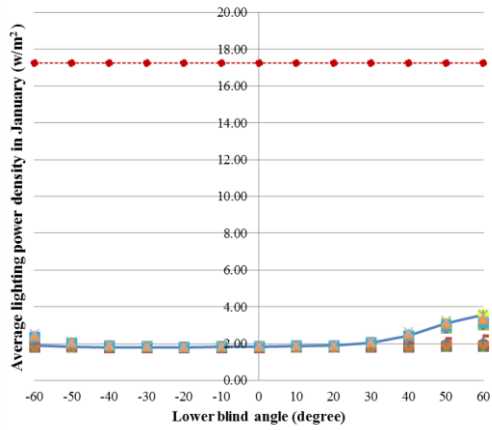
a) Room depth of 3 m in January   b) Room depth of 3 m in June
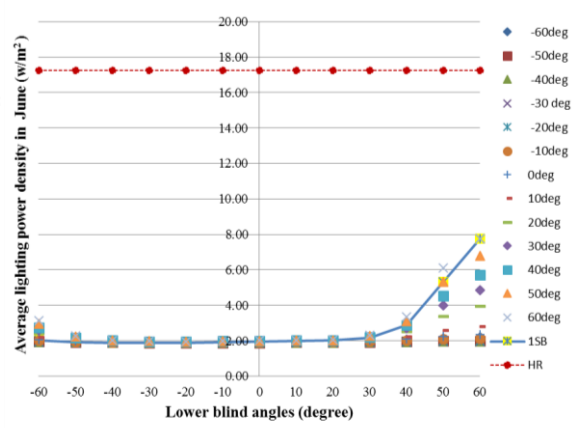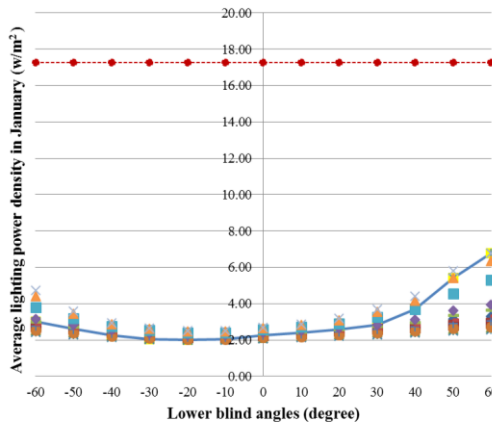
c) Room depth of 6 m in January   d) Room depth of 6 m in June
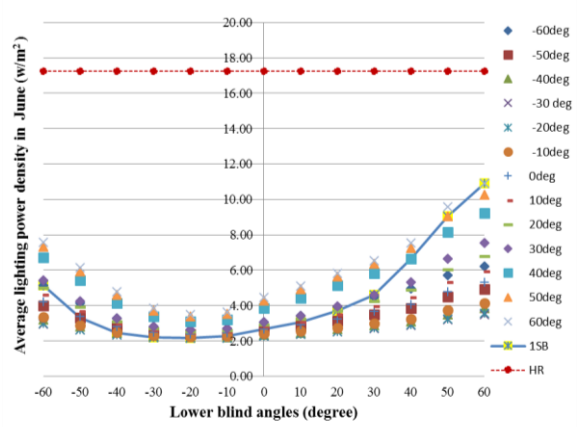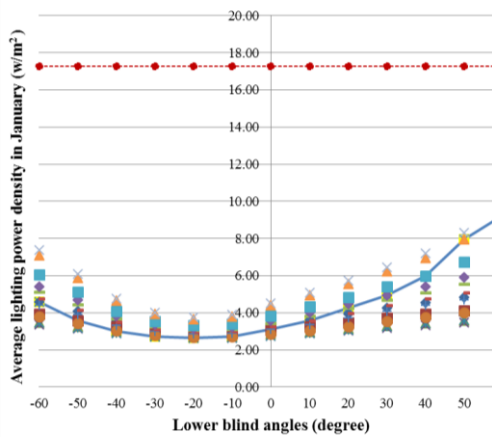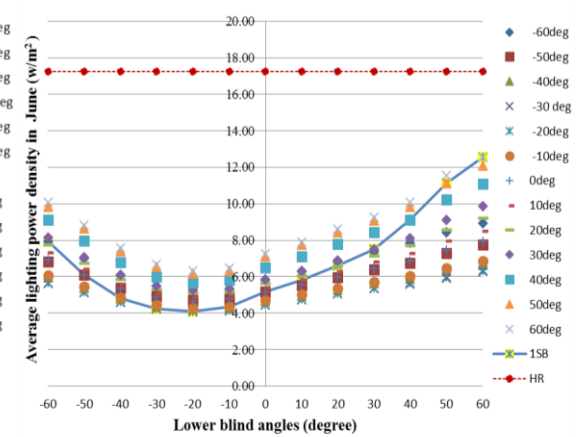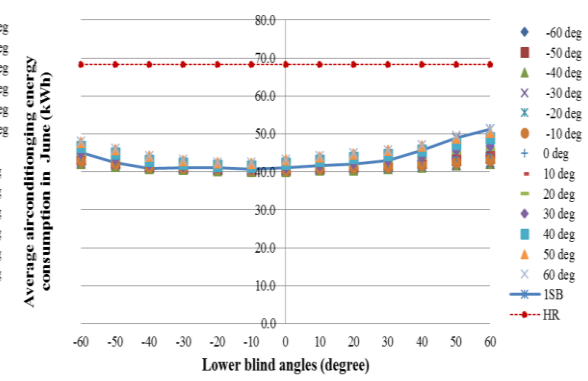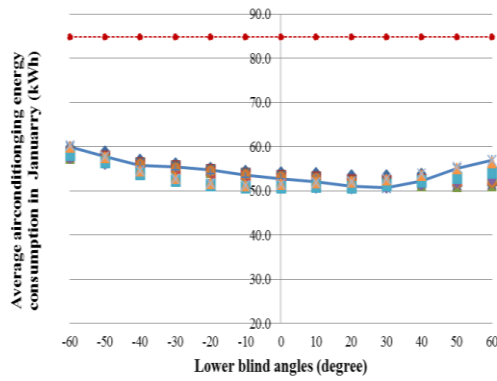
e) Room depth of 9 m in January   f) Room depth of 9 m in June

Figure A3 Average light power density at 500 lux in January and June
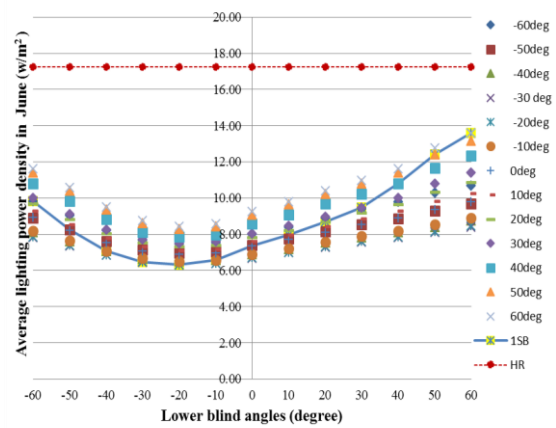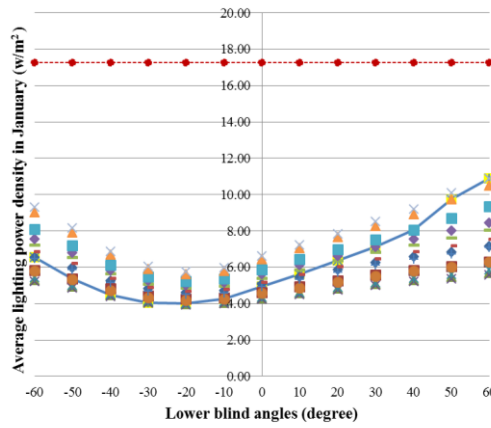
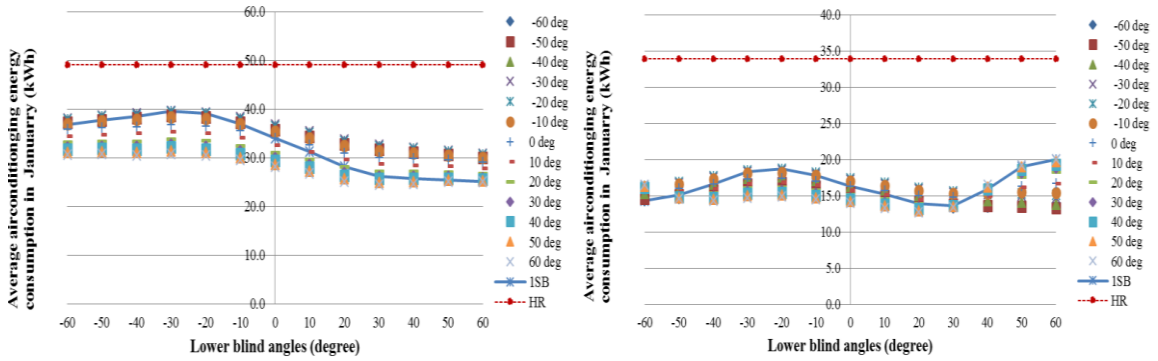g) Room depth of 12 m in January

h) Room depth of 12 m in June
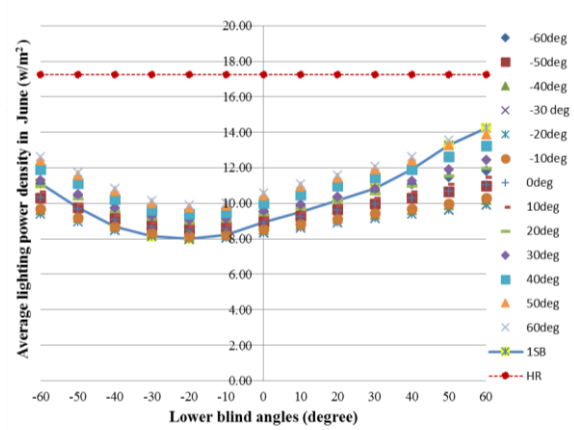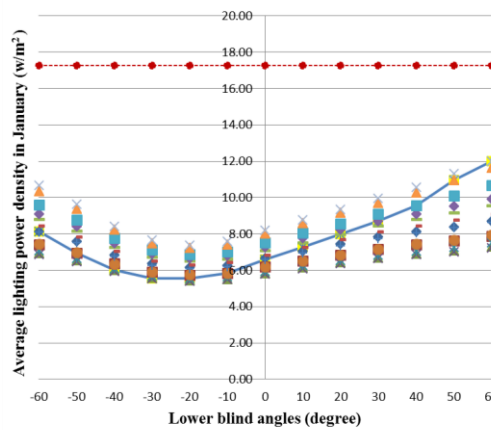
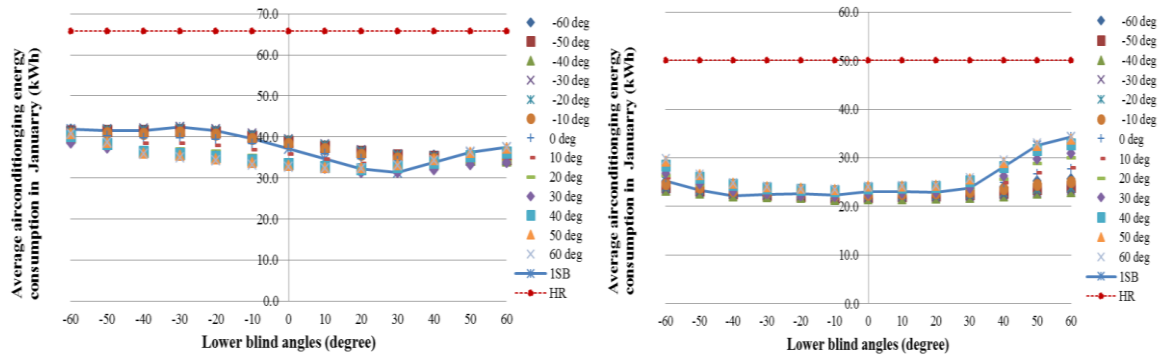i) Room depth of 15 m in January

j) Room depth of 15 m in June

Figure A3 Average light power density at 500 lux in January and June

Average light power density at 800 lux
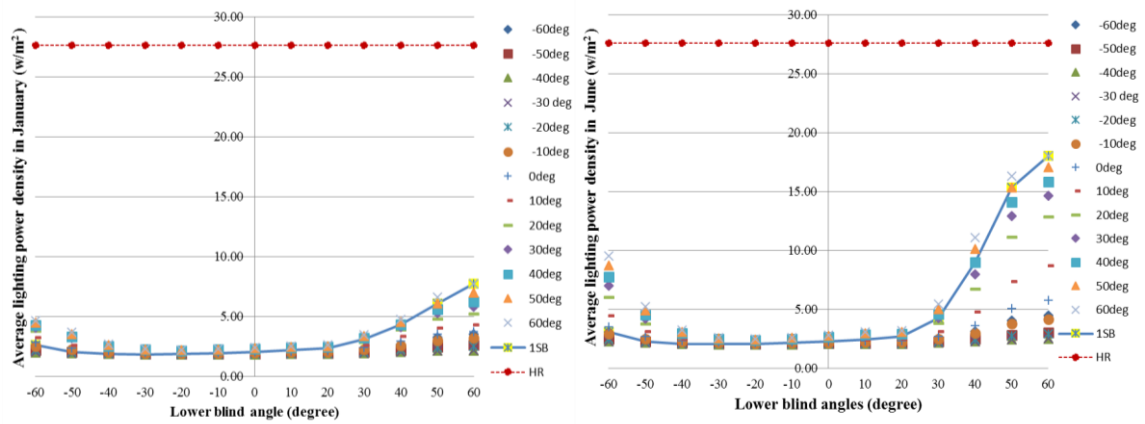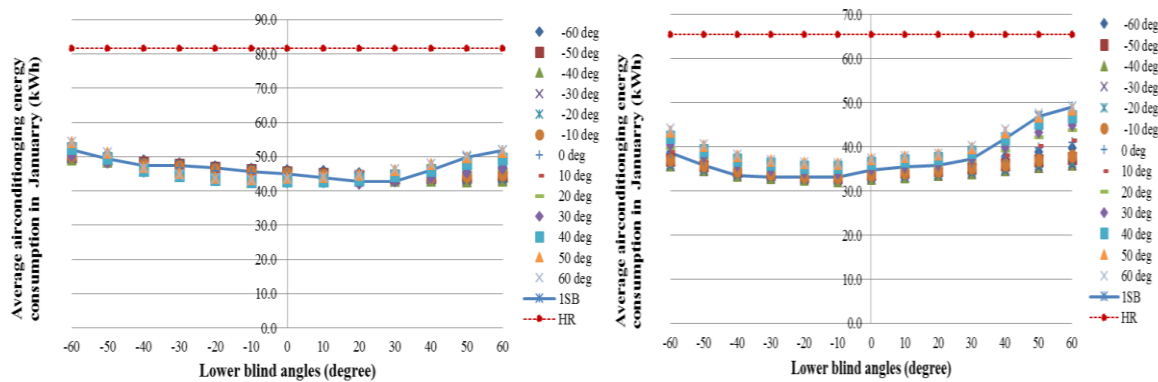

a) Room depth of 3 m in January   b) Room depth of 3 m in June
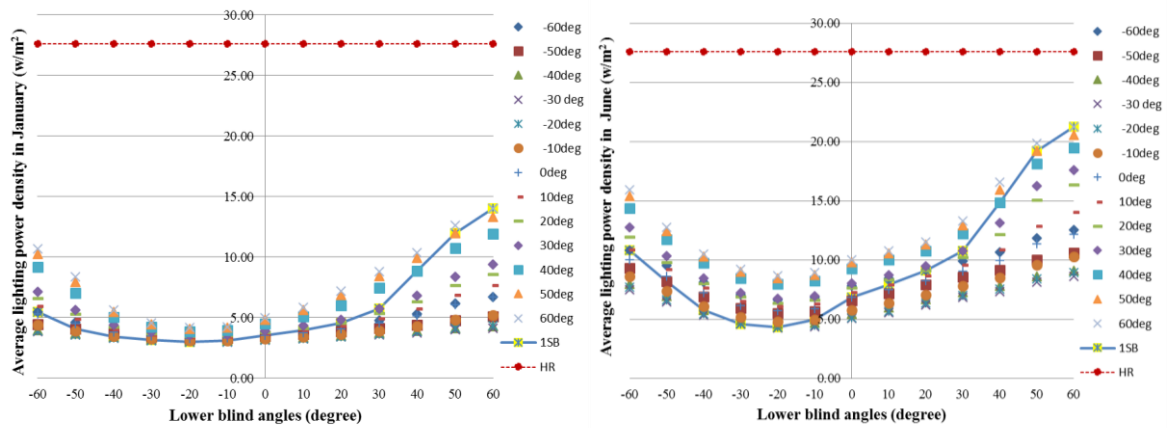
c) Room depth of 6 m in January   d) Room depth of 6 m in June
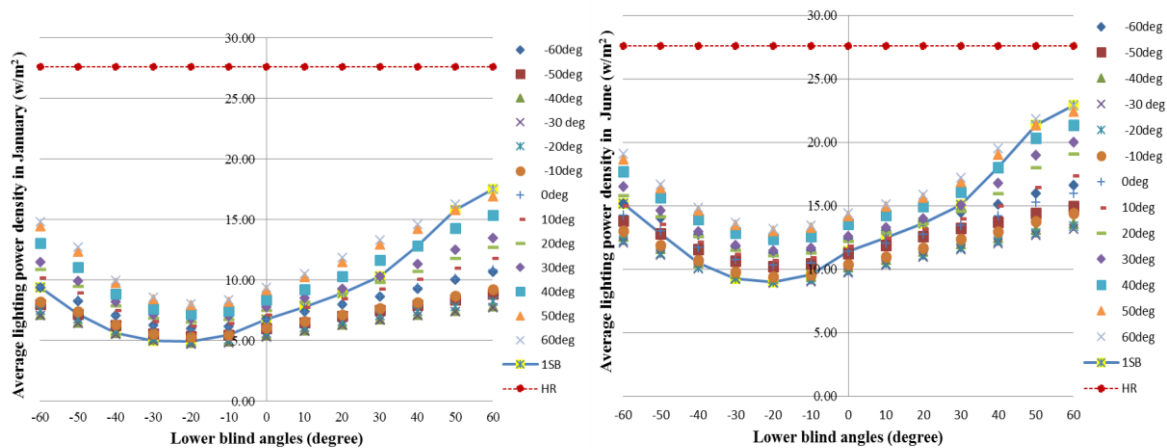
e) Room depth of 9 m in January   f) Room depth of 9 m in June

Figure A4 Average light power density at 500 lux in January and June
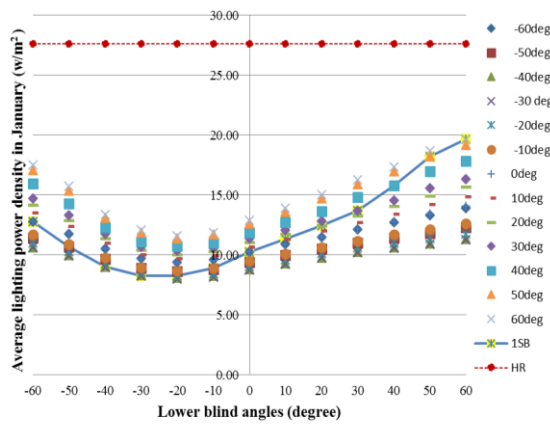
g) Room depth of 12 m in January
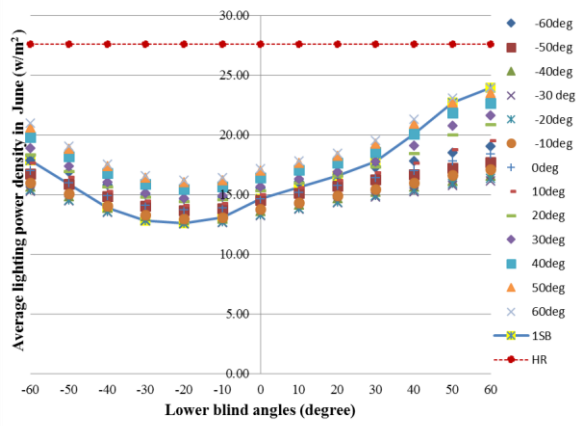
h) Room depth of 12 m in June
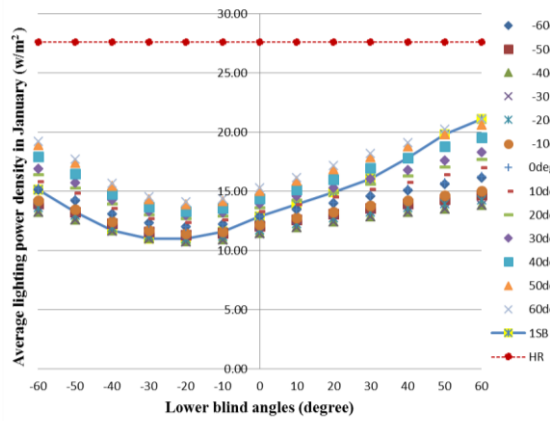
i) Room depth of 15 m in January
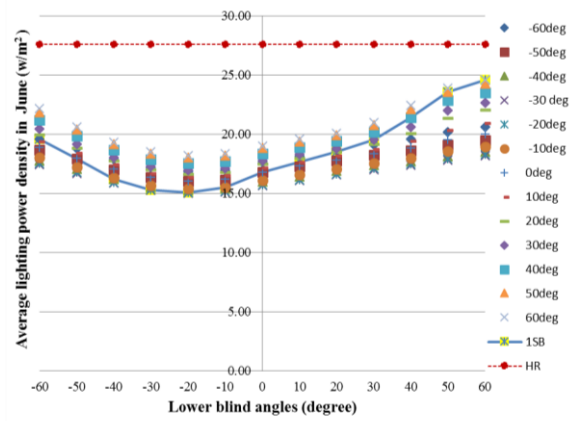
j) Room depth of 15 m in June

Figure A4 Average light power density at 800 lux in January and June (continued)
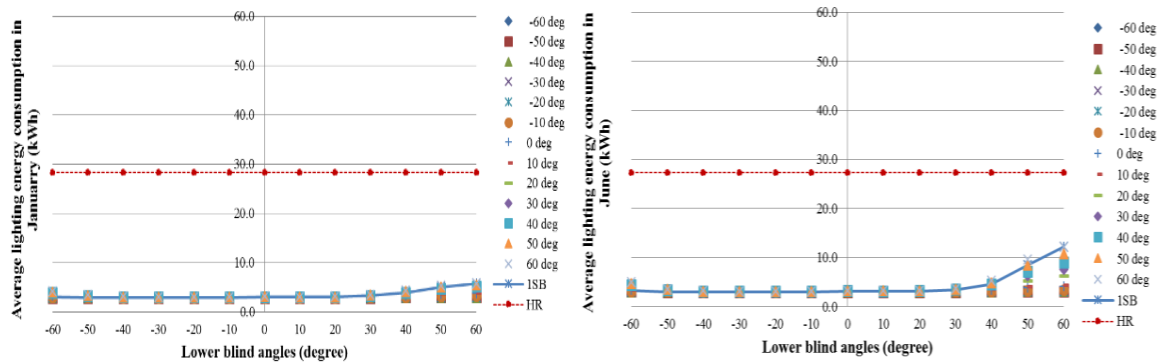
Average lighting energy consumption at 500 lux

a) Room depth of 3 m in January   b) Room depth of 3 m in June
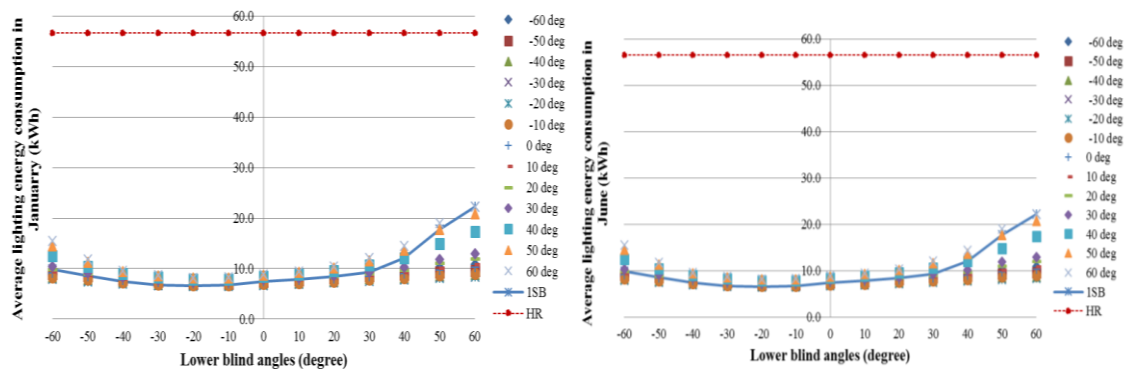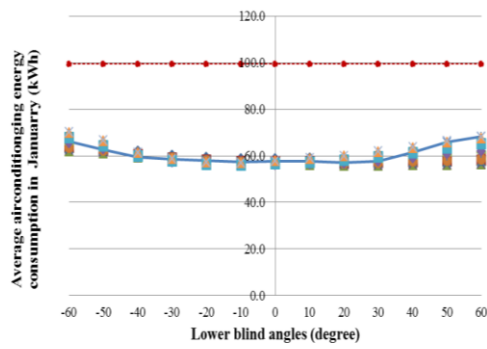

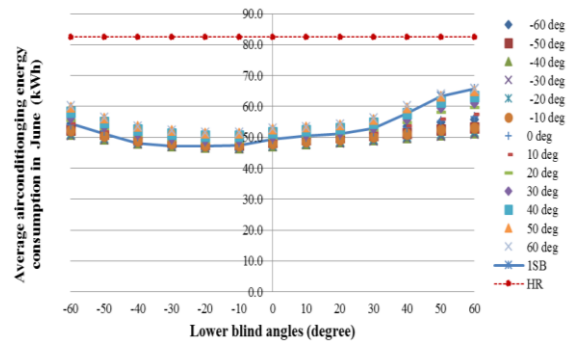c) Room depth of 6 m in January   d) Room depth of 6 m in June
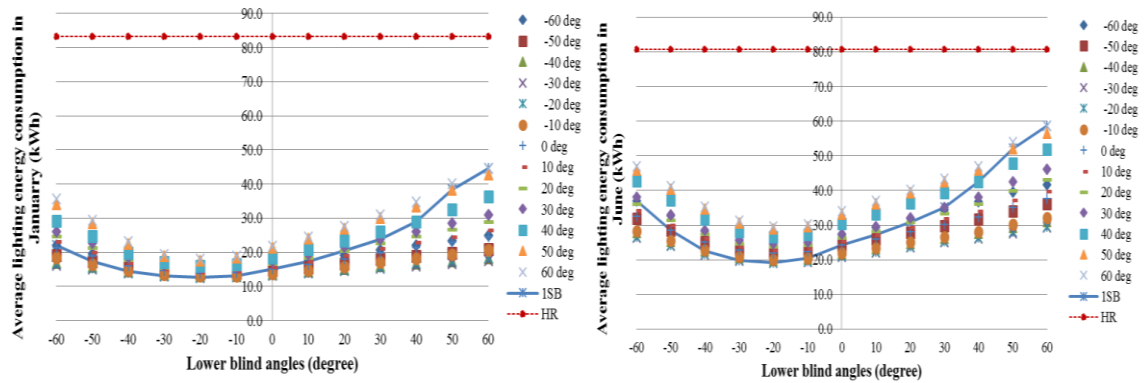
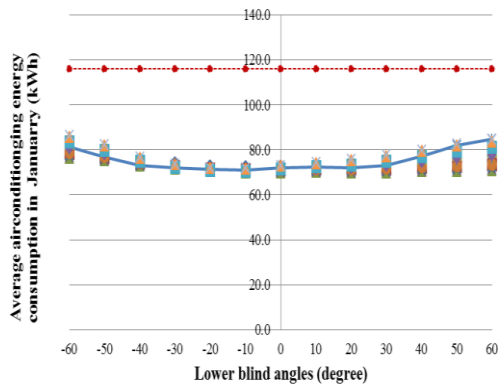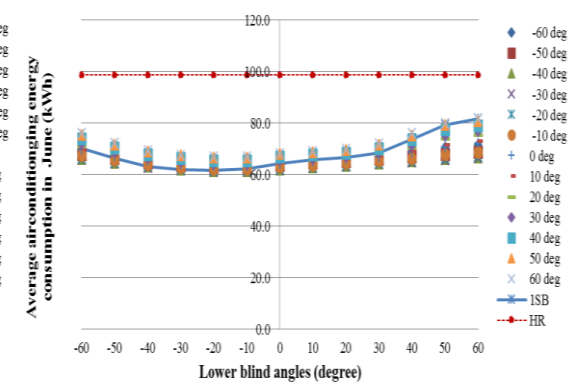e) Room depth of 9 m in January   f) Room depth of 9 m in June

Figure A5 Average lighting energy consumption at 500 lux in January and June
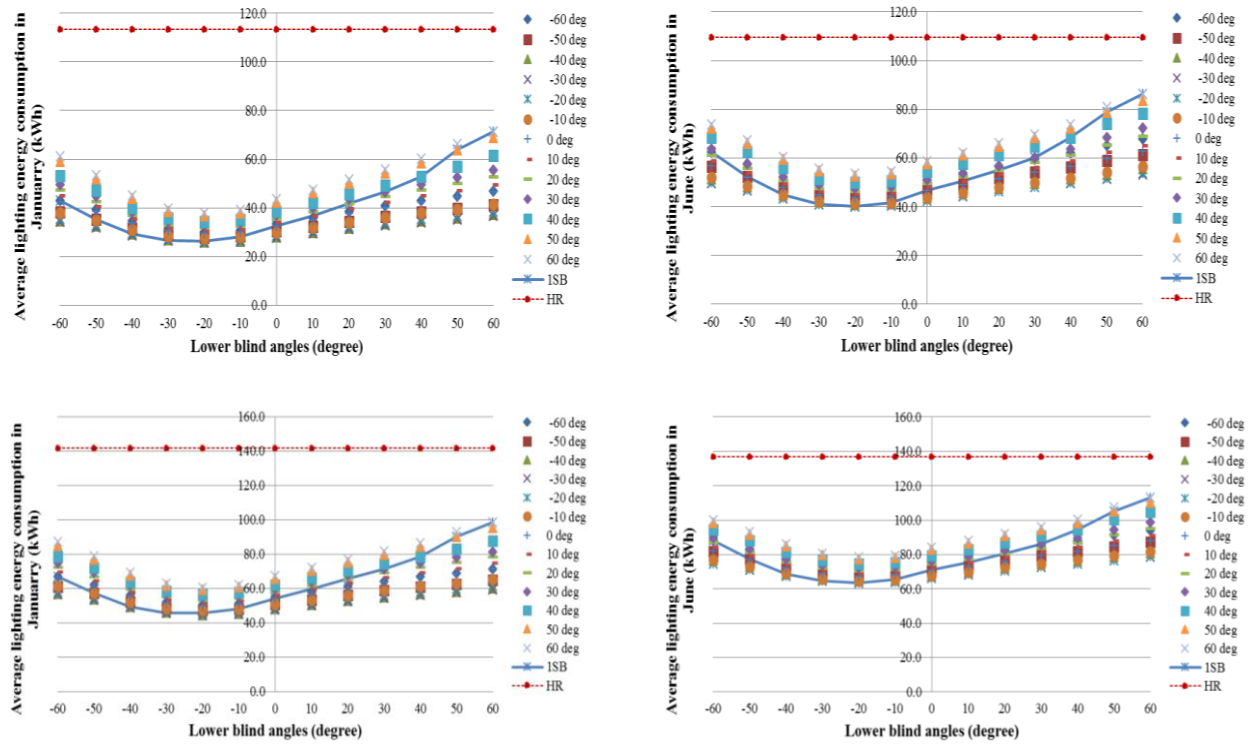
Figure A5 Average lighting energy consumption at 500 lux in January and June

(continued)

Average lighting energy consumption at 800 lux

a) Room depth of 3m in January

b) Room depth of 3m in June

c) Room depth of 6 m in January

d) Room depth of 6 m in June

e) Room depth of 9 m in January

f) Room depth of 9 m in June

Figure A6 Average lighting energy consumption at 800 lux in January and June

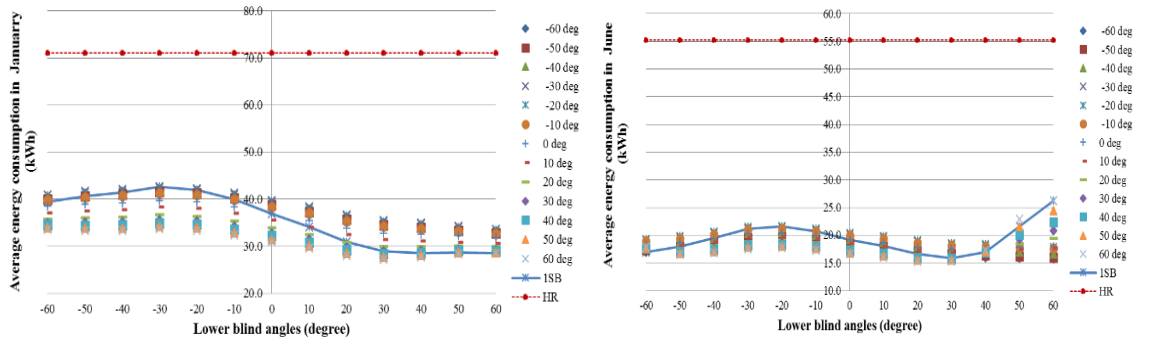g) Room depth of 12m in January

h) Room depth of 12m in June

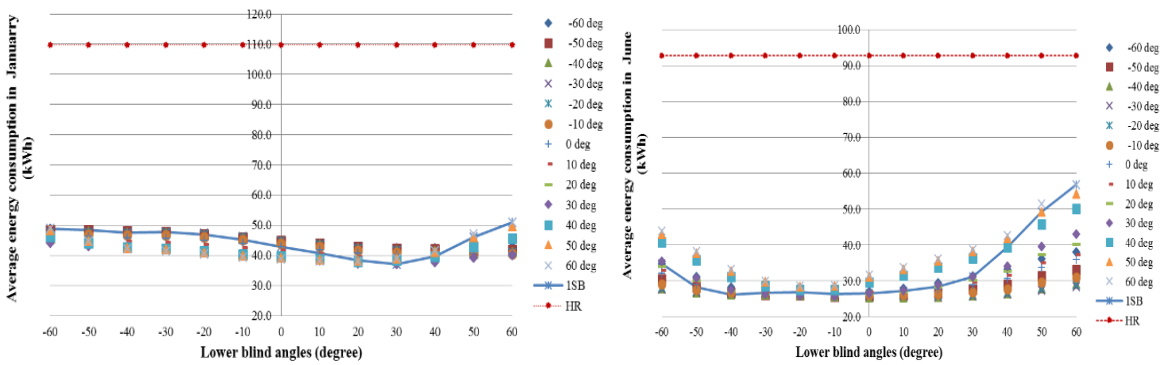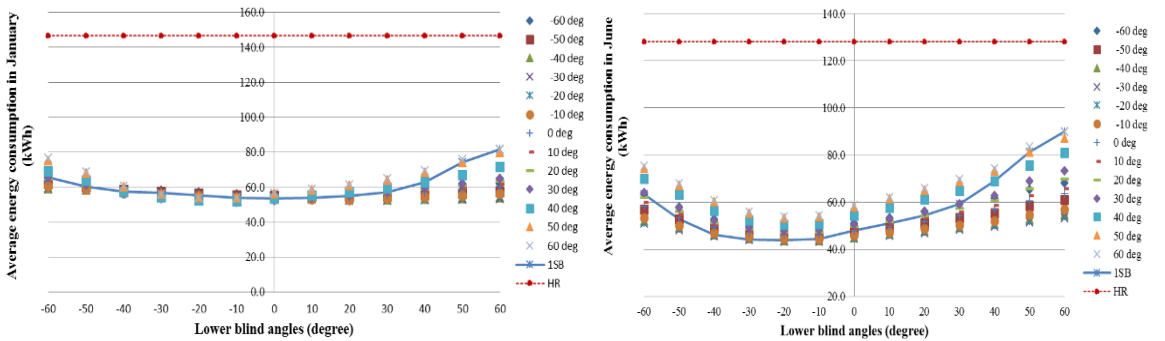h) Room depth of 15m in January

i) Room depth of 15m in June

Figure A6 Average lighting energy consumption at 800 lux in January and June

(continued)

Average Air-conditioning energy consumption at 500 lux

a) Room depth of 3 m in January

b) Room depth of 3 m in June

c) Room depth of 6 m in January
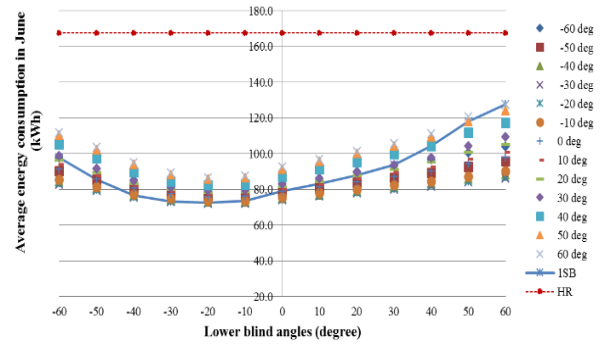
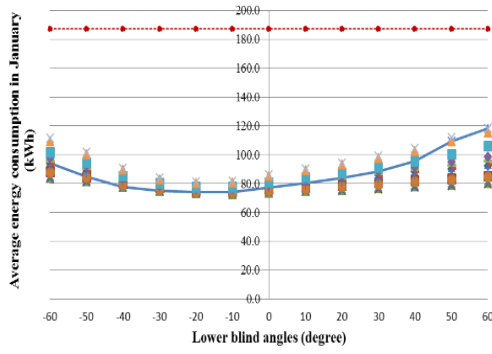d) Room depth of 6 m in June
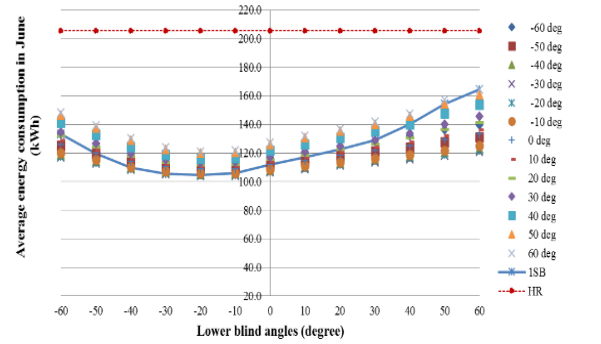

e) Room depth of 9 m in January

f) Room depth of 9 m in June

Figure A7 Average air-conditioning energy consumption at 500 lux in January and June

g) Room depth of 12 m in January

h) Room depth of 12 m in June

h) Room depth of 15 m in January

i) Room depth of 15 m in June

Figure A7 Average air-conditioning energy consumption at 500 lux in January and June

(continued)

Average Air-conditioning energy consumption 800 lux

a) Room depth of 3 m in January   b) Room depth of 3 m in June

c) Room depth of 6 m in January   d) Room depth of 6 m in June
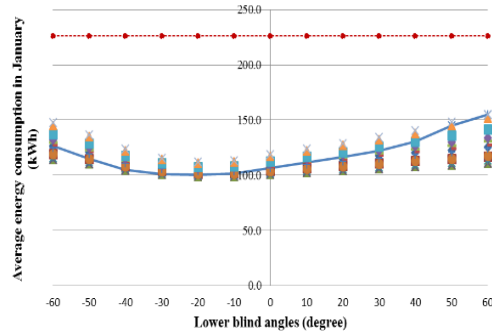
e) Room depth of 9 m in January   f) Room depth of 9 m in June

Figure A8 Average air-conditioning energy consumption at 800 lux in January and June

g) Room depth of 12 m in January
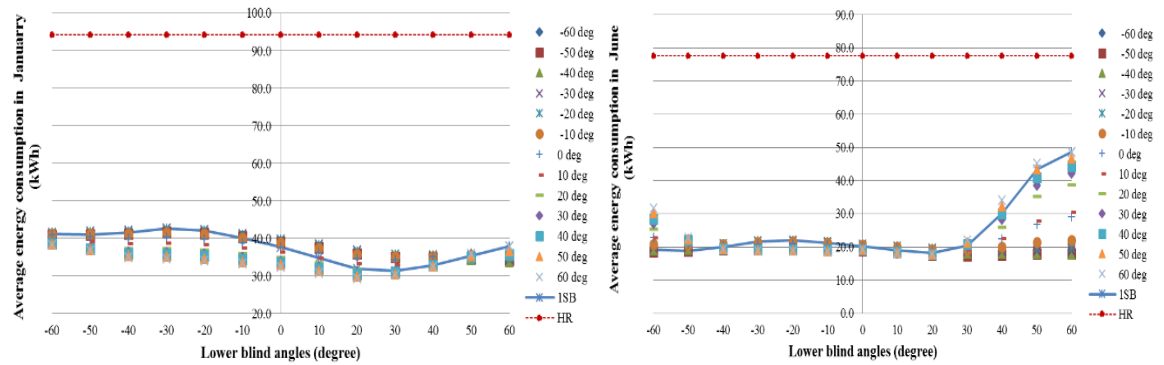
h) Room depth of 12 m in June

h) Room depth of 15 m in January
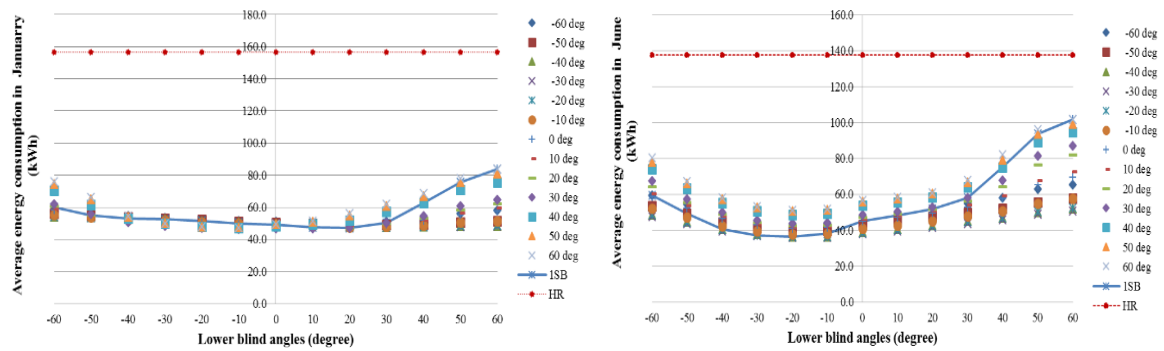
i) Room depth of 15 m in June

Figure A8 Average air-conditioning energy consumption at 800 lux in January and June

(continued)
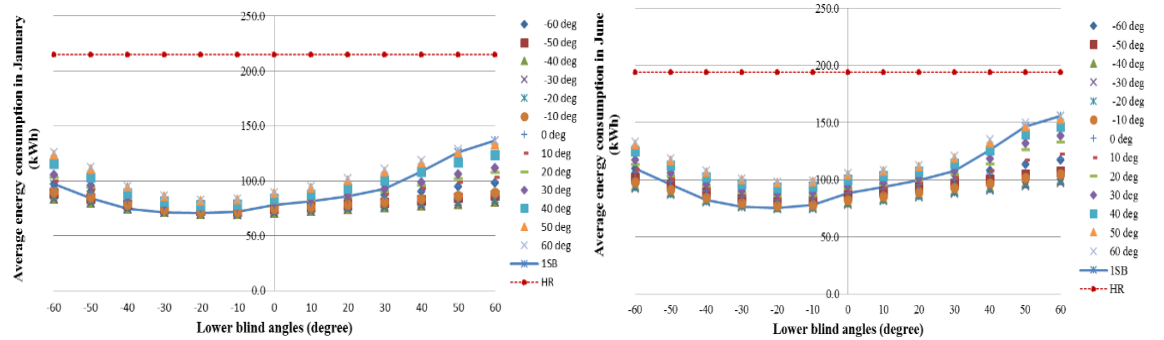
Average Total energy consumption500lux

a) Room depth of 3 m in January
b) Room depth of 3 m in June

c) Room depth of 6 m in January
d) Room depth of 6 m in June

e) Room depth of 9 m in January
f) Room depth of 9 m in June

Figure A9 Average total energy consumption at 500 lux in January and June

82

g) Room depth of 12m in January   h) Room depth of 12m in June

h) Room depth of 15m in January   i) Room depth of 15m in June

Figure A9 Average total energy consumption at 500 lux in January and June (continued)

Average Total energy consumption 800 lux

a) Room depth of 3 m in January

b) Room depth of 3 m in June
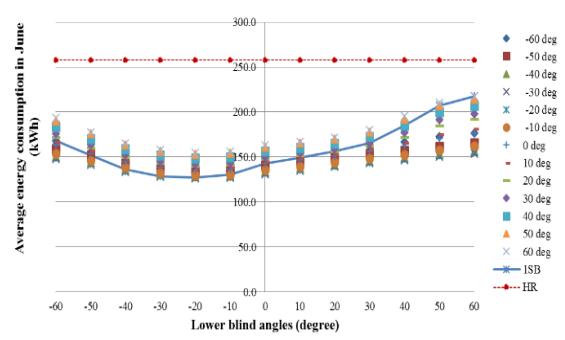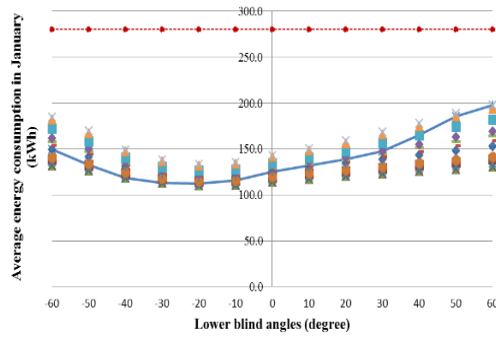

c) Room depth of 6 m in January

d) Room depth of 6 m in June
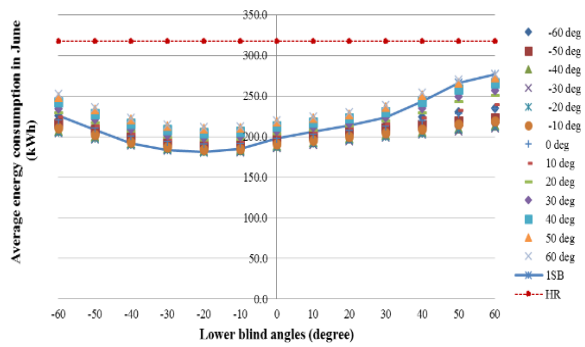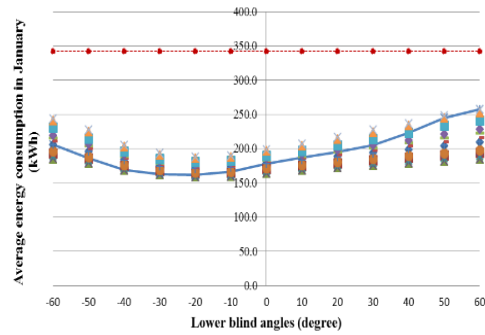

e) Room depth of 9 m in January

f) Room depth of 9 m in June

Figure A10 Average total energy consumption at 800 lux in January and June

g) Room depth of 12 m in January   h) Room depth of 12 m in June

h) Room depth of 15 m in January   i) Room depth of 15 m in June

Figure A10 Average total energy consumption at 800 lux in January and June (continued)